

**ANALYSIS OF DRILLING FLUID RHEOLOGY AND TOOL JOINT
EFFECT TO REDUCE ERRORS IN HYDRAULICS
CALCULATIONS**

A Dissertation

by

MARILYN VILORIA OCHOA

Submitted to the Office of Graduate Studies of
Texas A&M University
in partial fulfillment of the requirements for the degree of

DOCTOR OF PHILOSOPHY

August 2006

Major Subject: Petroleum Engineering

**ANALYSIS OF DRILLING FLUID RHEOLOGY AND TOOL JOINT
EFFECT TO REDUCE ERRORS IN HYDRAULICS
CALCULATIONS**

A Dissertation
by
MARILYN VILORIA OCHOA

Submitted to the Office of Graduate Studies of
Texas A&M University
in partial fulfillment of the requirements for the degree of
DOCTOR OF PHILOSOPHY

Approved by:

Chair of Committee,
Committee Members,

Head of Department,

Hans C. Juvkam-Wold
Jerome J. Schubert
Peter P. Valkó
Victor M. Ugaz
Stephen A. Holditch

August 2006

Major Subject: Petroleum Engineering

ABSTRACT

Analysis of Drilling Fluid Rheology and Tool Joint Effect to Reduce Errors in
Hydraulics Calculations. (August 2006)

Marilyn Vilorio Ochoa, B.S., Zulia University;

M.A., Zulia University

Chair of Advisory Committee: Dr. Hans C. Juvkam-Wold

This study presents a simplified and accurate procedure for selecting the rheological model which best fits the rheological properties of a given non-Newtonian fluid and introduces five new approaches to correct for tool joint losses from expansion and contraction when hydraulics is calculated. The new approaches are enlargement and contraction (E&C), equivalent diameter (ED), two different (2IDs), enlargement and contraction plus equivalent diameter (E&C+ED), and enlargement and contraction plus two different IDs (E&C+2IDs).

In addition to the Newtonian model, seven major non-Newtonian rheological models (Bingham plastic, Power law, API, Herschel-Bulkley, Unified, Robertson and Stiff, and Casson) provide alternatives for selecting the model that most accurately represents the shear-stress/shear-rate relationship for a given non-Newtonian fluid.

The project assumes that the model which gives the lowest absolute average percent error (E_{AAP}) between the measured and calculated shear stresses is the best one for a given non-Newtonian fluid.

The results are of great importance in achieving correct results for pressure drop and hydraulics calculations and the results are that the API rheological model

(RP 13D) provides, in general, the best prediction of rheological behavior for the mud samples considered ($E_{AAP}=1.51$), followed by the Herschel-Bulkley, Robertson and Stiff, and Unified models. Results also show that corrections with E&C+2IDs and API hydraulics calculation give a good approximation to measured pump pressure with 9% of difference between measured and calculated data.

DEDICATION

This dissertation is dedicated to my husband Jairo and my son Jairo Raul. They have always provided an atmosphere of love and understanding that helped me achieve my goal. I specifically dedicate my dissertation to my husband whose encouragement, love and good suggestions have made my dream of conquering a doctoral degree possible.

Also, I can not forget in this moment, my family in Venezuela.

They always have provided emotional support to help me finish this goal.

Finally, I want to dedicate this success in my life to my always remembered friend Sergei, who always was close to me when I needed him. Thank you my friend; I will follow all your advice, every single day of my life. You will be my good angel forever.

ACKNOWLEDGMENTS

I would like to sincerely thank Dr. Juvkam-Wold for supervising this study. I am thankful to him for his ideas and for pointing out the proper direction for this work.

Thanks to Dr. Schubert for reading, correcting and giving me good ideas of how to present this report, and for his support and good mood since the beginning of this research.

I am also grateful to Dr. Ugaz and Dr. Valkó for reading this report and giving me good suggestions.

I am very thankful to Universidad del Zulia-CIED-PDVSA for their financial support provided for my studies.

Thanks to my entire Colombian, Peruvian and Venezuelan friends that, in one way or another, helped me to conclude this doctoral degree.

TABLE OF CONTENTS

	Page
ABSTRACT	iii
DEDICATION	v
ACKNOWLEDGMENTS	vi
TABLE OF CONTENTS.....	vii
LIST OF FIGURES	x
LIST OF TABLES	xiii
 CHAPTER	
I INTRODUCTION	1
1.1 Definition of the Problem.....	3
1.2 Importance	3
II BACKGROUND RESEARCH	4
2.1 Literature Review	4
III RHEOLOGY	9
3.1 Understanding Drilling Fluid Rheology	9
3.2 Component of Rheological Research.....	9
3.3 Viscosity	9
3.4 Shear-Dependent Viscosity of Non-Newtonian Liquids	11
3.5 Linear Viscoelasticity	12
3.6 Viscoplastic or “Yield Stress” Fluid	12
3.7 Time Effects in Non-Newtonian Liquids.....	13
3.8 Rheology in Suspensions.....	14
3.9 Oil-Based Mud Rheological Properties as a Function of Temperature and Pressure	16

CHAPTER	Page
IV	ACCURATE PROCEDURE FOR SELECTING THE BEST RHEOLOGICAL MODELS 23
	4.1 Newtonian Model..... 24
	4.2 Bingham Plastic Model..... 27
	4.3 Power-Law Model..... 30
	4.4 API-Model (RP 13D)..... 33
	4.5 Herschel-Bulkley Model..... 36
	4.6 Unified Model 39
	4.7 Robertson and Stiff Model..... 42
	4.8 Casson Model 45
V	HYDRAULICS 49
	5.1 Friction Pressure Loss Calculation 50
VI	TOOL JOINT 71
	6.1 Weld-On Tool Joint..... 71
VII	STUDY APPROACHES TO ESTIMATE PRESSURE LOSSES BY CORRECTING FOR TOOL JOINT LOSSES 77
	7.1 Enlargement and Contraction..... 78
	7.2 Equivalent Diameter 83
	7.3 Two Different IDs..... 83
	7.4 Enlargement and Contraction Plus Equivalent Diameter..... 85
	7.5 Enlargement and Contraction Plus Two Different IDs 85
VIII	DATA USED TO VALIDATE THE NEW APPROACHES 86
IX	RESULTS ANALYSIS 89
X	CONCLUSIONS AND RECOMMENDATIONS 98
	10.1 Conclusions..... 98
	10.2 Recommendations 99
	NOMENCLATURE..... 100

	Page
REFERENCES	105
APPENDIX A.....	109
APPENDIX B.....	118
APPENDIX C.....	162
APPENDIX D.....	171
APPENDIX E.....	172
VITA.....	177

LIST OF FIGURES

	Page
Fig.2.1—Rheograms at various temperatures and pressures for unweighted oil-based mud, 80:20 oil/water ratio ⁷	6
Fig.2.2—Low-toxicity, biodegradable, organic-base fluid ⁸	7
Fig.3.1—Shear thinning or pseudoplastic fluid behavior (non-linear) ¹¹	11
Fig.3.2—Thixotropic effect (from Thivolle ³)	14
Fig.3.3—Effect of temperature and pressure on the viscosity of diesel oil (from Lummus ¹⁵)	17
Fig.3.4—Effect of pressure and temperature on plastic viscosity (from Bogotá Technical Center-Colombia)	18
Fig.3.5—Effect of pressure and temperature over yield point (from Bogotá Technical Center-Colombia)	19
Fig. 3.6—Effect of mud flow-rate on the drillstring fluid temperature above seafloor (from Lima ¹⁶).	20
Fig.3.7—Low-temperature PVT data for an IO1618 synthetic fluid run on a Huxley-Bertram HTHP viscometer (from Zamora and Sanjit ¹⁷)	21
Fig.3.8—Low-temperature and pressure effects on PV and YP of a 16-lb/gal, 85:15 oil/water ratio IO1618 synthetic mud (from Zamora and Sanjit ¹⁷)	22
Fig.4.1—Newtonian fluid rheogram	25
Fig.4.2—Comparison between measured data and calculated data for Newtonian model	27
Fig.4.3—Bingham plastic fluid rheogram	28
Fig.4.4—Comparison between measured data and calculated data for Bingham plastic model	29
Fig.4.5—Power-law fluid rheogram.....	31
Fig.4.6—Comparison between measured data and calculated data for Power law model.....	32
Fig.4.7—API “dual power law” fluid rheogram	34

	Page
Fig.4.8—Comparison between measured data and calculated data for API model	35
Fig.4.9—Herschel-Bulkley fluid rheogram	37
Fig.4.10—Comparison between measured data and calculated data for Herschel-Bulkley model	39
Fig.4.11— Comparison between measured data and calculated data for Unified model	42
Fig.4.12— Robertson and Stiff fluid rheogram.....	44
Fig.4.13— Comparison between measured data and calculated data for Robertson and Stiff model.....	45
Fig.4.14— Casson fluid rheogram	47
Fig.4.15—Comparison between measured data and calculated data for Casson model	48
Fig.5.1 —Diagram of the drilling fluid circulating system (from Mojisola ²⁵).	51
Fig.5.2—Critical Reynolds numbers for Bingham plastic fluids (from Bourgoyne ¹⁴).....	55
Fig.5.3— Critical Reynolds numbers for Casson fluids (data from Hanks ²⁹).....	68
Fig.6.1— API standards tool joint (from IADC manual ³¹).....	71
Fig.6.2— Diagram of tool joint ³²	72
Fig.6.3— Internal/external upset (from IADC manual ³¹)	73
Fig.6.4— Tool joint nomenclature (from IADC manual ³¹).....	75
Fig.6.5 —Schematic of the box and pin ends of a joint of pipe. ID = internal diameter, OD = outside diameter, FH = full hole ³²	76
Fig.7.1 —Schematic change of area, a_1 and a_2 , in a pipe with a tool joint (from tool joint to pipe) ³³	78
Fig.7.2 —Schematic change of area, a_1 and a_2 , in a pipe with a tool joint (enter from pipe to tool joint) ³³	79
Fig.7.3 —The angle, θ , is an important element in the enlargement and contraction equations ³³	80
Fig.7.4 —Schematic change of area in the annulus with presence of tool joint.....	82

	Page
Fig.8.1— Schematic of well and instrumentation for hydraulics study ⁹	88
Fig.9.1— Flow rate vs. pump pressure for eight rheological models at 150 °F.....	91
Fig.9.2— Flow rate vs. pump pressure with E&C correction.....	92
Fig.9.3— Flow rate vs. pump pressure with ED correction	93
Fig.9.4— Flow rate vs. pump pressure with correction for 2IDs	94
Fig.9.5— Flow rate vs. pump pressure with correction for E&C+ ED	95
Fig.9.6— Flow rate vs. pump pressure with correction for E&C+2IDs	96
Fig.B1— Critical Reynolds numbers for Casson fluids-example followed.....	156
Fig.D1— Rheograms for eight rheological models at 150 °F.....	171
Fig.E1— Flow rate vs. drillstring pressure loss with E&C correction.....	172
Fig.E2— Flow rate vs. annular pressure loss with E&C correction.....	172
Fig.E3— Flow rate vs. drillstring pressure loss with ED correction.....	173
Fig.E4— Flow rate vs. annulus pressure loss with ED correction	173
Fig.E5— Flow rate vs. drillstring pressure loss with 2IDs correction.....	174
Fig.E6— Flow rate vs. annular pressure loss with correction for 2IDs	174
Fig.E7— Flow rate vs. drillstring pressure loss with correction for E&C+2IDs	175
Fig.E8— Flow rate vs. annular pressure loss with correction for E&C+2IDs	175
Fig.E9— Flow rate vs. drillstring pressure loss with correction for E&C+ ED ...	176
Fig.E10— Flow rate vs. annular pressure loss with correction for E&C+ ED....	176

LIST OF TABLES

	Page
Table 4.1—Data from Fann 70 (from White and Zamora ⁹)	24
Table 4.2—Shear Stress Measured in Field Units	25
Table 4.3—Shear Stress Calculated as Function of Viscosity	26
Table 4.4—Shear Stress Calculated as Function of Plastic Viscosity and Yield Point	29
Table 4.5—Shear Stress Calculated as Function of Power Law Parameters	31
Table 4.6—Shear Stress Calculated as Function of API Parameters	35
Table 4.7—Shear Stress Calculated as Function of Herschel-Bulkley Parameters	38
Table 4.8—Shear Stress Calculated as Function of Unified Model Parameters	41
Table 4.9—Shear Stress Calculated as Function of Robertson and Stiff Model Parameters	44
Table 4.10—Square Roots of Variables Used To Graph Fig.4.14	46
Table 4.11—Shear Stress Calculated as Function of Casson Model Parameters	48
Table 6.1— Upset Drillpipe for Weld-On Tool Joints, Grades D and E (from IADC manual ³¹)	73
Table 6.2— Upset Drillpipe for Weld-On Tool Joints, Grades X, G and S (from IADC manual ³¹)	74
Table 7.1— Angles for Internal Upset (Drillpipe) for Weld-On Tool Joints	81
Table 7.2— Angles for External Upset (Annulus) for Weld-On Tool Joints	81
Table 9.1— E_{AAP} Value for Rheological Models	89
Table 9.2— Analysis of Five Corrections for Eight Rheological Models	96
Table A1—Rheology and Hydraulics Equations for Newtonian Model	109
Table A2—Rheology and Hydraulics Equations for Bingham Plastics Model	110
Table A3—Rheology and Hydraulics Equations for Power Law Model	111
Table A4—Rheology and Hydraulics Equations for API RP13D Model	112

	Page
Table A5—Rheology and Hydraulics Equations for Herschel-Bulkley Model	113
Table A6—Rheology and Hydraulics Equations for Unified Model.....	114
Table A7—Rheology and Hydraulics Equations for Robertson and Stiff Model “Original”	115
Table A8—Rheology and Hydraulics Equations for Robertson and Stiff Model “Yield Point”	116
Table A9—Rheology and Hydraulics Equations for Casson.....	117
Table B1— Pressure Drop Results Calculated with the Various Models ($q=100$ gpm).....	161
Table B2— Pressure Drop Results Calculated with the Various Models ($q=665$ gpm).....	161
Table C1— Angles for Internal Upset (Drillpipe) for Given Example.....	162
Table C2—Angles for Internal Upset (Annulus) for Given Example	164
Table D1— Rheological Properties for Eight Rheological Models	171

CHAPTER I

INTRODUCTION

The major applications of rheological properties for evaluating drilling fluid behavior are in solving problems of hole cleaning and hole erosion, suspension of cuttings, drilling fluid treatment, and hydraulics calculations. Hydraulics calculations are the focus of this project.

The viscosity of the drilling fluid must be known at all times because it determines the hydraulics in the well. The exact representation of this property differs depending on the type of fluid being pumped and rheological model being used for the evaluation of the fluid parameters. Many fluid properties depend on the system's rheology.

The rheology of dispersions, the most common drilling fluids today, is complex because they usually exhibit non-Newtonian behavior. Non-Newtonian fluids do not conform to a direct proportionality between shear stress and shear rate, and no single equation has been proved to describe exactly the rheogram of all such fluids. Shear stress in oil field terms is analogous to the pump pressure.

In addition to the Newtonian model, this study examined seven major non-Newtonian rheological models (Bingham, Power law, API RP 13D¹, Herschel-Bulkley, Unified, Robertson and Stiff, and Casson) to identify additional alternatives for selecting the model that represents most accurately the shear-stress/shear-rate relationship for a given non-Newtonian fluid. This approach assumed that the model that gives the lowest absolute average percent error (E_{AAP}) between the measured and calculated shear stresses is the best one for a given non-Newtonian fluid.

This dissertation follows the style and format of *SPE Journal*.

The first part of this study presents a simplified and accurate procedure for selecting the rheological model which best fits the rheological properties of a given non-Newtonian fluid.

The second part introduces five new approaches to correct for tool joint losses when hydraulics is calculated. These approaches are enlargement and contraction (E&C), equivalent diameter (ED), two different IDs (2IDs), enlargement and contraction plus equivalent diameter (E&C+ED), and enlargement and contraction plus two different IDs (E&C+2IDs).

Deep drilling needs high-strength drillpipe, which often has small-throated (internal upset) tool joints. These internal limitations cause flow losses that can be considerable. The pressure loss caused by entry into the tool joint is small compared with the exit losses.

On the other hand, the same problem can be experienced in the annulus between tool joint and casing due to the external upset of the tool joint. This space is narrower than the space between drillpipe and casing. The effect of expansion and contraction on the fluid flowing in the annulus is additional pressure loss.

The results of this research, methods to select the best rheological model and to estimate additional pressure loss from expansion and contraction of the fluid flowing through pipe and annuli, are of great importance in achieving correct results for pressure drop and hydraulics calculations.

Data from an offshore well showed that the API RP 13D model provides the best general prediction of rheological behavior for the mud samples considered ($E_{AAP}=1.51$). It was followed by Herschel-Bulkley, Robertson and Stiff, and the

Unified model. Also, correction with E&C+2IDs and the API hydraulics calculation gives a good approximation of measured pump pressure (9%).

1.1 Definition of the Problem

The drilling industry cannot without fail match calculated and actual pump pressures, Δp_p . For example, Δp calculations using API RP13D with synthetic-based mud (SBM) can be off as much as 35%.² The possible reasons could be that friction pressure losses are functions of drilling fluid properties, which are functions of the rheological model, temperature, and well geometry.³ As a result, current API RP13D equations seriously underestimate drillstring pressure losses, which account for the differences in pump pressure, Δp .

1.2 Importance

Many experimental studies deal with the flow of fluids through pipes and annuli for friction pressure loss calculations. Most of these studies have concentrated on rheological models, pipe roughness, and geometrical parameters. However, the effects of tool joints had yet been seriously investigated to estimate the friction pressure loss inside drillpipe and in the annulus. Additionally, selection of the best rheological model to obtain correct results for pressure drop and hydraulics have until now not been included in API RP13D.

This study of eight rheological models is expected to serve as a manual for the state of the art in rheology in drilling fluid, as well as in hydraulics calculation. This dissertation could also be used in an educational environment and for training purposes; it would help inform and educate the industry about rheology in drilling fluid and hydraulics calculation considering different rheological models as well as tool joint corrections.

CHAPTER II

BACKGROUND RESEARCH

2.1 Literature Review

Advances in the areas of drilling fluid rheology, tool joint effects, and hydraulics in drilling wells offer insight into the obstacles to choose appropriate equations.

2.1.1 Drilling Fluid Rheology

Most drilling fluid muds are non-Newtonian fluids, with viscosity decreasing as shear rate increases.³

Herzhaft *et al.*⁴ showed that plastic viscosity is the parameter most affected by temperature changes. On deepwater wells, the cooling effect of the riser will result in higher plastic viscosity in the drilling fluid. Additionally, the length of the riser enhances the cooling effect during circulation and during trips, creating major changes in rheology if oil-based or synthetic mud is used. Changes in mud viscosity may also lead to problems with surge and swab, transmission of measurement-while-drilling (MWD) pulses, increased equivalent circulating density and variations in hole-cleaning efficiency.

Zamora and Power² detailed in their paper a new unified rheological model. The rheological parameters for this model are the plastic viscosity (μ_p), yield point (τ_y), and yield stress (τ_0). A fourth parameter, the ratio τ_0/τ_y , is a useful tool to help characterize fluids rheologically, although it is not necessary for solving the model. However, many RP 13D elements are still valid and in use, but some need to be updated. Mud rheology needs adjustment for downhole conditions, especially in ultradeepwater wells drilled with oil or synthetic mud.

Power and Zamora⁵ showed that the ratio τ_0/τ_y is a useful parameter to characterize fluids rheologically. The acceptable range of τ_0/τ_y values is 0 to 1 for rheological models used in drilling. It will be better explained in Chapter III.

2.1.2 Pressure and Temperature Effect in the Rheology of Drilling Fluid

Politte⁶ concluded from his analysis of rheological data for emulsion that drilling fluid yield point is not a strong function of pressure, and becomes progressively less so as temperature increases. The effects of temperature on the yield point, however, are difficult to predict as they require chemical particle effects.

Davison *et al.*⁷ concluded from their study of rheological data obtained from a viscosimeter that the effect of low temperature on both oil-based mud (OBM) and synthetic mud (SBM) viscosity is quite pronounced. On the other hand, when pressure was increased at various temperatures, viscosity of both oil-based and SBMs increased, especially at higher shear rates. The pressure effects don't appear to be dependent on the temperature. **Fig. 2.1** shows some results.

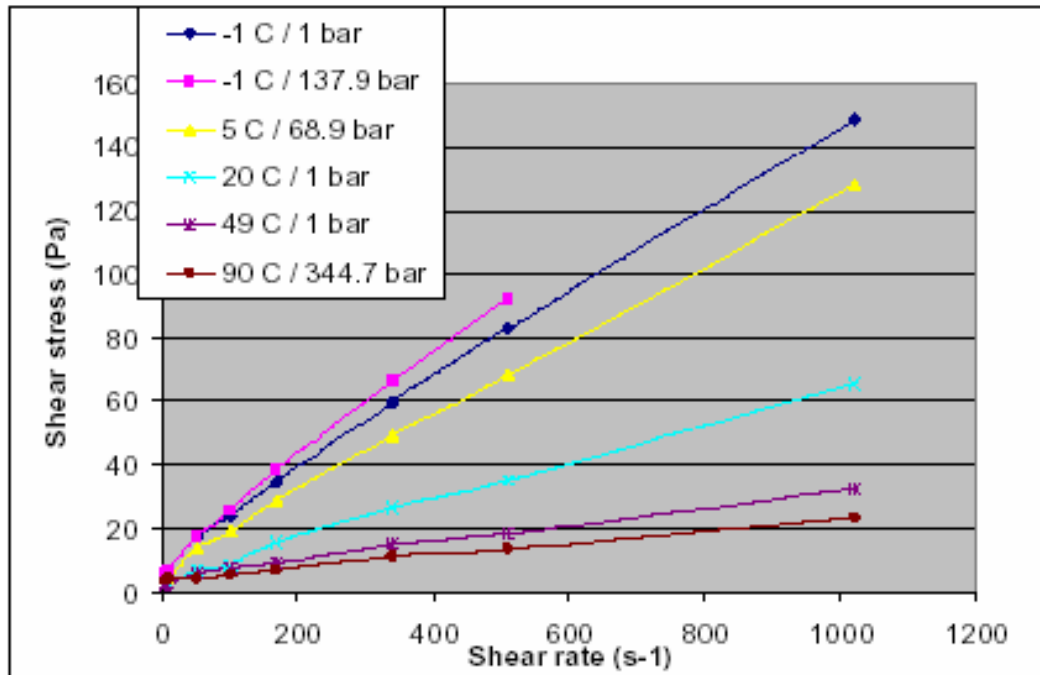


Fig. 2.1—Rheograms at various temperatures and pressures for unweighted oil-based mud, 80:20 oil/water ratio.⁷

Prediction of hydrostatic pressure requires pressure/volume/temperature (PVT) data for the mud in addition to an accurate simulation of the downhole temperature profile. The compressibility of a drilling fluid depends on its base fluid; the solids are incompressible.

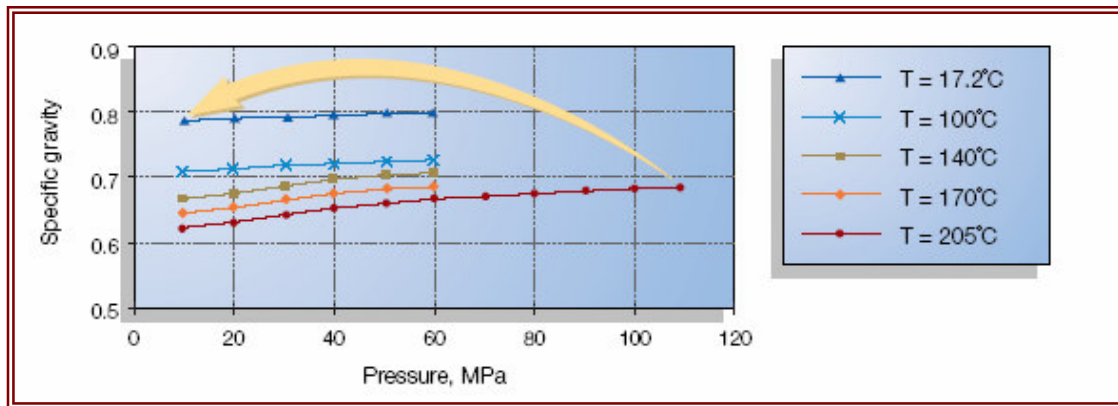


Fig. 2.2— Low-toxicity, biodegradable, organic-base fluid.⁸

Fig. 2.2 is the PVT diagram for the low-toxicity, biodegradable, organic-base fluid of the ULTIDRILL system, which has been used at 395°F and at weights up to 19 ppg. The specific gravity of the base fluid under these conditions at a depth of 16,000 feet is 0.68. The same fluid (arrow) returned to surface temperature and pressure has a specific gravity of 0.79, a 14% decrease in base fluid density at total depth, which is important in computing static pressure.⁸

2.1.3 Hydraulics in Deepwater

Zamora and Power² evaluated the inability of API equations from RP 13D to match field data in critical drilling, because these equations have to incorporate the effects of temperature and pressure on SBM density and rheological properties.

2.1.4 Tool Joints

White and Zamora⁹ established from a comparison between field and calculated data that one possible opportunity for discrepancies is increase in pressure caused by sudden contraction and expansion of the mud when passing through the tool joints, which is not considered in any published hydraulics calculation.

Denison¹⁰ concluded that internally constricted drillstring elements can drastically affect the rig hydraulics. Also, the pressure loss caused by entry into the tool joint is small compared with the exit losses.

Yeon-Tae and Subhash¹¹ found that the effect of the presence of tool joints on the annular friction pressure is significant, and they proposed an accurate prediction method for annular pressure loss.

CHAPTER III

RHEOLOGY

3.1 Understanding Drilling Fluid Rheology

The term “rheology” means the study of the deformation and flow of matter, including such widely differing materials as asphalt, lubricants, paints, plastics and rubber, which gives some idea of the scope of the subject and also the numerous scientific disciplines which are likely to be involved.¹²

Currently, the scope is even wider. Significant advances have been made in bio-rheology, in polymer rheology, in suspension rheology, and in the chemical processing and oil industries.¹²

3.2 Components of Rheological Research

3.2.1 Rheometry

Rheometry is the science of reproducing deformation and measuring the consequences on materials of interest. A rheometer reproduces deformation under controlled conditions representative of those found in real production processes such as temperature and deformation rate.

3.2.2 Constitutive Equations

In practice, rheology has usually been restricted to the study of the fundamental relations, called constitutive relations, between force and deformation in materials, primarily liquid.¹³

3.3 Viscosity

Viscosity is traditionally regarded as a most important material property, and any practical study requiring knowledge of material response would automatically turn to the viscosity.¹²

The concept of viscosity was introduced by Newton's postulate, in which the shear-stress (τ) was related to the velocity gradient, or shear rate ($\dot{\gamma}$), through the equation:

$$\tau = \mu \dot{\gamma} \quad \dots\dots\dots 3.1$$

For Newtonian liquids, μ is sometimes called the coefficient of viscosity, but it is now more commonly referred to simply as the viscosity. Such a terminology is helpful within the context of rheology, since, for most liquids, μ is not a coefficient, but a function of the shear rate ($\dot{\gamma}$).

3.3.1 Practical Ranges of Variables Which Affect Viscosity

The viscosity of real materials can be significantly affected by such variables as temperature and pressure, and it is clearly important for drilling fluid engineers to understand the way viscosity depends on such variables.¹²

For all liquids, viscosity decreases with increasing temperature and decreasing pressure. The strong temperature dependence of viscosity is such that, to produce accurate results, great care has to be taken with temperature control in viscometry. For liquids of higher viscosity, given their stronger viscosity dependence on temperature, even greater care has to be taken.¹²

The viscosity of liquids increases exponentially with isotropic pressure. Water below 30°C is the only exception; the viscosity of water first decreases before eventually increasing exponentially. The changes are quite small for pressures differing from atmospheric pressure (14.7 psi). Therefore, for most practical purposes, the pressure effect is ignored by viscometer users. In some situations, however, this would not be justified. For example, the oil industry requires measurements of the viscosity of lubricants and drilling fluids at elevated pressures.¹²

3.4 The Shear-Dependent Viscosity of Non-Newtonian Liquids

In the vast majority of drilling fluids, viscosity decreases with increase in shear rate, giving rise to what is now generally called “shear-thinning” behavior although the terms “temporary viscosity loss” and “pseudoplasticity” have also been employed.

In some cases (although few in number) the viscosity increases with shear rate. Such behavior is generally called “shear-thickening,” although the term “dilatancy” has also been used.¹²

The very act of deforming a material can cause rearrangement of its microstructure such that the resistance to flow increases with shear rate.¹¹ Many shear-thinning fluids will exhibit Newtonian behavior at extreme shear rates, both low and high. These two extremes are sometimes known as the lower and upper Newtonian regions respectively. For such fluids, when the apparent viscosity is plotted against log of shear rate, we see a curve as shown in **Fig. 3.1**.

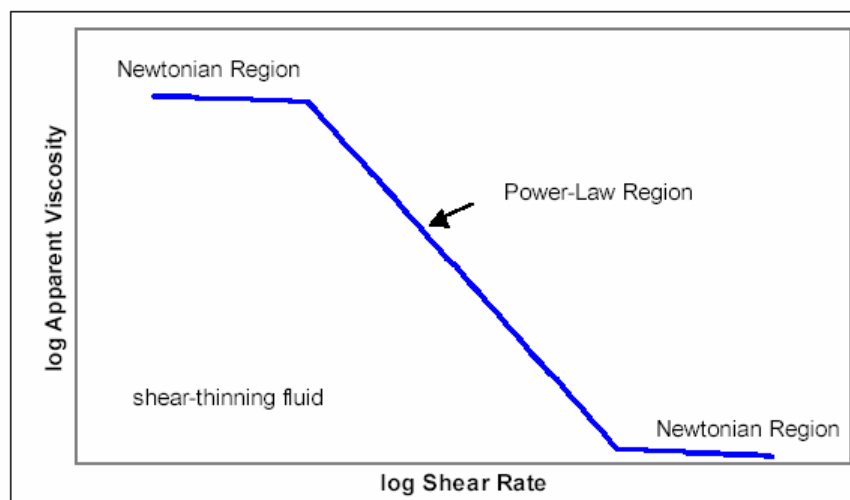


Fig. 3.1— Shear thinning or pseudoplastic fluid behavior (non-linear).¹¹

The terms "first Newtonian region" and "second Newtonian region" have also been used to describe the two regions where the viscosity reaches constant values.¹²

3.5 Linear Viscoelasticity

During the latter half of the nineteenth century, scientists began to note that a number of materials showed time dependence in their elastic response. Today we call this time-dependent response "viscoelasticity."¹³

The word "viscoelastic" means the simultaneous existence of viscous and elastic properties in a material. All real materials are viscoelastic; i.e., in all materials, both viscous and elastic properties coexist. The particular response of a sample in a given experiment depends on the time scale of the experiment in relation to a natural time of the material. Thus, if the experiment is relatively slow, the sample will appear to be viscous rather than elastic, whereas if the experiment is relatively fast, it will appear to be elastic rather than viscous. At intermediate time scales a mixed (viscoelastic) response is observed. An example of a common viscoelastic liquid is egg-white.¹²

3.6 Viscoplastic or "Yield Stress" Fluid

Another important type of non-Newtonian fluid is a viscoplastic or "yield stress" fluid. This is a fluid which will not flow when only a small shear stress is applied. The shear stress must exceed a critical value known as the yield stress, τ_0 , for the fluid to flow. For example, a tube of toothpaste should not flow at the slightest amount of shear stress; we need to apply an adequate force before the toothpaste starts flowing. So, viscoplastic fluids behave like solids when the applied shear stress is less than the yield stress. Once it exceeds the yield stress, the viscoplastic fluid will flow just like a fluid. Bingham plastics are a

special class of viscoplastic fluids that exhibit a linear behavior of shear stress against shear rate.

3.7 Time Effects in Non-Newtonian Liquids

We have so far assumed by implication that a given shear rate results in a corresponding shear stress, whose value does not change so long as the value of the shear rate is maintained. This is often not the case. The measured shear stress, and hence the viscosity, can either increase or decrease with time of shearing. Such changes can be reversible or irreversible.¹²

According to the accepted definition, a gradual decrease of the viscosity under shear stress followed by a gradual recovery of structure when the stress is removed is called “thixotropy.” The opposite type of behavior, involving a gradual increase in viscosity under stress, followed by recovery, is called “negative thixotropy” or “antithixotropy”.¹¹

Thixotropy usually occurs in circumstances where the liquid is shear-thinning (in the sense that viscosity levels decrease with increasing shear rate, other things being equal). In the same way, antithixotropy is usually associated with shear-thickening behavior. **Fig. 3.2** shows the behavior to be expected from relatively inelastic colloidal materials with the shear rate increasing continuously and linearly in time from zero to some maximum value and then decreasing to zero in the same way.¹²

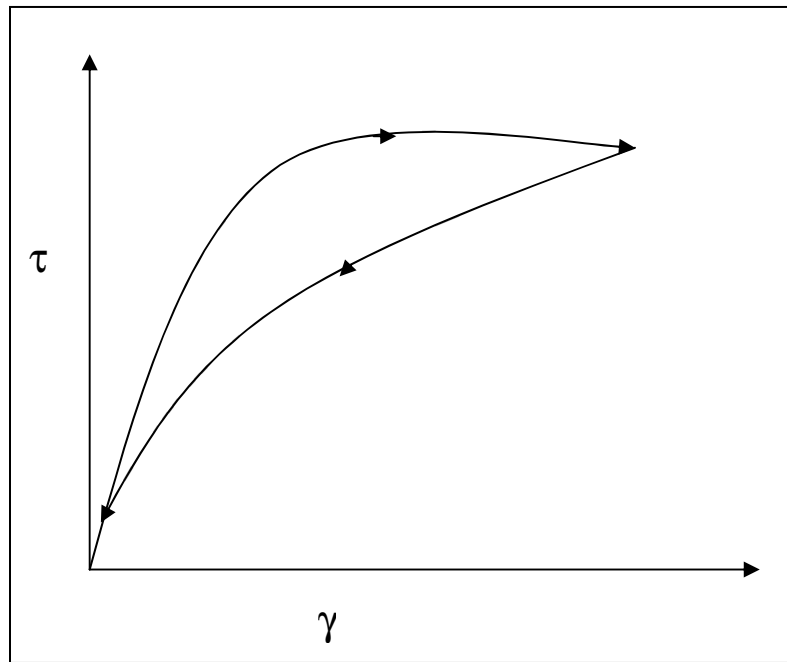


Fig. 3.2— Thixotropic effect (from Thivolle³).

The occurrence of thixotropy implies that the flow history must be taken into account when making predictions of flow behavior. For instance, flow of a thixotropic material down a long pipe is complicated by the fact that the viscosity may change with distance down the pipe.¹³

The bentonite suspensions used in drilling fluids are often thixotropic because the breakage and restoring of the network are reversible and not instantaneous, so that fluid properties are governed by different levels of structure.

3.8 Rheology of Suspensions

A suspension, or more broadly dispersion, consists of discrete particles randomly distributed in a fluid medium. Generally we divide suspensions into three categories: solid particles in a liquid medium (often the word “suspension”

is restricted to this meaning), liquid droplets in a liquid medium (or an emulsion), and gas in a liquid.¹³

Adding a particle does not simply change the magnitude of viscosity; it also can introduce all the known deviations from Newtonian behavior.

The first Newtonian plateau at low shear rate is followed by the Power-law shear- thinning region and then by a flattening out to the upper (second) Newtonian plateau. At some point, usually in this upper Newtonian region, viscosity can increase for suspensions of solid particles, given the appropriate conditions. In certain situations the first Newtonian plateau is sometimes so high as to be inaccessible to measurement. In such cases the low shear rate behavior is often described by an apparent yield stress.¹²

3.8.1 Forces Acting on Particles Suspended in a Liquid

Three kinds of forces coexist to various degrees in flowing suspensions. First, are those of colloidal origin that arise from interactions between the particles. These are controlled by properties of the fluid such as polarizability, but not by viscosity. These forces can result in an overall repulsion (electrostatic charges) or attraction between the particles. The Brownian force is strongly size dependent, ensures that the particles are in constant movement, and any description of the spatial distribution of the particles is a time average. The viscous forces acting on the particles are proportional to the local velocity difference between the particle and the surrounding fluid. For this reason, suspension viscosity is usually considered as the viscosity relative to that of the continuous phase. Clearly, the rheology measured macroscopically is strongly depending on this microstructure consideration.¹²

3.9 Oil-Based Mud Rheological Properties as a Function of Temperature and Pressure

Drilling fluids are called “oil-based mud” (OBM) if the continuous phase is composed of a liquid hydrocarbon. Diesel usually is used for the oil phase because of its viscosity characteristic, low flammability, and low solvency for rubber. In addition to diesel oil, weathered crude oils and various refined oils have been used as the oil phase for OBMs.¹⁴

Recently, several mineral oils have been developed that have a lower toxicity than diesel oil. These oils were developed to help solve the potential pollution problems associated with use of oil muds in a marine environment. The chosen oil should exhibit an acceptable viscosity over the entire range of temperatures and pressures to be encountered in the well. The effects of temperature and pressure on the viscosity of diesel oil are shown in **Fig. 3.3**.

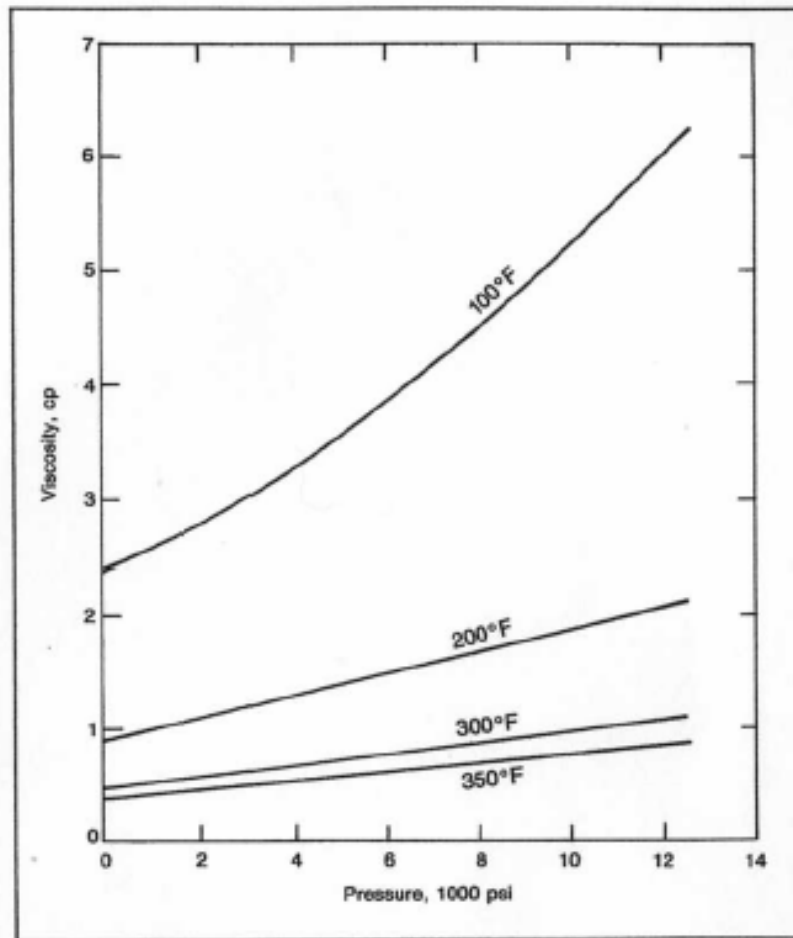


Fig. 3.3—Effect of temperature and pressure on the viscosity of diesel oil (from Lummus¹⁵).

Figs. 3.4 and 3.5 show real data for OBM from a Fann 70 viscometer. This data was obtained from Bogotá Technical Center-Colombia. The sample used diesel as the liquid phase in an OBM of 80:20 oil/water ratio.

The figures show how plastic viscosity and yield point (rheological properties from the Bingham plastic model) behave with variation of pressure and temperature.

Increasing pressure at constant temperature increases plastic viscosity and yield point. When temperature increases at constant pressure, the properties decrease.

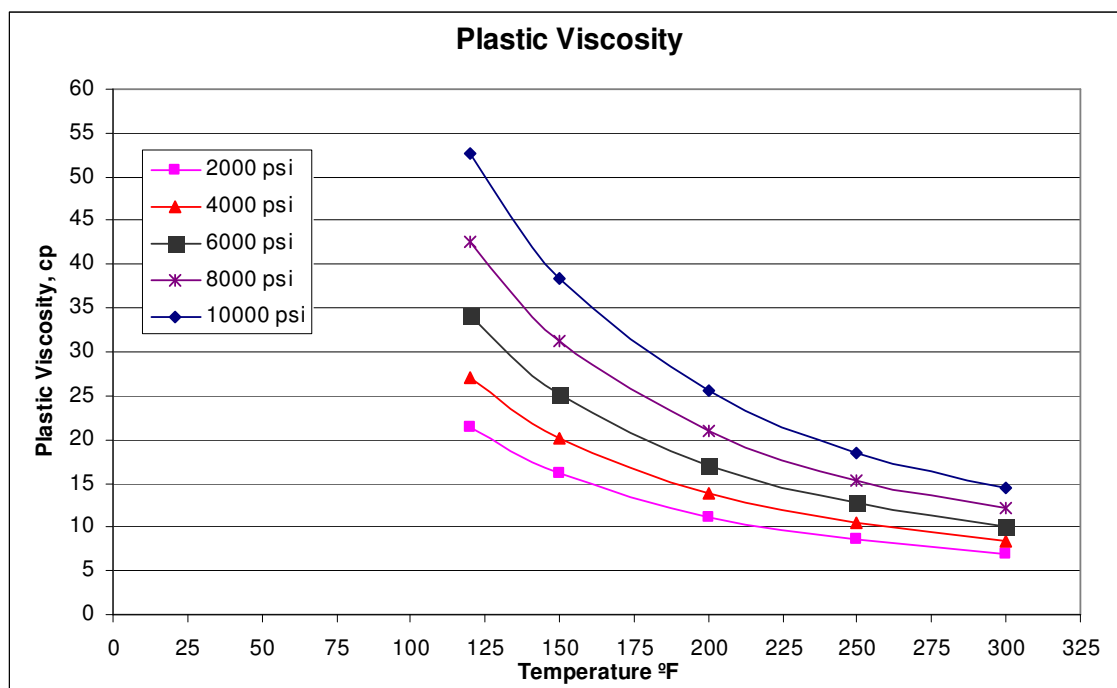


Fig. 3.4—Effect of pressure and temperature on plastic viscosity (from Bogotá Technical Center-Colombia[†]).

[†] Data provided by Ecopetrol, Bogotá- Colombia. 2005.

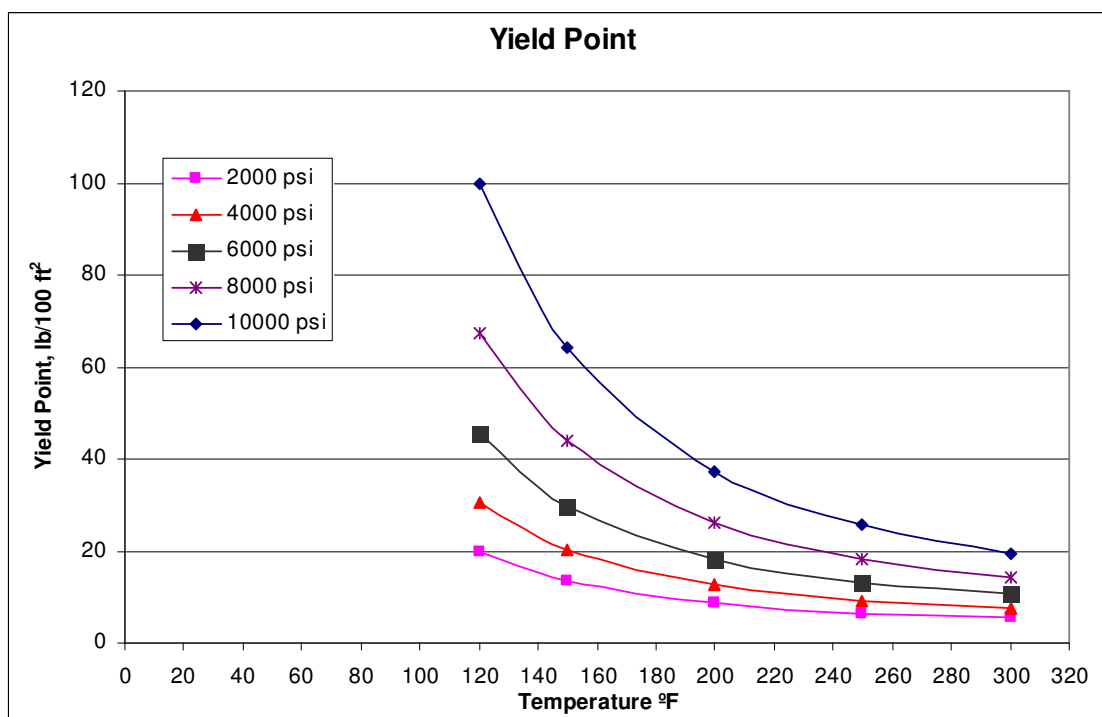


Fig. 3.5—Effect of pressure and temperature on yield point.
(from Bogotá Technical Center-Colombia[‡]).

In the deepwater environment, water temperatures easily reach 40 °F (5 °C) and below. This low-temperature environment effectively cools down the drilling fluid, significantly increasing fluid viscosity, which in turn impacts equivalent circulating densities. Narrow drilling margins (i.e., the window between fracture gradient and pore pressure) encountered in deepwater drilling operations often make such rheological increases intolerable, resulting in severe losses of SBM and thus significant increasing fluid cost and rig time. **Fig. 3.6** shows that for low circulation rates the temperature drops very rapidly and the fluid enters the wellbore almost at the same temperature to sea water profile.¹⁶

[‡] Data provided by Ecopetrol, Bogotá- Colombia. 2005.

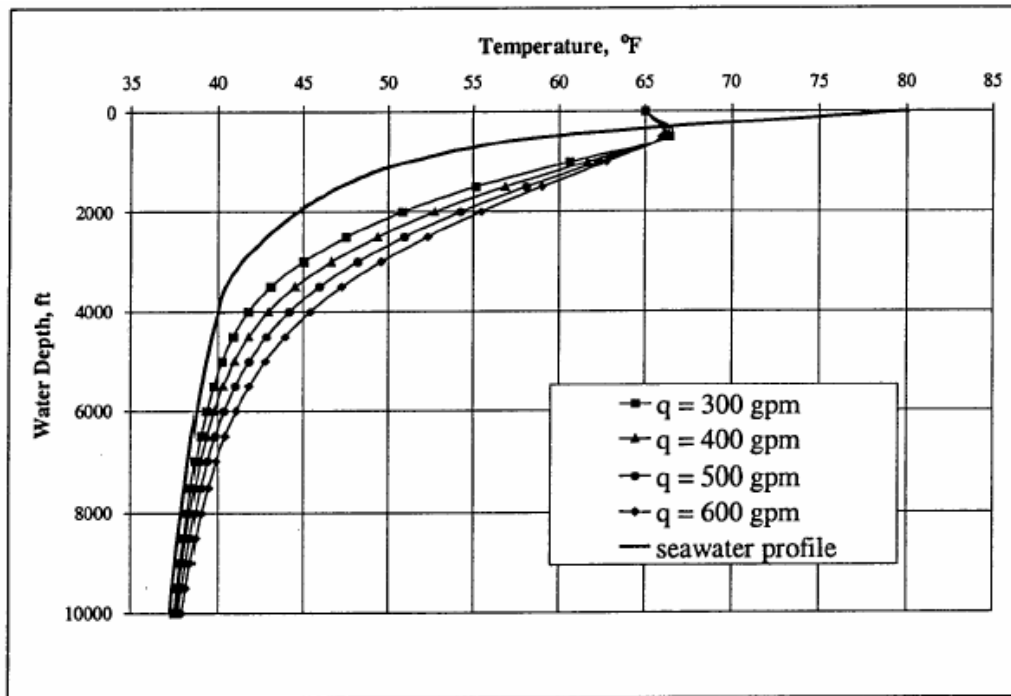


Fig. 3.6—Effect of mud flow-rate on the drillstring fluid temperature above seafloor (from Lima¹⁶).

Fig. 3.7 shows low-temperature PVT data taken on a Huxley-Bertram unit for an IO1618 fluid commonly used to formulate deepwater, SBMs.¹⁷

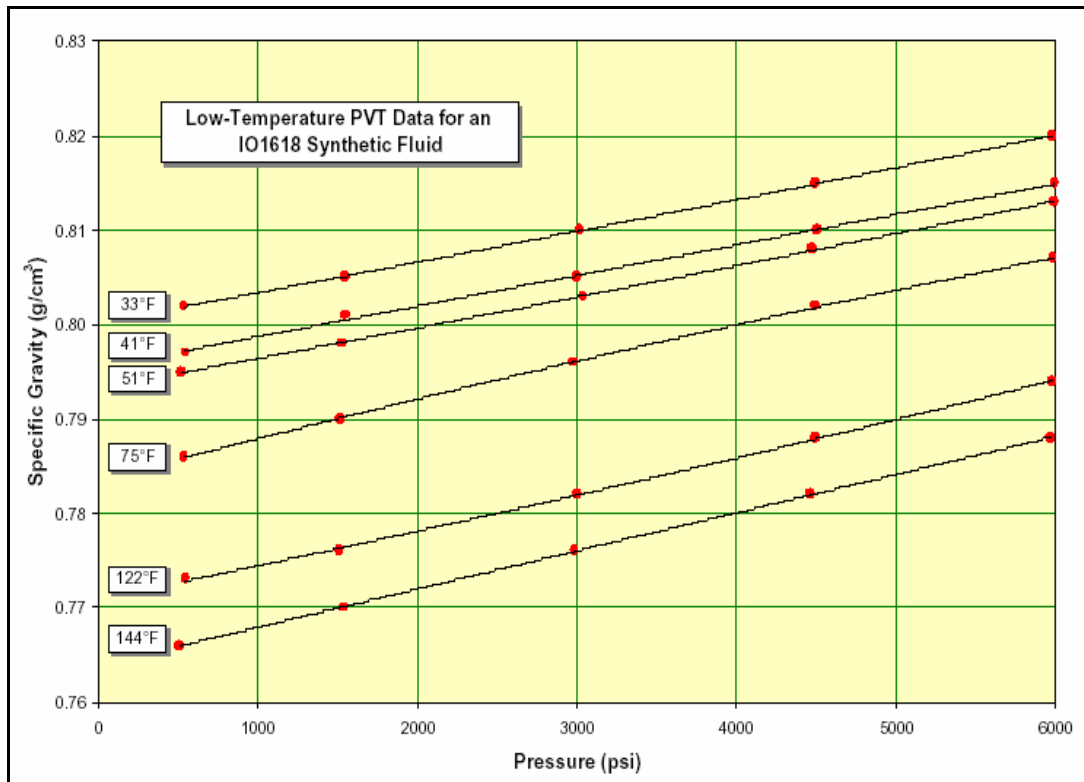
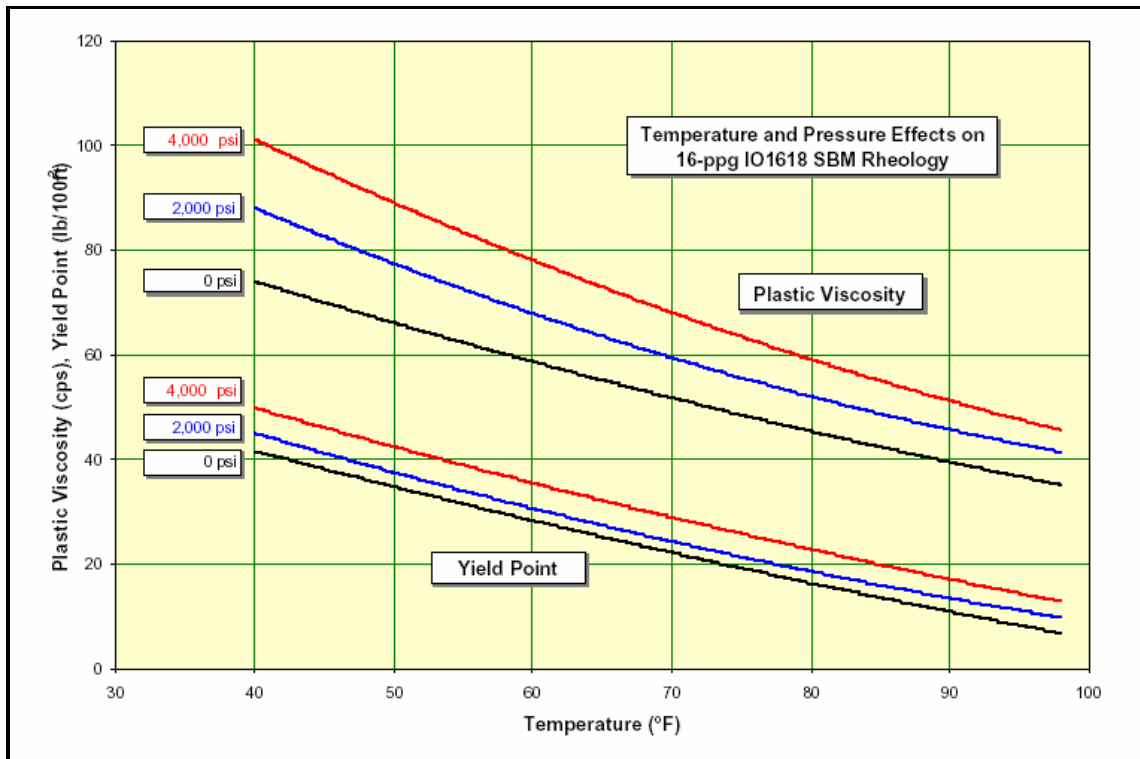


Fig. 3.7 - Low-temperature PVT data for an IO1618 synthetic fluid run on a Huxley-Bertram HTHP viscometer (from Zamora and Sanjit¹⁷).

Fig. 3.8 presents temperature and pressure effects on basic rheological parameters of a 16.0-lb/gal IO1618 SBM as measured on a Fann Model 75 viscometer.



3.8 – Low-temperature and pressure effects on PV and YP of a 16-lb/gal, 85:15 oil/water ratio IO1618 synthetic mud (from Zamora and Sanjit¹⁷).

The impact of cold temperatures experienced in deep water is clearly demonstrated in the last two figures. One consequence is that mud weights must be associated with the temperature at which they are measured. Another is that rheology on deepwater rigs is now routinely measured at three or more different temperatures and synchronized with Fann Model 70/75 viscometer tests run periodically in the lab.¹⁷

CHAPTER IV

ACCURATE PROCEDURE FOR SELECTING THE BEST RHEOLOGICAL MODELS

Most drilling fluids used today are dispersions. Many fluid properties depend on the system's rheology. The rheology of dispersions is complex, since they usually exhibit non-Newtonian behavior. Non-Newtonian fluids are those fluids that do not conform to a direct proportionality between shear stress and shear rate, and no single equation has been proved to describe exactly the rheogram of all such fluids.

Conventional rheological models in widespread use for the past half century in the oil industry include the Bingham plastic, Power-law, and Newtonian models. Of these, the Bingham plastic is advantageous because it includes a yield point that is a positive shear stress at zero shear rate, which most drilling fluids, cement slurries, and spaces have.¹⁸

More recently, the Herschel-Bulkley model has seen increased usage because it accommodates the existence of a yield point (Bingham plastic) as well as the nonlinearity of the relationship of shear stress to shear rate (Power-law).⁵

This study investigated seven major non-Newtonian rheological models to get more alternatives for selecting the best model that represents accurately the shear stress-shear rate relationship for a given non-Newtonian fluid. These models are the Bingham, Power-law, API RP 13D, Herschel-Bulkley, Unified, Robertson and Stiff, and Casson. To determine which rheological model best fit the behavior of the drilling fluid, we plotted the shear stress versus shear rate data of the drilling fluid.

We assumed that the model which gives the lowest absolute average percent error (E_{AAP}) between the measured and calculated shear stresses is the best one for a given non-Newtonian fluid.

Selection of the best model is of great importance in achieving correct results for pressure drop and hydraulics calculations.

4.1 Newtonian Model

A fluid that has a constant viscosity at all shear rates at a constant temperature and pressure is called a Newtonian fluid. Also, it can be described by a one-parameter rheological model. An equation describing a Newtonian fluid is given below:

$$\tau = \mu\gamma \dots\dots\dots(4.1)$$

When the shear stress (τ) of a Newtonian fluid is plotted against the shear rate (γ) in linear coordinates a straight line through the origin results. The Newtonian viscosity (μ) is the slope of this line.

Table 4.1 is an example to follow through this entire chapter.

Table 4.1—Data from Fann 70 (from White and Zamora⁹)

RPM	Reading
600	92
300	58
200	46
100	32
6	10
3	8

To transform the laboratory data units to field engineering units (**Table 4.2**), we have to apply conversion factors:

$$\gamma = 1.703 V, \dots\dots\dots (4.2)$$

$$\tau = 1.067 R. \dots\dots\dots (4.3)$$

Table 4.2—Shear Stress Measured in Field Units

γ (sec ⁻¹)	τ (lbf/100ft ²)
1021.8	98.164
510.9	61.886
340.6	49.082
170.3	34.144
10.22	10.67
5.11	8.536

Fig. 4.1 shows the Newtonian rheogram; from the equation of straight line we can estimate the slope, $\mu = 0.1066$ lbf.sec/100 ft². The straight line was obtained using linear regression techniques.

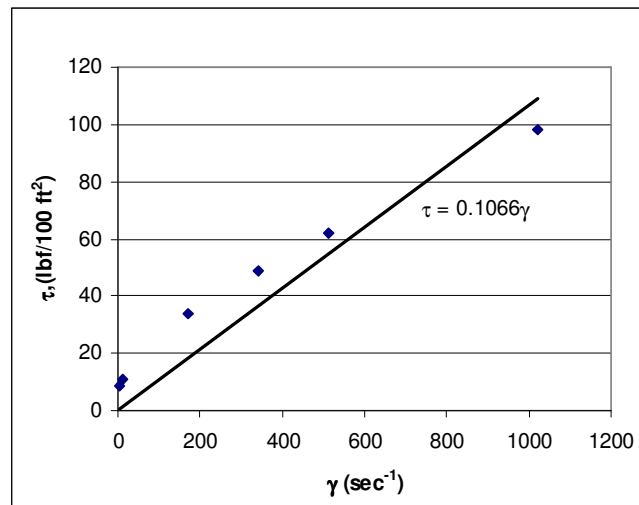


Fig. 4.1—Newtonian fluid rheogram.

To estimate viscosity in field units (cp) we have to convert by the following equation:

$$\mu = 47880m/100. \dots\dots\dots (4.4)$$

Our result is 51 cp.

Now, we can estimate the shear stresses as function of viscosity. **Table 4.3** shows the results

Table 4.3—Shear Stress Calculated as Function of Viscosity

$\gamma \text{ (sec}^{-1}\text{)}$	$\tau \text{ lbf/100ft}^2$
1021.8	108.92388
510.9	54.46194
340.6	36.30796
170.3	18.15398
10.218	1.0892388
5.109	0.5446194

To estimate the E_{AAP} , we used a statistical method. This method is used between the measured and calculated shear stresses:

$$E_{AAP} = \left[\left(\frac{1}{N} \right) \sum \left| \frac{(\tau_{\text{measured}} - \tau_{\text{calculated}})}{\tau_{\text{measured}}} \right| \right] \times 100. \dots\dots\dots (4.5)$$

Using this example, for the Newtonian model $E_{AAP} = 46.54\%$. **Fig. 4.2** shows a comparison between measured and calculated data.

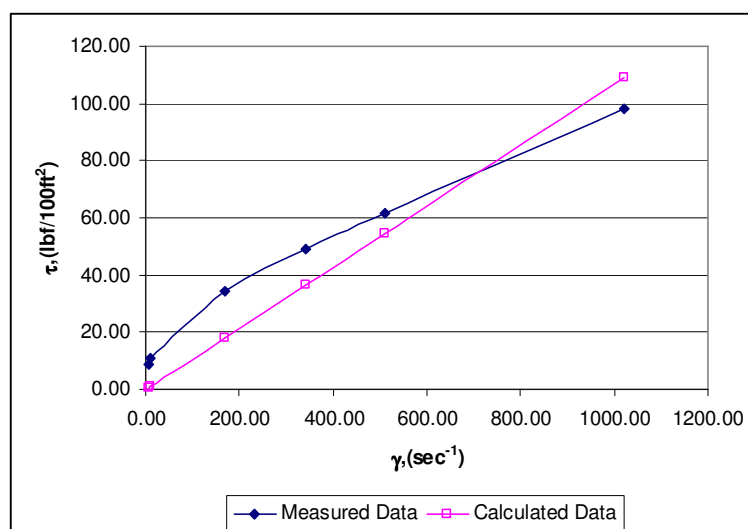


Fig. 4.2— Comparison between measured data and calculated data for Newtonian model.

Note that estimation of Newtonian viscosity can be made in an easier way by estimating the viscosity equal to the reading at 300 RPM, R_{300} .¹⁴

Then for our case, $\mu = 58$ cp. This equation is used for hydraulics calculations.

4.2 Bingham Plastic Model

The Bingham plastic model was the first two-parameter model that gained widespread acceptance in the drilling industry and is simple to visualize. However, it does not represent accurately the behavior of the drilling fluid at very low shear rates (in the annulus) or at very high shear rate (at the bit).¹⁹

$$\tau = \mu_p \gamma + \tau_y \quad (4.6)$$

The Bingham parameters, yield point (τ_y) and plastic viscosity (μ_p) can be read from a graph or can be calculated by the following equations,¹⁴

$$\mu_p = R_{600} - R_{300} \quad (4.7)$$

$$\tau_y = R_{300} - \mu_p \quad (4.8)$$

Let us consider the same data used in the Newtonian model to show the calculations for the Bingham plastic model. **Fig. 4.3** and **Table 4.4** show the results.

The straight line was obtained using linear regression techniques.

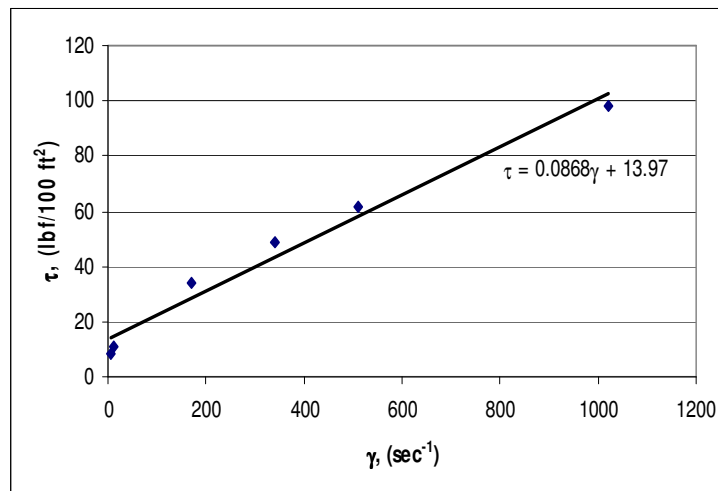


Fig. 4.3— Bingham plastic fluid rheogram.

To estimate viscosity in field units (cp), we have to convert with Eq. 4.4:

$$\mu_p = 0.0868 \times 47880 / 100 = 41.55 \text{ cp.}$$

$$\tau_y = 13.97 \text{ lbf}/100 \text{ ft}^2.$$

Using Eq. 4.7 and Eq. 4.8, we have¹⁴

$$\mu_p = 92 - 58 = 34 \text{ cp.}$$

$$\tau_y = 58 - 34 = 24 \text{ lbf}/100 \text{ ft}^2.$$

Note, we are considering the graph to estimate E_{AAP} and Eq. 4.7 and Eq. 4.8 for hydraulics.

Table 4.4—Shear Stress Calculated as Function of Plastic Viscosity and Yield Point

γ (sec ⁻¹)	τ lbf/100ft ²
1021.8	102.635866
510.9	58.30296813
340.6	43.5253355
170.3	28.74770289
10.218	14.85672822
5.109	14.41339924

Eq. 4.5 was used to estimate the absolute average percent error (E_{AAP}), which for this example, for the Bingham plastic model, is 24.26%. **Fig. 4.4** shows a comparison between measured and calculated data.

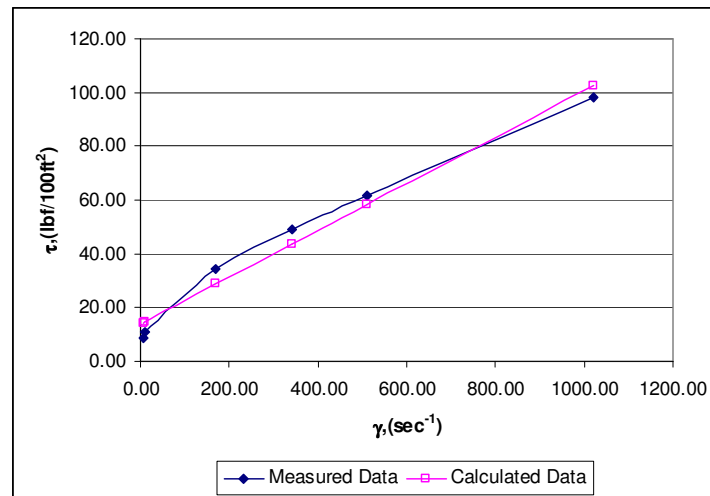


Fig. 4.4— Comparison between measured data and calculated data for Bingham plastic model.

Note that the yield strength, τ_0 , is the true shear stress at zero shear-rate and relates to the state of flocculation of the drilling fluid at rest. It is more representative of the structure formed at rest than the yield point value. And its value is usually approximated by measuring the shear stress at 3 RPM.

4.3 Power Law Model

The Bingham plastic model assumes a linear relationship between shear stress and shear rate. However, a better representation of the behavior of a drilling fluid is to consider a Power-law relationship between viscosity and shear rate such that:

$$\tau = k\dot{\gamma}^n, \dots\dots\dots (4.10)$$

where k is the consistence index and n is flow behavior index.

Eq. 4.10 was linearized as follows:

$$\log \tau = \log k + n \log \dot{\gamma}, \dots\dots\dots (4.11)$$

where n is determined from the slope and k is the intercept.

The Power-law model provides more information in the low-shear-rate condition but still has a weakness at high shear rates.¹⁹

Let us consider the data given in the Newtonian model to illustrate the calculations. The first step is to obtain a logarithmic graph shear rate and shear stress from Table 4.2.

Fig. 4.5 and **Table 4.5** show the results. The straight line was obtained using linear regression techniques (least-squares regression).

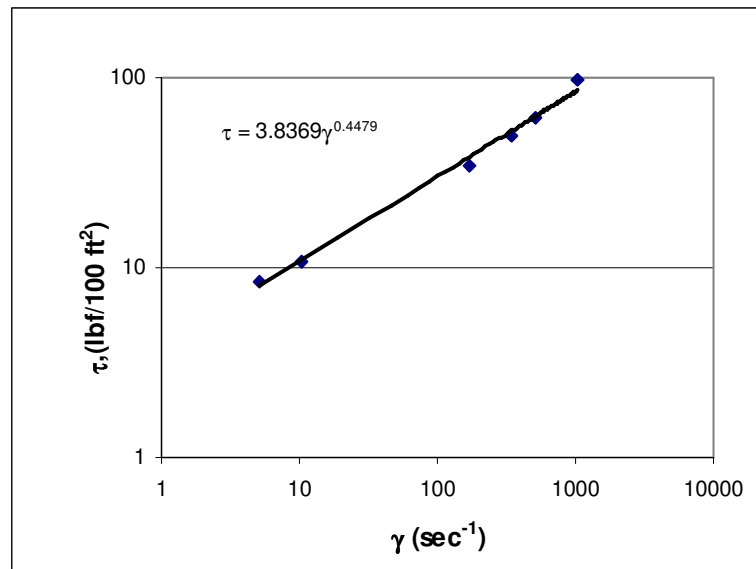


Fig. 4.5— Power-law fluid rheogram.

From **Fig. 4.5** the Power law parameters are:

$$n = 0.4479$$

$$k = 3.8369 \text{ lbf} \cdot \text{sec}^n / 100 \text{ ft}^2$$

Table 4.5—Shear Stress Calculated as Function of Power Law Parameters

γ (sec ⁻¹)	τ lbf/100ft ²
1021.8	85.455419
510.9	62.65009346
340.6	52.24663401
170.3	38.30367391
10.218	10.86498097
5.109	7.965464115

One of the obvious disadvantages of the Power law is that it fails to describe the low-shear-rate region. Since n is usually less than one, at low shear rate μ goes to infinity (only as $\dot{\gamma} \rightarrow 0$) rather than to a constant, as usually observed experimentally. Viscosities also become Newtonian at high shear rates for many suspensions and dilute polymer solutions.¹³

Using Eq. 4.5, $E_{AAP} = 6.88\%$. **Fig. 4.6** shows a comparison between measured and calculated data.

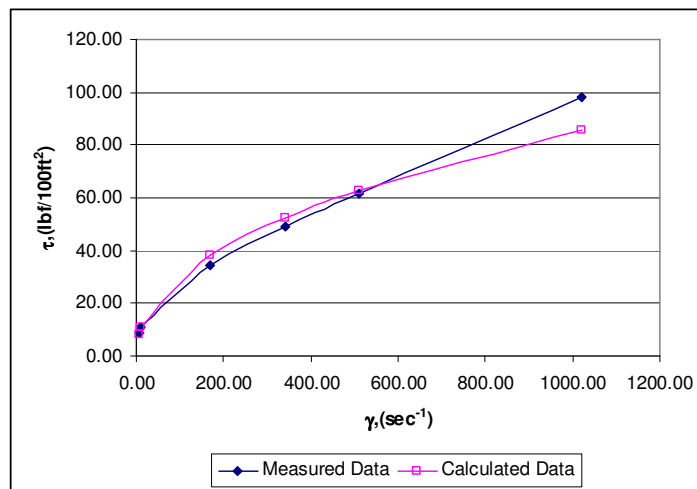


Fig. 4.6— Comparison between measured data and calculated data for Power law model.

Note that the estimations of Power-law parameters can be made by the following equations¹⁴:

$$n = 3.32 \log \left(\frac{R_{600}}{R_{300}} \right), \dots\dots\dots (4.12)$$

$$k = 510 R_{600} / 511^n. \dots\dots\dots (4.13)$$

Then for our case, $n = 0.6652$ and $k = 467.06 \text{ dyne}\cdot\text{sec}^n/100\text{cm}^2$. These equations to estimate Power law parameters are used for hydraulics calculation in Chapter V.

4.4 API Model (RP 13D)

API published their API RP 13D¹ in 1995. In this publication, the API recommends using a modified Power-law model to calculate pressure losses in pipes and annuli. For a Power-law model, the apparent viscosity decreases with increasing shear rate (Eq. 4.10).

The API Power law tries to match shear rates from the viscometer with shear rates actually experienced inside the drillpipe and annulus. Inside the drillpipe, 600 and 300 RPM readings are used for rheology and pressure loss calculations.

- Pipe Flow

$$n_p = 3.32 \log \left(\frac{R_{600}}{R_{300}} \right) \dots\dots\dots (4.14)$$

$$k_p = \frac{5.11 R_{600}}{1,022^{n_p}} \dots\dots\dots (4.15)$$

Inside the annulus, 3 and 100 RPM readings are used for rheology and pressure- loss calculations.

- Annulus Flow:

$$n_a = 0.657 \log \left(\frac{R_{100}}{R_3} \right) \dots\dots\dots (4.16)$$

$$k_a = \frac{5.11 R_{100}}{170.2^{n_a}} \dots\dots\dots (4.17)$$

As shown, RP 13D is based on a “dual Power law,” the lower shear rate segment for the annulus and the upper segment for inside the drillstring. Fig. 4.7 and Table 4.6 show the results. The straight lines were obtained using linear regression techniques.

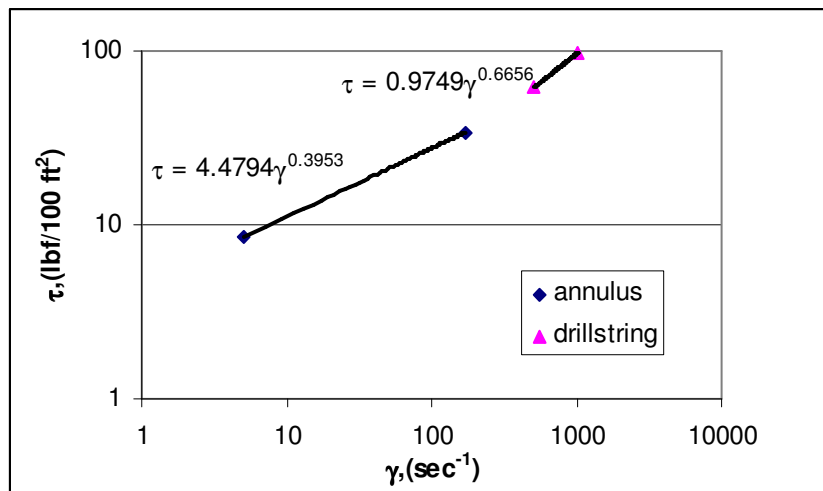


Fig. 4.7— API “dual power law” fluid rheogram.

From **Fig. 4.7** the API parameters are:

$$n_p = 0.6656.$$

$$n_a = 0.3953.$$

$$k_p = 0.9749 \text{ lbf} \cdot \text{sec}^n / 100 \text{ ft}^2.$$

$$k_a = 4.4794 \text{ lbf} \cdot \text{sec}^n / 100 \text{ ft}^2.$$

From Eq. 4.14 to Eq. 4.17,

$$n_p = 3.32 \log(92/58) = 0.66519465$$

$$n_a = 0.657 \log(32/8) = 0.395553$$

$$k_p = 5.11 (92/1022^{0.6652}) = 4.6808 \text{ dyne} \cdot \text{sec}^n / \text{cm}^2$$

$$k_a = 5.11 (32/170.2^{0.3956}) = 21.4291 \text{ dyne} \cdot \text{sec}^n / \text{cm}^2$$

Table 4.6—Shear Stress Calculated as Function of API Parameters

γ (sec ⁻¹)	τ lbf/100ft ²
1021.8	98.17344076
510.9	61.89113501
340.6	47.2522078
170.3	34.17388941
10.218	11.22874048
5.109	8.535787172

Using Eq. 4.5, $E_{AAP} = 1.51\%$. **Fig. 4.8** shows a comparison between measured and calculated data.

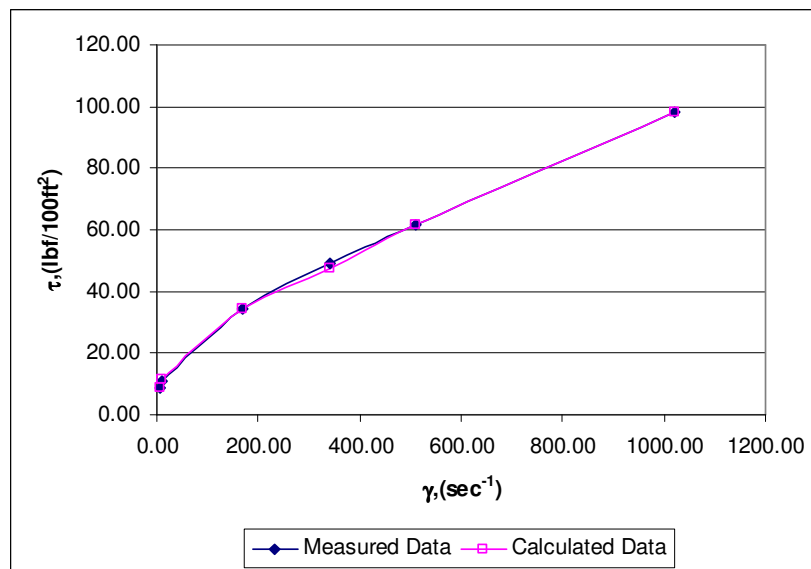


Fig. 4.8— Comparison between measured data and calculated data for API model.

This is a good choice for pressure loss calculations. The approach technically is a “generalized correlation” for which explicit laminar flow solutions are both available and straightforward. However, this approach does not consider a yield stress term that has become central to evaluating and optimizing hole cleaning, barite sag, suspension, and other key drilling concerns.¹⁸

4.5 Herschel-Bulkley

The Herschel-Bulkley model defines a fluid by three-parameter and can be described mathematically as follows:

$$\tau = \tau_0 + k\dot{\gamma}^n \quad \dots\dots\dots(4.18)$$

$$\log(\tau - \tau_0) = \log(k) + n \log(\dot{\gamma}) \quad \dots\dots\dots(4.19)$$

For $\tau < \tau_0$ the material remains rigid. For $\tau > \tau_0$, the material flows as a Power-law fluid.

The Herschel-Bulkley equation is preferred to Power-law or Bingham relationships because it results in more accurate models of rheological behavior when adequate experimental data are available. The yield stress is normally taken as the 3 RPM reading. However, we are taking Versan and Tolga's²⁰ approach to obtain τ_0 . Then n and k values can be calculated from the 600 and 300 RPM values or graphically. The Power-law model described above is valid for fluids for which the shear stress is zero when the strain rate is zero.

The Herschel-Bulkley model is commonly used to describe materials such as concrete, mud, dough, and toothpaste, for which a constant viscosity after a critical shear stress is a reasonable assumption when a log-log graph is made. In addition to the transition behavior between a flow and no-flow regime, the Herschel-Bulkley model can also exhibit a shear-thinning or shear thickening behavior depending on the value of n .

Since this is a three-parameter model, an initial calculation of τ_0 is required for other parameter calculations. τ_0 is calculated by Versan and Tolga²⁰.

$$\tau_0 = \frac{\tau^{*2} - \tau_{\min} \times \tau_{\max}}{2 \times \tau^* - \tau_{\min} - \tau_{\max}}, \quad \dots\dots\dots(4.20)$$

where τ^* is the shear stress value corresponding to the geometric mean of the shear rate, γ^* .

$$\gamma^* = \sqrt{\gamma_{\min} \gamma_{\max}} \cdot \dots\dots\dots(4.21)$$

From Eq. 4.21, $\gamma^* = 72.25 \text{ sec}^{-1}$. Then using this value we can interpolate between values of shear stress in Table 4.2,

$$\tau^* = 19.77 \text{ lbf}/100\text{ft}^2.$$

Finally, from Eq. 4.20: $\tau_0 = 6.66 \text{ lbf}/100\text{ft}^2$.

Fig. 4.9 and **Table 4.7** show the results. The straight line was obtained using linear regression techniques.

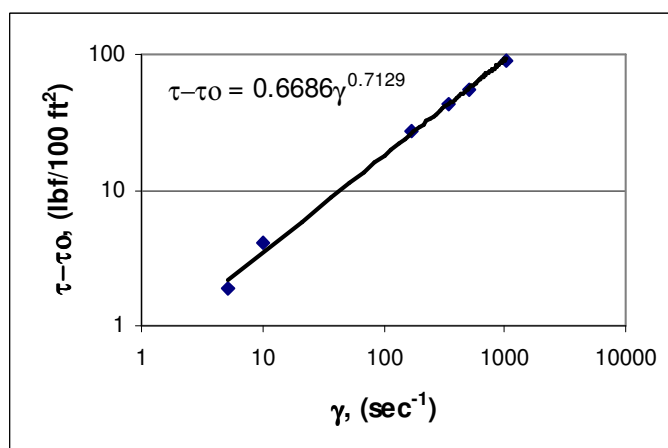


Fig. 4.9— Herschel-Bulkley fluid rheogram.

From **Fig. 4.9** the Herschel-Bulkley parameters are:

$$n = 0.7129.$$

$$k = 0.6686 \text{ lbf} \cdot \text{sec}^n / 100 \text{ft}^2$$

Table 4.7—Shear Stress Calculated as Function of Herschel-Bulkley Parameters

$\gamma \text{ (sec}^{-1}\text{)}$	$\tau \text{ lbf/100ft}^2$
1021.8	100.0862
510.9	63.6589
340.6	49.3504
170.3	32.7048
10.218	10.1635
5.109	8.7968

Using Eq. 4.5, $E_{AAP} = 2.90\%$. **Fig. 4.10** shows a comparison between measured and calculated data.

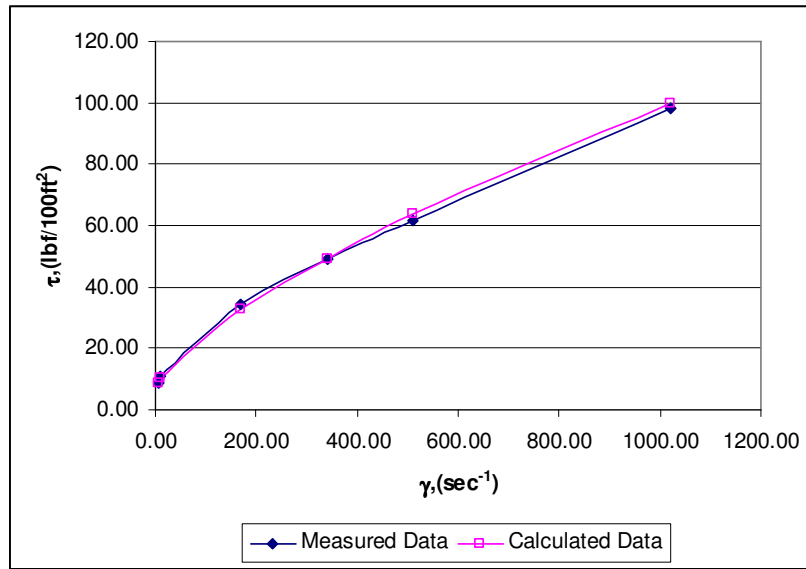


Fig. 4.10— Comparison between measured data and calculated data for Herschel-Bulkley model.

4.6 Unified Model

The Unified model² is an improved version of a simplified Herschel-Bulkley model established by the drilling industry years ago. See Eq. 4.18 and Eq. 4.19. The calculations of rheological parameters for the Unified model n and k involve previous estimation of plastic viscosity (μ_p), yield point (τ_y), and yield stress (τ_0).

See Eq. 4.7 and Eq. 4.8 for estimation of plastic viscosity and yield point respectively.

To estimate τ_0 for the Unified model, Zamora and Power² give the following alternative: Take low shear yield point (τ_{yL}) as τ_0 . This is calculated from Eq. 4.22.

$$\tau_{yL} = (2R_3 - R_6)1.066, \dots\dots\dots(4.22)$$

where τ_{yL} is lower shear yield point.

For the example that we have been following:

$$\tau_{yL} = (2 \times 8 - 10) \times 1.066 = 6.396 \text{ lbf}/100\text{ft}^2.$$

The equations proposed for this model to estimate n_p and n_a , and k_p and k_a are the following:

- Pipe Flow

$$n_p = 3.32 \log \left(\frac{2\mu_p + \tau_y}{\mu_p + \tau_y} \right) \dots\dots\dots (4.23)$$

$$k_p = 1.066 \left(\frac{\mu_p + \tau_y}{511^{n_p}} \right) \dots\dots\dots (4.24)$$

- Annular Flow

$$n_a = 3.32 \log \left(\frac{2\mu_p + \tau_y - \tau_o}{\mu_p + \tau_y - \tau_o} \right) \dots\dots\dots (4.25)$$

$$k_a = 1.066 \left(\frac{\mu_p + \tau_y - \tau_o}{511^{n_a}} \right) \dots\dots\dots (4.26)$$

Now, let estimate n and k for the example that we have been following:

- Pipe Flow

$$n_p = 3.32 \log \left(\frac{2 \times 34 + 24}{34 + 24} \right) = 0.665.$$

$$k_p = 1.066 \left(\frac{34 + 24}{511^{0.665}} \right) = 0.971 \text{ lbf} \cdot \text{sec}^n / 100\text{ft}^2.$$

- Annular Flow

$$n_a = 3.32 \log \left(\frac{2 \times 34 + 24 - 6.396}{34 + 24 - 6.396} \right) = 0.73.$$

$$k_a = 1.066 \left(\frac{34 + 24 - 6.396}{511^{0.73}} \right) = 0.577 \text{ lbf} \cdot \text{sec}^n / 100\text{ft}^2.$$

The ratio τ_0/τ_y is another parameter which is a useful tool to help characterize fluids rheologically, although it is not necessary for solving the model. Some fluids may exhibit more plastic behavior in one part of the well and more pseudoplastic behavior in another. This is important for hole cleaning and barite sag considerations.

As the ratio τ_0/τ_y approaches 1, ($\tau_0 \rightarrow \tau_y$), fluids take on Bingham plastic behavior. For τ_0/τ_y approaching 0, ($\tau_0 \rightarrow 0$), they behave more like pseudoplastic (Power-law) fluids.

For our example:

$$\tau_0/\tau_y = 6.4/24 = 0.27$$

Clearly, the fluid behaves more like a pseudoplastic.

Table 4.8 shows the result of shear stress calculation using the parameter estimated above.

Table 4.8—Shear Stress Calculated as Function of Unified Model Parameters

γ (sec ⁻¹)	τ lbf/100ft ²
1021.8	97.48
510.9	61.47
340.6	46.94
170.3	30.93
10.218	9.55
5.109	8.30

Using Eq. 4.5, $E_{AAP}=4.74\%$. **Fig. 4.11** shows a comparison between measured and calculated data.

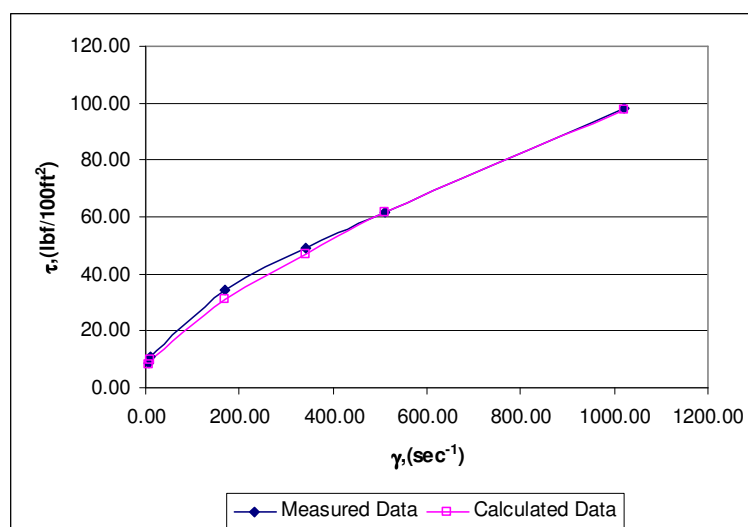


Fig. 4.11— Comparison between measured data and calculated data for Unified model.

4.7 Robertson and Stiff Model

Robertson and Stiff²¹ developed a more general model to describe the rheological behavior of drilling fluids and cement slurries. The basic equation is:

$$\tau = A (\dot{\gamma} + C)^B, \dots\dots\dots(4.27)$$

where A , B , and C are model parameters. A and B can be considered similar to the parameters k and n of the Power-law model. The third parameter C is a correction factor to the shear rate, and the term $(\dot{\gamma} + C)$ is considered effective shear rate.

Eq. 4.28 represents the yield stress for the Robertson and Stiff model.

$$\tau_0 = AC^B. \dots\dots\dots(4.28)$$

Despite the fact that some investigators²² have meticulously shown that the Robertson and Stiff model is superior to Bingham and Power-law models, it has

found little relevance in the drilling industry because of the relative complexity in evaluating the three parameters, A , B and C .

The major advantage of the model over the Power-law and Bingham plastic models is the superior fit of rheological stress/rate of strain data.²¹

To evaluate the parameters,²² we plotted the shear stress corresponding to several shear rates. The logarithm from Eq. 4.27 plots a straight line on log-log coordinates:

$$\log(\tau) = \log(A) + B \log(\dot{\gamma} + C) \quad \dots\dots\dots(4.29)$$

Thus, if τ is plotted vs. $(\dot{\gamma} + C)$ on log-log coordinates, B is the slope and A is the intercept where $(\dot{\gamma} + C) = 1.0$.

$$C = (\dot{\gamma}_{\min} \dot{\gamma}_{\max} - \dot{\gamma}^{*2}) / (2\dot{\gamma}^* - \dot{\gamma}_{\min} - \dot{\gamma}_{\max}), \quad \dots\dots\dots(4.30)$$

where $\dot{\gamma}^*$ is the shear rate value corresponding to the geometric mean of the shear stress, τ^* .

The geometric mean of the shear stress (τ^*) is then calculated from:

$$\tau^* = (\tau_{\min} \times \tau_{\max})^{1/2} \quad \dots\dots\dots(4.30)$$

From Eq. 4.30, $\tau^* = 28.95$ lbf/100ft². Then with this value we can interpolate between the values of shear rates in **Table 4.2**, $\dot{\gamma}^* = 134.86$ 1/sec^B.

Finally, from Eq. 4.30, $C = 17.12$ 1/sec^B.

The **Fig. 4.12** shows the results. The straight line was obtained by using linear regression techniques.

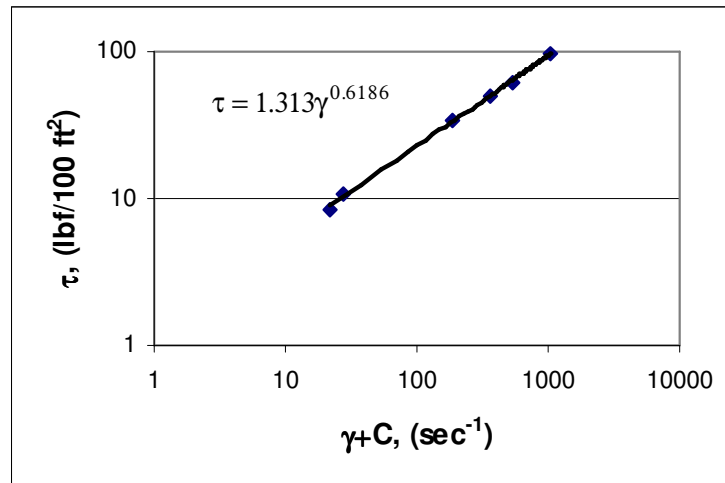


Fig. 4.12— Robertson and Stiff fluid rheogram.

From Fig. 4.12 the Robertson and Stiff parameters are:

$$A = 1.31297551 \text{ lbf} \cdot \text{sec}^B / 100 \text{ ft}^2.$$

$$B = 0.618576471.$$

Table 4.9 shows the result of shear-stress calculation using the parameter estimated above.

Table 4.9—Shear Stress Calculated as Function of Robertson and Stiff Parameters

γ (sec ⁻¹)	τ lbf/100ft ²
1021.8	96.4372
510.9	63.4492
340.6	49.8680
170.3	33.4329
10.218	10.1637
5.109	8.9430

Using Eq. 4.5, $E_{AAP}=2.9137\%$. **Fig. 4.13** shows a comparison between measured and calculated data.

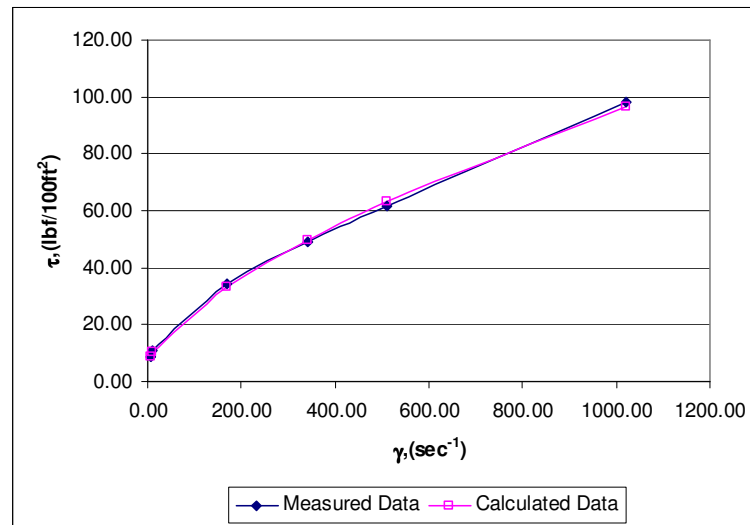


Fig. 4.13— Comparison between measured data and calculated data for Robertson and Stiff model.

4.8 Casson Model

Casson's 1959 model described the flow of viscoelastic fluids. This model has a more gradual transition from Newtonian to the yield region. For many materials, such as blood and food products, it provides a better fit. Note that values of the parameters for the Casson model also depend on the range of shear rates considered.¹³

This model is used by petroleum engineers in the characterization of cement slurry and is better for predicting high shear-rate viscosities when only low and intermediate shear-rate data are available. The Casson model is more accurate at both very high and very low shear rate.¹⁹

The Casson model has been used in other industries to give a more accurate representation of high shear rate viscosities when only low and intermediate shear-rate data are available. Thus, this model will improve our ability to predict viscosities at the bit.¹⁹

Casson considered rigid primary particles aggregating into long rods. Under shear, the rod length progressively decreases until at very high shear rate, the rod is completely broken down into primary particles.¹⁹

The empirical equation for the 1D form of the Casson model is given by¹³

$$\gamma = 0 \quad \text{For } \tau < \tau_c. \quad \dots\dots\dots(4.31)$$

$$\tau^{\frac{1}{2}} = \tau_c^{\frac{1}{2}} + \mu_c^{\frac{1}{2}} \gamma^{\frac{1}{2}} \quad \text{For } \tau \geq \tau_c, \quad \dots\dots\dots(4.32)$$

where τ_c is the Casson yield stress and μ_c is the Casson plastic viscosity.

Table 4.10 shows the values of shear rates and shear stresses needed to build **Fig. 4.14**.

Table 4.10—Square Roots of Variables Used to Graph Fig. 4.14

γ (sec ⁻¹)	τ (lbf/100ft ²)
1021.8	101.1646
510.9	61.7832
340.6	47.4246
170.3	31.5577
10.218	10.9202
5.109	9.5159

The straight line in **Fig. 4.14** was obtained by linear regression techniques.

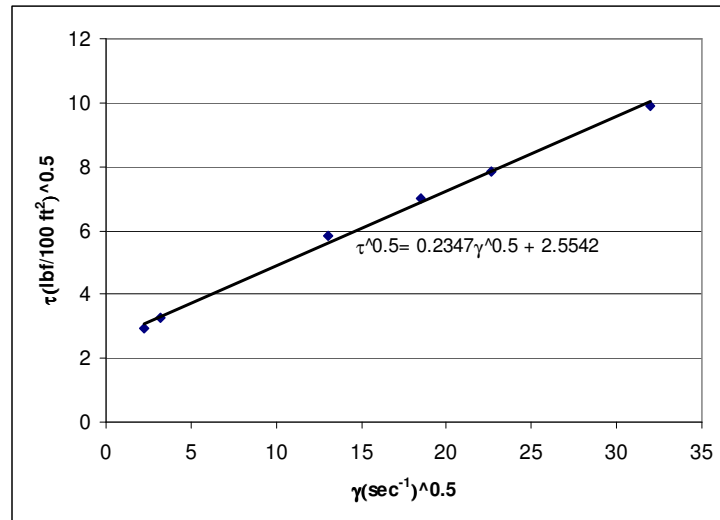


Fig. 4.14— Casson fluid rheogram.

Then we can obtain from **Fig. 4.14** the Casson model parameters:

$$\tau_c^{0.5} = 2.554 \text{ lbf}/100 \text{ ft}^2,$$

$$\mu_c^{0.5} = 0.2347 \text{ lbf}\cdot\text{sec}/100 \text{ ft}^2,$$

or

$$\tau_c = 6.5238 \text{ lbf}/100 \text{ ft}^2.$$

and

$$\mu_c = 0.0551 \text{ lbf}\cdot\text{sec}/100 \text{ ft}^2.$$

Table 4.11 shows the result of shear-stress calculation using the parameters estimated above.

Table 4.11—Shear Stress Calculated as Function of Casson Model
Parameters

γ (sec ⁻¹)	τ lbf/100ft ²
1021.8	101.1646
510.9	61.7832
340.6	47.4246
170.3	31.5577
10.218	10.9202
5.109	9.5159

Using Eq. 4.5, $E_{AAP} = 4.66\%$. **Fig. 4.15** shows a comparison between measured and calculated data.

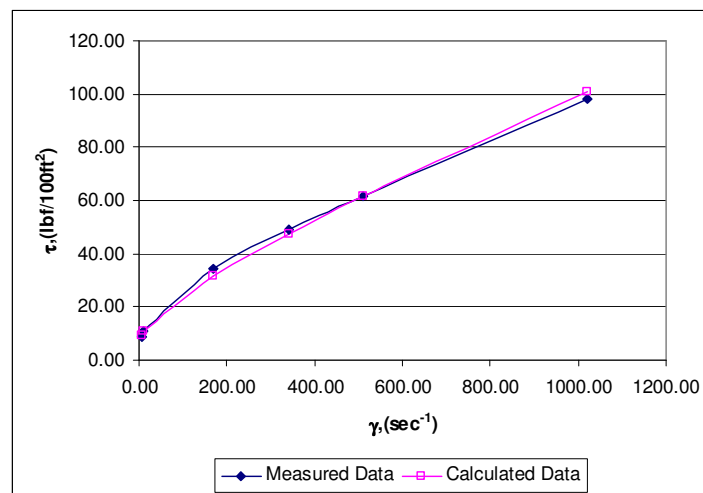


Fig. 4.15— Comparison between measured data and calculated data for Casson model.

CHAPTER V

HYDRAULICS

Conventional calculations of downhole pressure, which assume constant drilling fluid properties, are both practical and accurate enough for routine wells. Downhole static pressures are easy to calculate from mud weight measured at the surface, while additional pressures caused by circulation can be calculated using established relationships between pump rate and drilling fluid rheological properties.²³

Errors that result from ignoring variations in mud properties are small in relatively shallow wells. In these settings, mud engineers can concentrate on formulating drilling fluid properties for maximum rates of penetration and optimal hole conditions. Formations can commonly withstand moderate overpressure before being fractured, which permits mud engineers to add a comfortable safety margin when weighting the mud.²³

On the other hand, in high pressure and high temperature (HPHT), extended reach, and deepwater wells as established before, mud properties do vary with downhole pressure and temperature, affecting the accuracy of both surface measurements and downhole estimations of mud weight and viscosity. In these wells these variations can be significant because of the limited safety margins available.²³

Clearly the ability to predict these effects is critical to the successful drilling of HPHT, extended reach, and deepwater wells. Small but serious errors in computing the drilling fluid pressure at the reservoir may result from ignoring uncertainties in either temperature or fluid properties. Simulation of downhole

temperature profiles at all phases of the drilling operation is therefore the key to understanding the behavior of drilling fluids.²⁴

Equivalent circulating density (ECD) is often much higher than equivalent mud weight (EMW) in HPHT, extended reach, and deepwater wells due to the small annular clearances between the drillpipe and hole wall. ECD is computed from the dimensions of the annulus and, for a given fluid viscosity, increases with pump rate. The calculation becomes increasingly complicated when changes of viscosity with temperature are considered.²³

5.1 Frictional Pressure Loss Calculation

During circulating of drilling fluid, friction between the drilling fluid and the wall of the drill pipe and annulus cause pressure loss.¹⁴ Actually, the pump pressure, Δp_p , is affected by:

1. Frictional pressure losses (Δp_s) in the surface equipment such as Kelly, swivel, standpipe.
2. Frictional pressure losses (Δp_{ds}) inside the drillstring (drillpipe, Δp_{dp} and drill collar, Δp_{dc}).
3. Frictional pressure losses across the bit, Δp_b .
4. Frictional pressure losses in the annulus around the drillstring, Δp_a .

The mathematical expression for this is as given:

$$\Delta p_p = \Delta p_s + \Delta p_{ds} + \Delta p_b + \Delta p_a. \dots\dots\dots(5.1)$$

Error in Δp_p is a combination of errors in the four elements. In general, frictional pressure losses across the bit, Δp_b , and the surface pipe system can be evaluated fairly accurately.

Error in Δp_p consists primarily of errors from friction pressure losses in the drillstring and annulus. The drillstring pressure losses represent the largest component of error in the pump pressure.

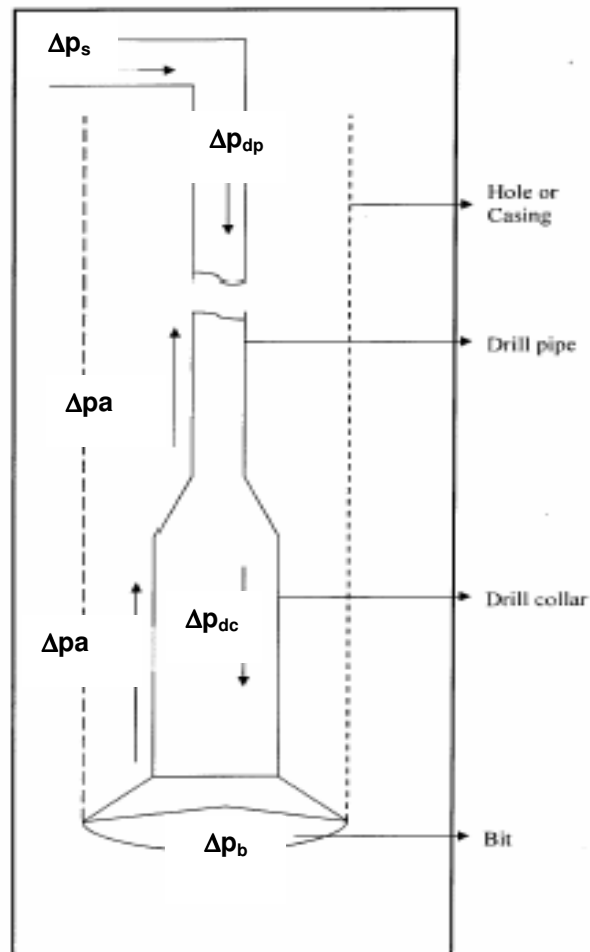


Fig. 5.1— Diagram of the drilling fluid circulating system (from Mojisola²⁵).

Frictional pressure loss is a function of several factors such as rheology behavior of the drilling fluid (Newtonian or non-Newtonian), flow regime of the drilling fluid (laminar, turbulent, or intermediate flow), drilling fluid properties

(density and viscosity), flow rate of the drilling fluid (q), drillstring configuration and wellbore geometry. See **Fig. 5.1**

When the best-fit rheological model has been chosen and the fluid rheological properties have been determined as shown in Chapter IV, the flow regime can then be determined by calculating the Reynolds number (N_{Re}) at a particular fluid flow rate using the appropriate equations.

The calculated value of N_{Re} is compared to a critical value N_{Rec} to decide if the flow is laminar or turbulent. The next step is to calculate the friction factor, f . This factor is a function of the fluid rheological properties, pipe roughness, and the Reynolds number for some model.

Once the friction factor has been determined, the frictional pressure loss can be calculated using the appropriate equation from each rheological model. This chapter shows how this procedure works with each rheological model.

Appendix A shows the rheological and hydraulic equations for eight models. Appendix B also shows a numerical example for each rheological model to illustrate the pump pressure calculation.

5.1.1 Frictional Pressure Loss Calculation for Newtonian Fluid

- Pipe flow¹⁴

a. Pipe velocity:

$$v_p = \frac{0.408q}{D_p^2} \dots\dots\dots(5.2)$$

b. Reynolds number:

$$N_{Re} = \frac{928D_p v_p \rho}{\mu_a} \dots\dots\dots(5.3)$$

c. Critical Reynolds number value, $N_{Rec} = 2100$.

d. Regime flow determination,

Comparison between N_{Re} and N_{Rec}

If $N_{Re} < N_{Rec} \rightarrow$ flow is laminar.

$$f = 16 / N_{Re}. \quad (5.4)$$

If $N_{Re} > N_{Rec} \rightarrow$ flow is turbulent.

$$f = 0.0791 / N_{Re}^{0.25}. \quad (5.5)$$

e. Frictional pressure loss calculation inside drillstring:

$$\left(\frac{dp}{dL} \right) = \frac{fv_p^2 \rho}{25.81 D_p}. \quad (5.6)$$

$$\Delta p_{ds} = \left(\frac{dp}{dL} \right) \Delta L, \quad (5.7)$$

where (dp/dL) is the pressure gradient, psi/ft.

- Annular Flow

a. Annular velocity:

$$v_a = \frac{0.408q}{(D_2^2 - D_1^2)}. \quad (5.8)$$

b. Reynolds number:

$$N_{Re} = \frac{757(D_2 - D_1)v_a \rho}{\mu_a}. \quad (5.9)$$

c. Critical Reynolds Number value, $N_{Rec} = 2100$.

d. Regime flow determination:

Comparison between N_{Re} and N_{Rec}

If $N_{Re} < N_{Rec} \rightarrow$ flow is laminar.

$$f = 16 / N_{Re}. \quad (5.4)$$

If $N_{Re} > N_{Rec} \rightarrow$ flow is turbulent.

$$f = 0.0791 / N_{Re}^{0.25}. \quad (5.5)$$

e. Frictional pressure loss calculation in the annulus:

$$\left(\frac{dp}{dL}\right) = \frac{fv_a^2 \rho}{25.81(D_2 - D_1)} \cdot \dots\dots\dots(5.10)$$

$$\Delta p_a = \left(\frac{dp}{dL}\right) \Delta L \cdot \dots\dots\dots(5.11)$$

- Frictional pressure losses across the bit, Δp_b :

$$\Delta p_b = \frac{156 \rho q^2}{(D_{N1}^2 + D_{N2}^2 + D_{N3}^2)^2} \cdot \dots\dots\dots(5.12)$$

where D_{N1} , D_{N2} , D_{N3} are diameters of the three nozzles.

5.1.2 Frictional Pressure Loss Calculation for Bingham Plastic Fluid

To calculate velocity, Reynolds numbers, critical Reynolds number value, regime flow, and frictional pressure losses, follow the procedure outlined in Section 5.1.1 (annulus and pipe).¹⁴ Note: Use the apparent viscosity estimate for this model from Eqs. 5.13 and 5.14. Use Eqs. 4.7 and 4.8 to estimate plastic viscosity and yield point.

- Pipe Flow

$$\mu_a = \mu_p + \frac{5\tau_y D_p}{v_p} \cdot \dots\dots\dots(5.13)$$

- Annular Flow

$$\mu_a = \mu_p + \frac{5\tau_y (D_2 - D_1)}{v_a} \cdot \dots\dots\dots(5.14)$$

Another way to determine the flow is using the Hedstrom number, N_{He} , to estimate the critical Reynolds number from **Fig. 5.2**. Also, we have to work with plastic viscosity to calculate the Reynolds number. Finally, we have to compare Eqs. 5.14 and 5.15.

$$N_{He} = \frac{37100 \rho \tau_y D_p^2}{\mu_p^2} \dots\dots\dots(5.15)$$

$$N_{Re} = \frac{928 D_p v_p \rho}{\mu_p} \dots\dots\dots(5.16)$$

If $N_{Re} < N_{Rec} \rightarrow$ flow is laminar.

If $N_{Re} > N_{Rec} \rightarrow$ flow is turbulent.

Note that we also can use this second technique with the annulus.

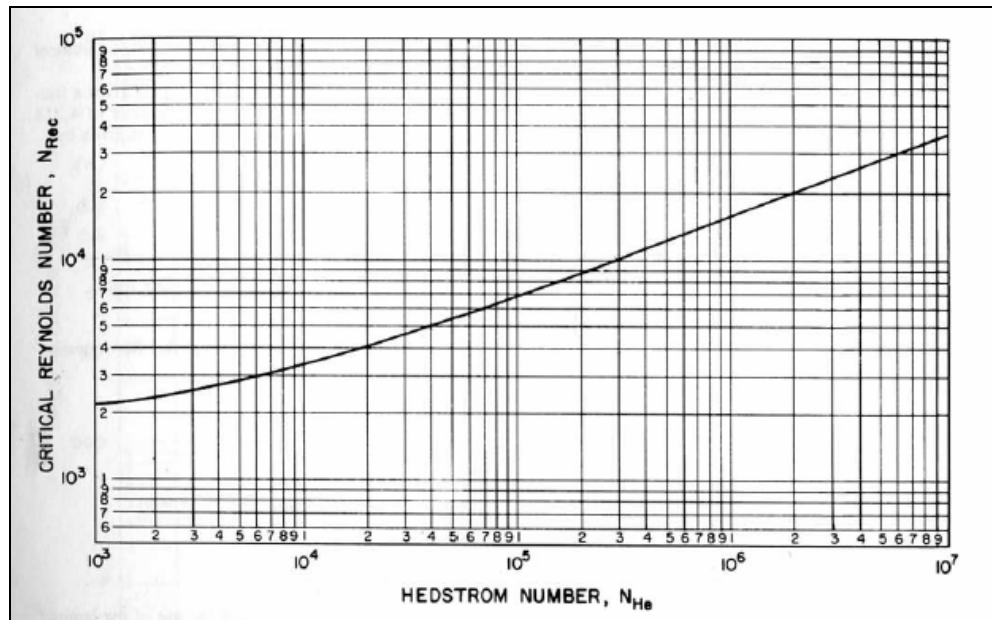


Fig. 5.2— Critical Reynolds numbers for Bingham plastic fluids (from Bourgoyne¹⁴).

5.1.3 Frictional Pressure Calculation for Power Law Fluid

To estimate velocity, we follow the procedure outlined in Part a, Section 5.1.1 (annulus and pipe).¹⁴

- Pipe Flow

b. Reynolds Number:

$$N_{Re} = \frac{89100 v_p^{2-n} \rho}{k} \left(\frac{0.0416 D_p}{3 + \frac{1}{n}} \right)^n \dots\dots\dots (5.17)$$

$$n = 3.32 \log \left(\frac{R_{600}}{R_{300}} \right) \dots\dots\dots (4.12)$$

$$k = \frac{510 R_{300}}{511^n} \dots\dots\dots (4.13)$$

c. For laminar flow,²⁶ critical Reynolds number value, $N_{Rec} = 3470-1370n$.

For turbulent flow,²⁶ critical Reynolds number value $N_{Rec} = 4270-1370n$.

d. Regime flow determination:

Comparison between N_{Re} and N_{Rec}

If $N_{Re} < N_{Rec} \rightarrow$ flow is laminar.

The friction factor is included in Eq. 5.21.

If $N_{Re} > N_{Rec} \rightarrow$ flow is turbulent.²⁶

$$f = \frac{a}{N_{Re}^b} \dots\dots\dots (5.18)$$

$$a = \frac{\log n + 3.93}{50} \dots\dots\dots (5.19)$$

$$b = \frac{1.75 - \log n}{7} \dots\dots\dots (5.20)$$

e. Frictional pressure loss calculation inside drillstring:

Laminar:

$$\left(\frac{dp}{dL}\right) = \frac{k v_p^n \left(\frac{3 + 1/n}{0.0416}\right)^n}{144000 D_p^{1+n}} \cdot \dots\dots\dots (5.21)$$

Turbulent:

Use Eq. 5.6 to estimate pressure loss calculation for turbulent flow.

$$\Delta p_{ds} = \left(\frac{dp}{dL}\right) \Delta L \cdot \dots\dots\dots (5.7)$$

- Annular Flow

b. Reynolds number:

$$N_{Re} = \frac{109000 v_a^{2-n} \rho}{k} \left(\frac{0.0208(D_2 - D_1)}{2 + \frac{1}{n}} \right)^n \cdot \dots\dots\dots (5.22)$$

c. For laminar flow, the critical value $N_{Rec} = 3470-1370n$.

For turbulent flow, the critical value $N_{Rec} = 4270-1370n$.

d. Regime flow determination:

Comparison between N_{Re} and N_{Rec}

If $N_{Re} < N_{Rec} \rightarrow$ flow is laminar.

Friction factor included in Eq.5.23

If $N_{Re} > N_{Rec} \rightarrow$ flow is turbulent.

Follow the same procedure as for pipe flow.

e. Frictional pressure loss calculation inside annulus:

Laminar:

$$\left(\frac{dp}{dL}\right) = \frac{k v_a^n \left(\frac{2+1/n}{0.0208}\right)^n}{144000(D_2 - D_1)^{1+n}} \quad \dots\dots\dots(5.23)$$

Turbulent:

Use Eq.5.10 to estimate pressure loss calculation for turbulent flow.

$$\Delta p_a = \left(\frac{dp}{dL}\right) \Delta L \quad \dots\dots\dots(5.7)$$

5.1.4 Frictional Pressure Loss Calculation for API RP 13D Fluid

To estimate velocity, Reynolds numbers, and friction pressure losses, follow the procedure outlined in Parts *a*, *b* and *e* of Section 5.1.1 (annulus and pipe).¹

Note: Use the equivalent viscosity to estimate Reynolds number; see Eq. 5.25.

- Pipe Flow

b. Reynolds number:

$$N_{Re} = \frac{928 v_p \rho D_p}{\mu_e} \quad \dots\dots\dots(5.24)$$

$$\mu_e = 100k \left(\frac{96 v_p}{D_p}\right)^{n-1} \left(\frac{3n+1}{4n}\right)^n \quad \dots\dots\dots(5.25)$$

$$n = 3.32 \log \left(\frac{R_{600}}{R_{300}}\right) \quad \dots\dots\dots(4.12)$$

$$k = \frac{5.10 R_{600}}{1022^n} \quad \dots\dots\dots(4.15)$$

where μ_e is the equivalent viscosity, cp

c. Critical value $N_{Rec} = 2100$.

d. Regime flow determination:

Comparison between N_{Re} and N_{Rec}

If $N_{Re} < N_{Rec} \rightarrow$ flow is laminar.

Use Eq. 5.4.

If $N_{Re} > N_{Rec} \rightarrow$ flow is turbulent.

Use Eqs. 5.18-5.20.

- Annular Flow

b. Reynolds number:

$$N_{Re} = \frac{928 v_a \rho (D_2 - D_1)}{\mu_e} \dots\dots\dots (5.26)$$

$$\mu_e = 100k \left(\frac{144v}{D_2 - D_1} \right)^{n-1} \left(\frac{2n+1}{3n} \right)^n \dots\dots\dots (5.27)$$

$$n = 0.657 \log \left(\frac{R_{100}}{R_3} \right) \dots\dots\dots (4.16)$$

$$k = \frac{5.10 R_{100}}{170.2^n} \dots\dots\dots (4.17)$$

c. Critical value $N_{Rec} = 2100$.

d. Regime flow determination:

Comparison between N_{Re} and N_{Rec}

Use the same procedure followed for this model in pipe flow, but consider the friction factor for laminar flow as $f = 24 / N_{Re}$.

.

5.1.5 Frictional Pressure Loss Calculation for Herschel-Bulkley Fluid

To estimate velocity, follow the procedure outlined in Part *a* of Section 5.1.1 (annulus and pipe).^{23,26,27}

- Pipe Flow

b. Reynolds number:

$$N_{Re} = \frac{2(3n+1)}{n} \left[\frac{\rho v_p^{(2-n)} \left(\frac{D_p}{2} \right)^n}{\tau_0 \left(\frac{D_p}{2v_p} \right)^n + k \left(\frac{3n+1}{nC_c} \right)^n} \right] \cdot \dots\dots\dots(5.28)$$

c. Critical Reynolds numbers value, N_{Rec}

$$N_{Rec} = \left[\frac{4(3n+1)}{ny} \right]^{\frac{1}{1-z}} \cdot \dots\dots\dots(5.29)$$

$$y = \frac{\log(n) + 3.93}{50} \cdot \dots\dots\dots(5.30)$$

$$z = \frac{1.75 - \log(n)}{7} \cdot \dots\dots\dots(5.31)$$

d. Regime flow determination:

Comparison between N_{Re} and N_{Rec}

If $N_{Re} < N_{Rec} \rightarrow$ flow is laminar.

Friction factor included in Eq.5.34

If $N_{Re} > N_{Rec} \rightarrow$ flow is turbulent.

$$f = y(C_c N_{Re})^{-z} \cdot \dots\dots\dots(5.32)$$

$$C_c = 1 - \left(\frac{1}{2n+1} \right) \frac{\tau_0}{\tau_0 + k \left[\frac{(3n+1)q}{n\pi(D_p/2)^3} \right]^n} \cdot \dots\dots\dots(5.33)$$

e. Frictional pressure loss calculation inside the drillstring:

Laminar:

$$\left(\frac{dp}{dL}\right) = \frac{4k}{14400D_p} \left\{ \left(\frac{\tau_0}{k}\right) + \left[\left(\frac{3n+1}{nC_c}\right) \left(\frac{8q}{\pi D_p^3}\right) \right]^n \right\} \dots\dots\dots(5.34)$$

Turbulent:

$$\left(\frac{dp}{dL}\right) = \frac{fq^2\rho}{1421.22D_p^5} \dots\dots\dots(5.35)$$

$$\Delta p_{ds} = \left(\frac{dp}{dL}\right) \Delta L \dots\dots\dots(5.7)$$

- Annular Flow

b. Reynolds number:

$$N_{Re} = \frac{4(2n+1)}{n} \left\{ \frac{\rho v_a^{2-n} \left(\frac{D_2 - D_1}{2}\right)^n}{\tau_0 \left(\frac{D_2 - D_1}{2v_a}\right)^n + k \left[\frac{2(2n+1)}{nC_a^*}\right]^n} \right\} \dots\dots\dots(5.36)$$

where v_a is annular velocity in ft/sec and D_1, D_2 are diameters in ft.

c. Critical value N_{Rec}

$$N_{Rec} = \left[\frac{8(2n+1)}{ny} \right]^{\frac{1}{1-z}} \dots\dots\dots(5.37)$$

Use Eqs. 5.30 and 5.31 to estimate the values of z and y .

d. Regime flow determination:

Comparison between N_{Re} and N_{Rec}

If $N_{Re} < N_{Rec} \rightarrow$ flow is laminar.

Friction factor is included in Eq.5.46

If $N_{Re} > N_{Rec} \rightarrow$ flow is turbulent.

$$f = y(C_a^* N_{Re})^{-z} \dots\dots\dots (5.38)$$

$$C_a^* = 1 - \left(\frac{1}{n+1} \right) \frac{\tau_0}{\tau_0 + k \left\{ \frac{2q(2n+1)}{n\pi[(D_2/2) - (D_1/2)][(D_2/2)^2 - (D_1/2)^2]} \right\}^n} \dots\dots\dots (5.39)$$

e. Frictional pressure loss calculation inside annulus:

Laminar:

$$\left(\frac{dp}{dL} \right) = \frac{4k}{14400(D_2 - D_1)} \left\{ \left(\frac{\tau_0}{k} \right) + \left[\left(\frac{16(2n+1)}{n \times C_a^*(D_2 - D_1)} \right) \left(\frac{q}{\pi(D_2^2 - D_1^2)} \right) \right]^n \right\} \dots\dots\dots (5.40)$$

Turbulent:

$$\left(\frac{dp}{dL} \right) = \frac{fq^2 \rho}{1421.22(D_2 - D_1)(D_2^2 - D_1^2)^2} \dots\dots\dots (5.41)$$

$$\Delta p_a = \left(\frac{dp}{dL} \right) \Delta L \dots\dots\dots (5.7)$$

5.1.6 Frictional Pressure Loss Calculation for Unified Fluid

- Pipe Flow^{2,24}

a. Velocity:

$$v_p = \frac{24.5q}{D_p^2} \dots\dots\dots (5.42)$$

b. Reynolds number:

$$G = \frac{3n+1}{4n} \dots\dots\dots (5.43)$$

$$\gamma_w = \frac{1.6Gv_p}{D_p} \dots\dots\dots (5.44)$$

$$\tau_w = \left(\frac{4}{3} \right)^n \tau_0 + k\gamma_w^n \dots\dots\dots (5.45)$$

$$N_{Re} = \frac{\rho v_p^2}{19.36 \tau_w}, \dots\dots\dots(5.46)$$

where G is a unified model parameter, dimensionless.

c. Friction factor determination for any flow regime:

$$f_{laminar} = 16 / N_{Re} \cdot \dots\dots\dots(5.47)$$

$$f_{transient} = \frac{16 N_{Re}}{(3470 - 1370n)^2} \cdot \dots\dots\dots(5.48)$$

$$a = \frac{\log n + 3.93}{50} \cdot \dots\dots\dots(5.19)$$

$$b = \frac{1.75 - \log n}{7} \cdot \dots\dots\dots(5.20)$$

$$f_{turbulent} = \frac{a}{N_{Re}^b} \cdot \dots\dots\dots(5.49)$$

$$f_{partial} = (f_{transient}^{-8} + f_{turbulent}^{-8})^{-1/8} \cdot \dots\dots\dots(5.50)$$

$$f = (f_{partial}^{12} + f_{laminar}^{12})^{1/12} \cdot \dots\dots\dots(5.51)$$

d. Frictional pressure loss calculation inside drillstring:

$$\left(\frac{dp}{dL} \right) = \frac{1.076 f v_p^2 \rho}{10^5 D_p} \cdot \dots\dots\dots(5.52)$$

$$\Delta p_{ds} = \left(\frac{dp}{dL} \right) \Delta L \cdot \dots\dots\dots(5.7)$$

- Annular Flow

a. Velocity:

$$v_a = \frac{24.5q}{D_2^2 - D_1^2} \cdot \dots\dots\dots(5.53)$$

b. Number of Reynolds:

$$G = \left(\frac{2n+1}{3n} \right) \times 1.5. \quad \dots\dots\dots (5.54)$$

$$\gamma_w = \frac{1.6Gv_a}{D_2 - D_1}. \quad \dots\dots\dots (5.55)$$

$$\tau_w = \left(\frac{3}{2} \right)^n \tau_0 + k\gamma_w^n. \quad \dots\dots\dots (5.56)$$

$$N_{Re} = \frac{\rho v_a^2}{19.36\tau_w}. \quad \dots\dots\dots (5.57)$$

c. Friction factor determination for any flow regime:

$$f_{laminar} = 16 / N_{Re}. \quad \dots\dots\dots (5.47)$$

$$f_{transient} = \frac{16N_{Re}}{(3470 - 1370n)^2}. \quad \dots\dots\dots (5.48)$$

$$a = \frac{\log n + 3.93}{50}. \quad \dots\dots\dots (5.19)$$

$$b = \frac{1.75 - \log n}{7}. \quad \dots\dots\dots (5.20)$$

$$f_{turbulent} = \frac{a}{N_{Re}^b}. \quad \dots\dots\dots (5.49)$$

$$f_{partial} = (f_{transient}^{-8} + f_{turbulent}^{-8})^{-1/8}. \quad \dots\dots\dots (5.50)$$

$$f = (f_{partial}^{12} + f_{laminar}^{12})^{1/12}. \quad \dots\dots\dots (5.51)$$

d. Frictional pressure loss calculation inside annulus:

$$\left(\frac{dp}{dL} \right) = \frac{1.076fv_a^2\rho}{10^5(D_2 - D_1)}. \quad \dots\dots\dots (5.58)$$

$$\Delta p_a = \left(\frac{dp}{dL} \right) \Delta L. \quad \dots\dots\dots (5.7)$$

5.1.7 Frictional Pressure Loss Calculation for Robertson and Stiff Fluid

To estimate velocity follow the procedure outline in Part a of Section 5.1.6 (annulus and pipe).²⁶⁻²⁹

- Pipe Flow

b. Reynolds number:

$$N_{Re} = \frac{89100 v_p^{2-B} \rho}{A} \left(\frac{0.0416 D_p}{3 + \frac{1}{B}} \right)^B \dots\dots\dots (5.59)$$

c. For laminar flow,²⁶ critical value $N_{Rec} = 3470-1370B$.

For turbulent flow,²⁶ critical value $N_{Rec} = 4270-1370B$.

d. Regime flow determination:

Comparison between N_{Re} and N_{Rec}

If $N_{Re} < N_{Rec} \rightarrow$ flow is laminar.

Friction factor is included in Eq. 5.60.

If $N_{Re} > N_{Rec} \rightarrow$ flow is turbulent.²⁶

$$a = \frac{\log(B) + 3.93}{50} \dots\dots\dots (5.60)$$

$$b = \frac{1.75 - \log(B)}{7} \dots\dots\dots (5.61)$$

$$f_{\text{turbulent}} = \frac{a}{N_{Re}^b} \dots\dots\dots (5.49)$$

e. Frictional pressure loss calculation inside drillstring:

Laminar:

$$\left(\frac{dp}{dL} \right) = 8.33E-4 \times 2^{2+B} \times A \left\{ \left(\frac{1+3B}{B} \right) \left[\frac{0.2 v_p + \frac{C}{6} D_p}{D_p^{\left(\frac{1+B}{B} \right)}} \right] \right\}^B \dots\dots\dots (5.62)$$

Turbulent:

To estimate frictional pressure loss for turbulent flow, follow the procedure outlined in Part *e* of Section 5.1.1 (annulus and pipe).

$$\Delta p_{ds} = \left(\frac{dp}{dL} \right) \Delta L. \dots\dots\dots (5.7)$$

- Annular Flow

b. Reynolds number:

$$N_{Re} = \frac{109000 v_a^{2-B} \rho}{A} \left(\frac{0.0208(D_2 - D_1)}{2 + \frac{1}{B}} \right)^B. \dots\dots\dots (5.63)$$

To estimate flow regime, follow the procedure outlined in Parts *c* and *d* of Section 5.1.7 (pipe). For laminar flow in the annulus, use Eq. 5.62.

e. Frictional pressure loss calculation inside annulus:

Laminar:

$$\left(\frac{dp}{dL} \right) = 8.33E-4 \times 4^{1+B} \times A \left\{ \left(\frac{1+2B}{B} \right) \left[\frac{0.2v_a + \frac{C}{8}(D_2 - D_1)}{(D_2 - D_1)^{\left(\frac{1+B}{B} \right)}} \right] \right\}^B. \quad (5.64)$$

Note: To consider yield stress with this model, use the following equations and estimate the frictional pressure loss for laminar flow by iteration:

- Pipe Flow

$$\lambda = \frac{2(AC)^B}{\left(\frac{dp}{dL} \right)}. \dots\dots\dots (5.65)$$

General equation to estimate friction pressure loss:

$$q = \pi \left\{ \left[\frac{1}{2A} \left(\frac{dp}{dL} \right) \right]^{1/B} \left(\frac{B}{3B+1} \right) \left[\left(\frac{D}{2} \right)^{\frac{3B+1}{B}} - \lambda^{\frac{3B+1}{B}} \right] - \frac{C}{3} \left[\left(\frac{D}{2} \right)^3 - \lambda^3 \right] \right\}. \quad (5.66)$$

- Annular Flow

$$\lambda = \frac{(AC)^B}{\left(\frac{dp}{dL} \right)}. \quad \dots\dots\dots (5.67)$$

$$q = 2D \left\{ \left(\frac{1}{2A} * \left(\frac{dp}{dL} \right) \right)^{1/B} \left(\frac{B}{2B+1} \right) \left[\left(\frac{D}{2} \right)^{\frac{3B+1}{B}} - \lambda^{\frac{2B+1}{B}} \right] - \frac{C}{2} \left[\left(\frac{D}{2} \right)^3 - \lambda^3 \right] \right\}.$$

.....(5.68)

For the annulus, $D = D_2 - D_1$ and $D = D_p$ for pipe.

5.1.8 Frictional Pressure Loss Calculation for Casson Fluid

To calculate velocity and Reynolds numbers follow the procedure outlined in Parts *a* and *b* of Section 5.1.1 (annulus and pipe).^{17,19} Note: Use the Casson viscosity estimate for this model with Eqs. 5.13 and 5.14.

- Pipe Flow

c. Critical Reynolds number value, N_{Rec} from **Fig.5.3**.

$$C_a = \frac{D_p^2 \tau_c \rho}{32.174 \mu_c^2}. \quad \dots\dots\dots (5.69)$$

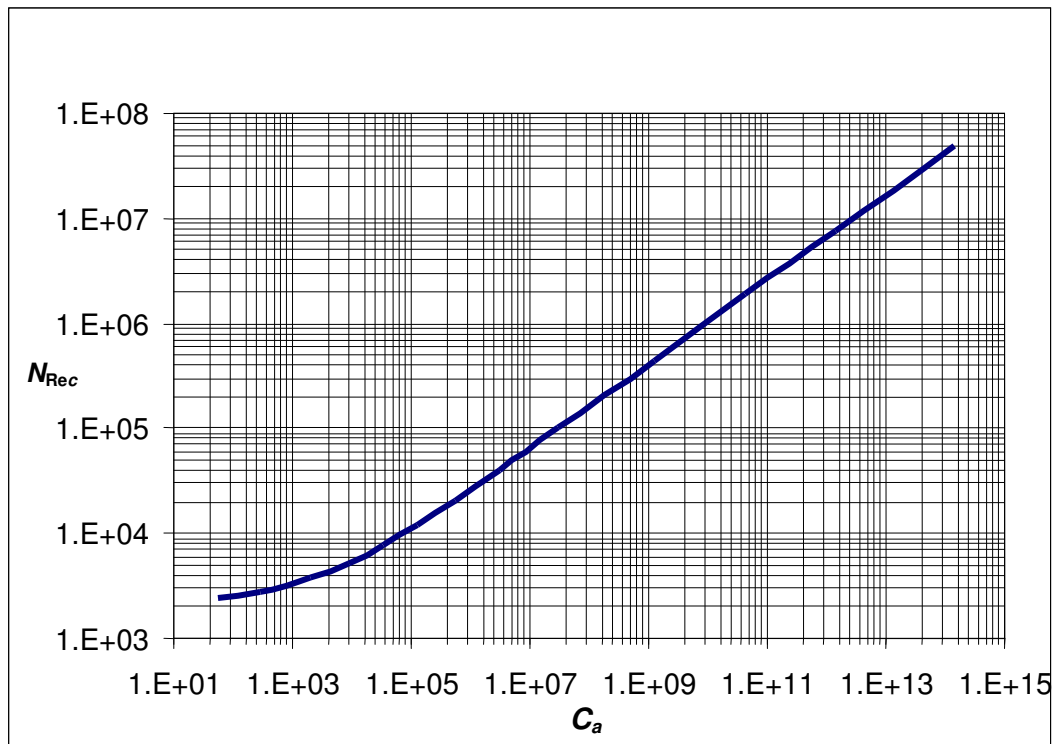


Fig. 5.3— Critical Reynolds numbers for Casson fluids (data from Hanks³⁰).

d. Regime flow determination:

Comparison between N_{Re} and N_{Rec}

If $N_{Re} < N_{Rec} \rightarrow$ flow is laminar.

Friction factor is included in Eq. 5.68.

If $N_{Re} > N_{Rec} \rightarrow$ flow is turbulent.

$$f = \frac{0.0791}{N_{Re}^{0.25}} \cdot \dots\dots\dots(5.5)$$

e. Frictional pressure loss calculation inside annulus:

Laminar:

$$q = \frac{\pi(D_2 - D_1)^3}{8(\mu_c^{1/2})^2} \times \left[\frac{(D_2 - D_1)\left(\frac{dp}{dL}\right)}{16} - \frac{4}{7}\sqrt{\tau_c} \sqrt{\frac{\left(\frac{dp}{dL}\right)(D_2 - D_1)}{4}} - \frac{64\tau_c^4}{84(D_2 - D_1)^3\left(\frac{dp}{dL}\right)^3} + \frac{\tau_c}{3} \right] \dots\dots\dots(5.72)$$

Where

$dp/dL = \text{lb/ft}^2/\text{ft}$

$$\Delta p_a = \left(\frac{dp}{dL}\right)\Delta L \dots\dots\dots(5.23)$$

Note that Eqs.5.70 and 5.72 need Solve from Excel in order to evaluate pressure drop gradient.

CHAPTER VI

TOOL JOINT

The tool joint is a necessary part to extend the drillpipe. These components are fabricated separately from the pipe body and welded onto the pipe at a manufacturing facility.

The tool joints provide high-strength, high-pressure threaded connections that are sufficiently robust to survive the rigors of drilling and numerous cycles of tightening and loosening at threads. Tool joints are usually made of steel that has been heat treated to a higher strength than the steel of the tube body.³¹

6.1 Weld-On Tool Joint

The flash-welded tool joint was introduced to the industry in 1938 and is now the only tool joint carried in API specifications, **Fig. 6.1**.

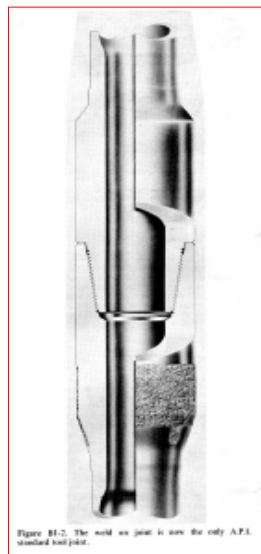


Fig. 6.1— API standards tool joint (from IADC manual³¹).

6.1.1 Upset and Designs

Upsets are necessary on drillpipe to which weld-on type tool joints are applied. These allow adequate safety factors in the weld area for mechanical strength and metallurgical considerations. **Fig. 6.2** shows an upset diagram. API upset for various sizes and weights of drillpipe are shown in **Fig. 6.3** and **Tables 6.1** and **6.2**.

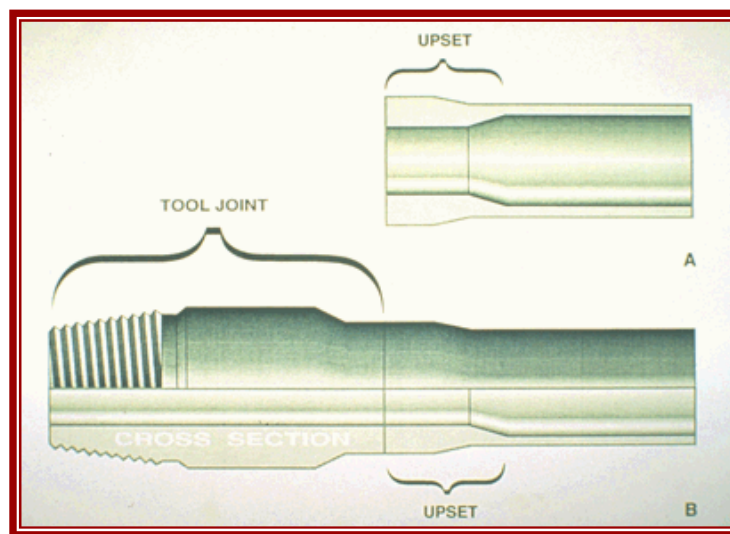


Fig. 6.2— Diagram of tool joint.³²

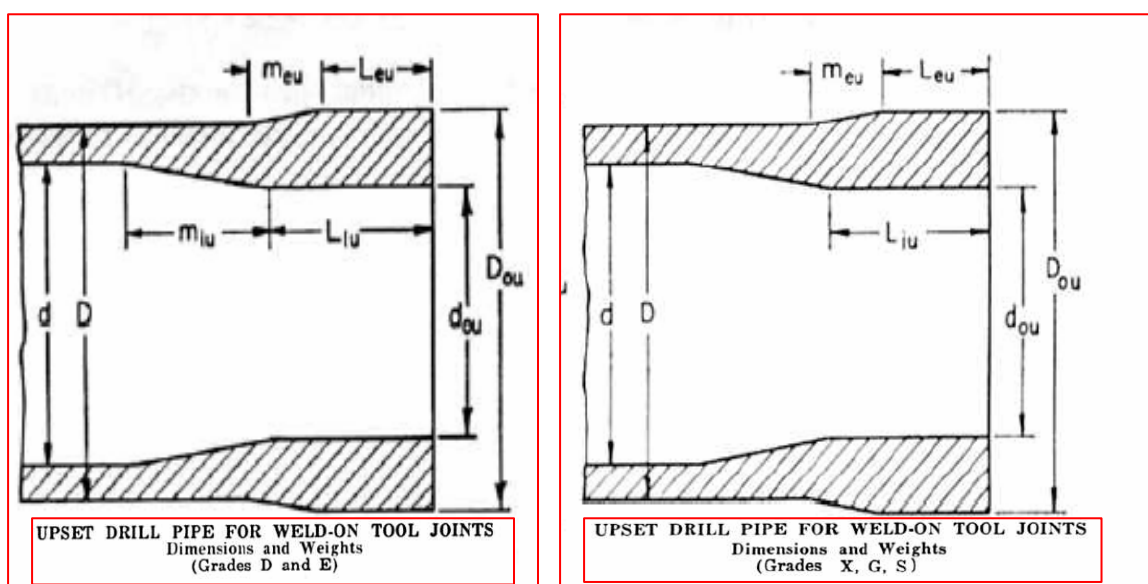


Fig. 6.3— Internal/external upset (from IADC manual³¹).

Table 6.1— Upset Drillpipe for Weld-On Tool Joints, Grades D and E
(from IADC manual³¹).

Pipe Size: Out- side Dia., in. <i>D</i>	Nomi- nal Wt.: ¹ lb/ft	Wall Thick- ness, in. <i>t</i>	Inside Diam- eter, in. <i>d</i>	Calculated Weight		³ Upset Dimensions, in.						
				Plain End lb/ft <i>w_{pe}</i>	Upset ⁴ lb <i>e₁₀</i>	Out- side Diam- eter, ² $+ \frac{1}{8},$ $- \frac{1}{32}$ <i>D_{ou}</i>	Inside Diameter at End of Upset, ³ $\pm \frac{1}{40}$ <i>d_{ou}</i>	Length of Internal Upset $+1\frac{1}{2}$ $- \frac{1}{2}$ <i>L_{iu}</i>	Length of Internal Taper, min. <i>m_{iu}</i>	Length of External Upset, min. <i>L_{eu}</i>	Length of External Taper, min. max. <i>m_{eu}</i>	
4½	20.00	0.430	3.640	18.69	8.60	4.781	3	2¼	2	1½	1	1½
5	19.50	0.362	4.276	17.93	8.60	5.188	3¼ ₁₆	2¼	2	1½	1	1½
5	25.60	0.500	4.000	24.03	7.80	5.188	3¾ ₁₆	2¼	2	1½	1	1½
5½	21.90	0.361	4.778	19.81	10.60	5.563	4	2¼	2	1½	1	1½
5½	24.70	0.415	4.670	22.54	9.00	5.563	4	2¼	2	1½	1	1½

Table 6.2— Upset Drillpipe for Weld-On Tool Joints, Grades X, G and S
(from IADC manual³¹).

Pipe Size: Out- side Diam., in. <i>D</i>	Nomi- nal Wt.: ¹ lb/ft	Wall Thick- ness, in. <i>t</i>	Inside Diam- eter, in. <i>d</i>	Calculated Weight		*Upset Dimensions, in.				
				Plain End lb/ft <i>w_{pe}</i>	Upset ⁴ lb <i>e_w</i>	Out- side Diam- eter, ² $+ \frac{1}{8},$ $- \frac{1}{32}$ <i>D_{os}</i>	Inside Diameter at End of Pipe, ³ $+ \frac{1}{16}$ <i>d_{os}</i>	Length of Internal Upset $+ 1\frac{1}{2}$ $- \frac{1}{2}$ <i>L_{is}</i>	Length of External Upset, min. <i>L_{es}</i>	Length End of Pipe to Taper Fadeout, Ext. Upset max. <i>L_{es} + m_{es}</i>
3½	15.50	0.449	2.602	14.63	11.00	3.781	1½ ₁₆	4¼	3	5½
4½	20.00	0.430	3.640	18.69	17.60	4.781	2¼ ₁₆	4¼	3	5½
5	19.50	0.362	4.276	17.93	16.80	5.188	3 ⁹ ₁₆	4¼	3	5½
5	25.60	0.500	4.000	24.03	15.40	5.188	3 ⁹ ₁₆	4¼	3	5½
5½	21.90	0.361	4.778	19.81	21.00	5.563	3¼ ₁₆	4¼	3	5½
5½	24.70	0.415	4.670	22.54	18.40	5.563	3¼ ₁₆	4¼	3	5½

Deepwater drilling necessitates high strength drillpipe which often has small throated (internal upset) tool joints.

Figs. 6.4 and 6.5 show the pin and box areas, which are the largest factor and are subject to the widest variation. The tool joint outside diameter (OD) and inside diameter (ID) largely determine the strength of the joint in torsion. The OD affects the box area the ID affects the pin area. Choice of OD and ID determines the areas of the pin and box and establishes the theoretical torsional strength.

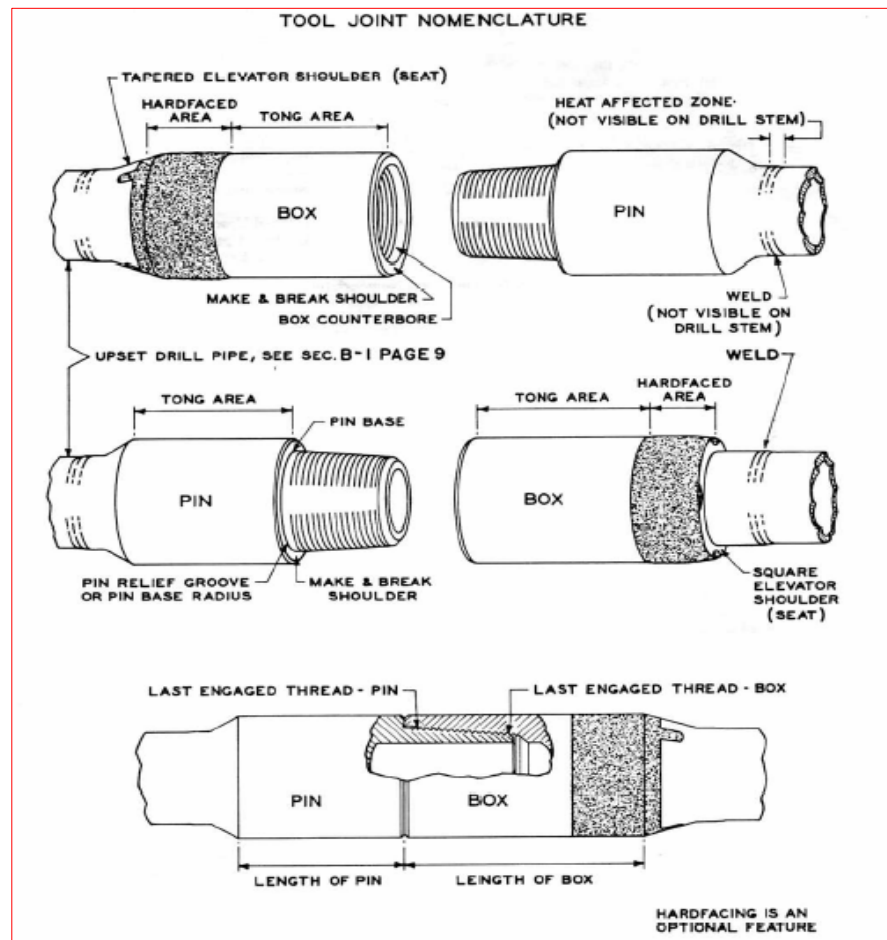


Fig. 6.4— Tool joint nomenclature (from IADC manual³¹).

6.1.2 Cleaning and Inspection

Pin and box threads and shoulders should be thoroughly cleaned in preparation to adding them to the string. Cleaning pays off in three ways. First, it removes foreign material and permits proper make-up, thereby reducing danger of galling and wobbles. Second, it permits better inspection. Third, it increases life of connections by elimination of abrasive materials. Connections should be carefully dried after cleaning so that the thread compound will properly adhere to the surface.

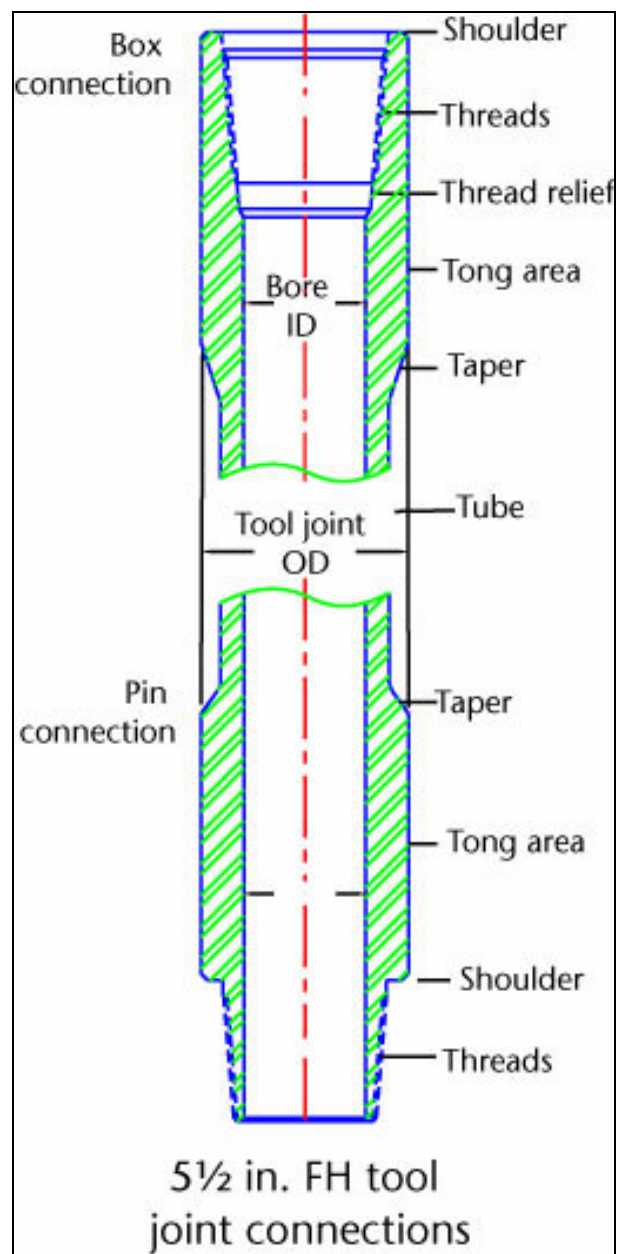


Fig. 6.5 —Schematic of the box and pin ends of a joint of pipe. ID = internal diameter, OD = outside diameter, FH = full hole.³²

CHAPTER VII

STUDY APPROACHES TO ESTIMATE PRESSURE LOSSES BY CORRECTING FOR TOOL JOINT LOSSES

The prediction of friction pressure losses is important in many field operations, including drilling, completion, fracturing, acidizing, workover and production. Also, deep drilling necessitates high-strength drillpipe which often has small-throated (internal upset) tool joints. These internal limitations cause flow losses which can be considerable. The pressure loss caused by entry into the tool joint is small compared with the exit losses.

On the other hand, external upset of tool joint can cause the same problem in the annulus between tool joint and casing. This space is narrower than the space between drillpipe and casing. As a result, the expansion and contraction of the annulus during fluid flow causes additional pressure loss.

This research proposes five approaches to correct pump pressure loss by tool joints, and Appendix C give an example of how these approaches work:

1. Enlargement and contraction (E&C).
2. Equivalent diameter (ED).
3. Two different IDs (2IDs).
4. Enlargement and contraction plus equivalent diameter (E&C+ED).
5. Enlargement and contraction plus two different IDs (E&C+2IDs).

7.1 Enlargement and Contraction

When fluid is flowing steadily in a long, straight pipe of uniform diameter, the flow pattern, as indicated by the velocity distribution across the pipe diameter, will assume a certain characteristic form. Any impediment in the pipe which changes the direction of the whole stream, or even part of it, will alter the characteristic flow pattern and create turbulence, causing an energy loss greater than that normally accompanying flow in straight pipe. This disturbance in the flow pattern produces an additional pressure drop.³³

7.1.1 Gradual Enlargement for Pipe

The losses due to gradual enlargement of pipes were investigated by Gibson,³⁴ and **Fig. 7.1** shows the geometry's change. Also, the resistance to flow may be expressed by the coefficient K_e . See Eq. 7.1.

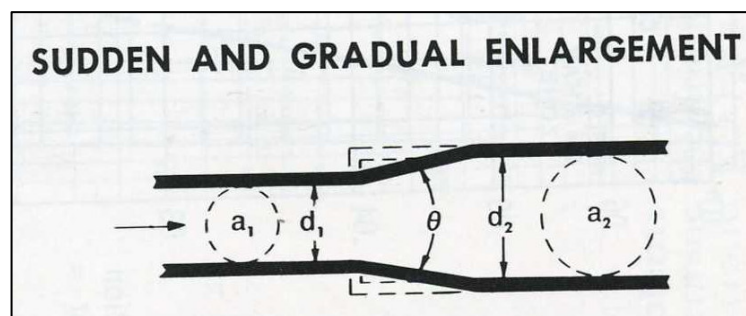


Fig. 7.1 —Schematic change of area, a_1 and a_2 , in a pipe with a tool joint (from tool joint to pipe).³³

$$45^\circ < \theta \leq 180^\circ$$

$$K_e = (1 - \beta^2)^2, \dots\dots\dots(7.1)$$

$$\theta \leq 45^\circ$$

$$K_e = 2.6 \sin\left(\frac{\theta}{2}\right) (1 - \beta^2)^2, \dots\dots\dots(7.2)$$

where β is the ratio of diameters of small to large pipes, dimensionless.

The mechanical energy loss, F_e , between two different successive diameters can be expressed by comparing Bernoulli equation at two points. See Eq.7.2

$$F_e = K_e \left(\frac{v^2}{2gc} \right). \dots\dots\dots(7.3)$$

The pressure loss then is calculated by multiplying the fluid density by mechanical energy loss for gradual enlargements.

$$\Delta p_e = 0.052 F_e \rho. \dots\dots\dots(7.4)$$

7.1.2 Gradual Contraction for Pipe

The same procedure is followed to obtain the pressure loss for gradual contraction. See **Fig. 7.2**.

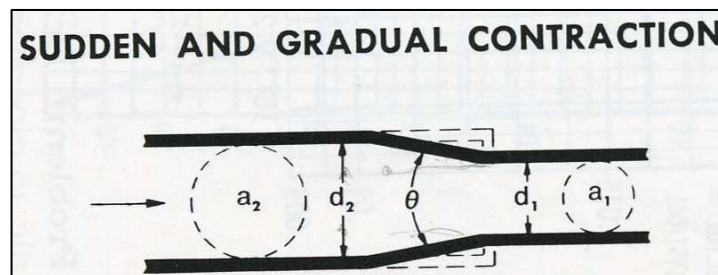


Fig. 7.2 —Schematic change of area, a_1 and a_2 , in a pipe with a tool joint (enter from pipe to tool joint).³³

$$45^\circ < \theta \leq 180^\circ$$

$$K_c = 0.5 \sqrt{\sin\left(\frac{\theta}{2}\right)} (1 - \beta^2) \dots\dots\dots (7.5)$$

$$\theta \leq 45^\circ$$

$$K_c = 0.8 \sin\left(\frac{\theta}{2}\right) (1 - \beta^2) \dots\dots\dots (7.6)$$

Then;

$$F_c = K_c \left(\frac{v^2}{2gc} \right) \dots\dots\dots (7.7)$$

$$\Delta p_c = 0.052 F_c \rho \dots\dots\dots (7.8)$$

Note the convergence or divergence angle can be estimated using tables and figures in Chapter VI. Also, see **Fig. 7.3** and **Tables 7.1** and **7.2**.

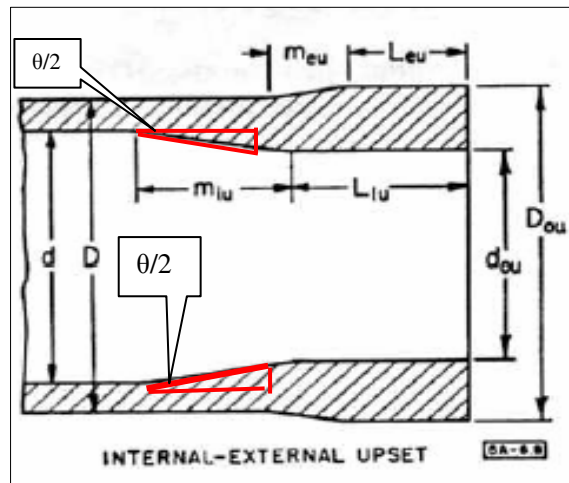


Fig. 7.3 —The angle, θ , is an important element in the enlargement and contraction equations.³³

Table 7.1— Angles for Internal Upset (Drillpipe) for Weld-On Tool Joints

Pipe				tool joint			angle calculation	
OD,in	wt(lbf/ft)	Grade	d,in	miu,in	dou,in	d-dou	$\theta/2$	θ
4.5	20	D,E	3.6400	2	3.0000	0.6400	17.7500	35.5000
5	19.5	D,E	4.2760	2	3.6875	0.5885	16.4000	32.8000
5	25.6	D,E	4.0000	2	3.3750	0.6250	17.3500	34.7000
5.5	21.9	D,E	4.7780	2	4.0000	0.7780	21.2500	42.5000
5.5	24.7	D,E	4.6700	2	4.0000	0.6700	18.5200	37.0400
3.5	15.5	X,G,S	2.6020	2	1.9375	0.6645	18.3800	36.7600
4.5	20	X,G,S	3.6400	2	2.8125	0.8275	22.4800	44.9600
5	19.5	X,G,S	4.2760	2	3.5625	0.7135	19.6300	39.2600
5	25.6	X,G,S	4.0000	2	3.3125	0.6875	18.9600	37.9200
5.5	21.9	X,G,S	4.7780	2	3.8125	0.9655	25.7700	51.5400
5.5	24.7	X,G,S	4.6700	2	3.8125	0.8575	23.2100	46.4200

Table 7.2— Angles for External Upset (Annulus) for Weld-On Tool Joints

Pipe				tool joint			angle calculation	
D,in	wt(lbf/ft)	Grade	d,in	meu,in	Dou,in	Dou-D	$\theta/2$	θ
4.5	20	D,E	3.6400	1.5	4.7810	0.2810	10.6100	21.2200
5	19.5	D,E	4.2760	1.5	5.1880	0.1880	7.1400	14.2800
5	25.6	D,E	4.0000	1.5	5.1880	0.1880	7.1400	14.2800
5.5	21.9	D,E	4.7780	1.5	5.5630	0.0630	2.4000	4.8000
5.5	24.7	D,E	4.6700	1.5	5.5630	0.0630	2.4000	4.8000
3.5	15.5	X,G,S	2.6020	2.5	3.7810	0.2810	6.4100	12.8200
4.5	20	X,G,S	3.6400	2.5	4.7810	0.2810	6.4100	12.8200
5	19.5	X,G,S	4.2760	2.5	5.1880	0.1880	4.3000	8.6000
5	25.6	X,G,S	4.0000	2.5	5.1880	0.1880	4.3000	8.6000
5.5	21.9	X,G,S	4.7780	2.5	5.5630	0.0630	1.4400	2.8800
5.5	24.7	X,G,S	4.6700	2.5	5.5630	0.0630	1.4400	2.8800

7.1.3 Gradual Enlargement and Contraction for Annulus

The procedure is the same as followed in Sections 7.1.1 and 7.1.2. However, notice that the velocity used to estimate the pressure loss by enlargement and contraction corresponds to the narrow annulus. See **Fig. 7.4**.

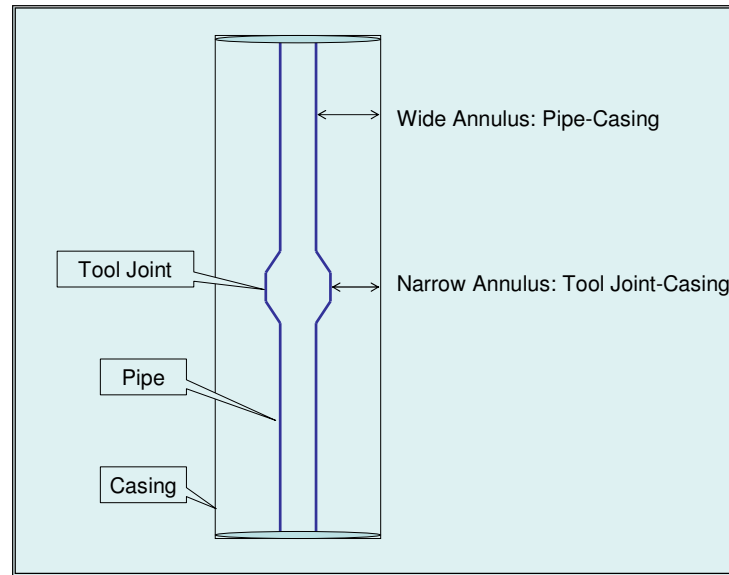


Fig. 7.4 —Schematic change of area in the annulus with presence of tool joint.

7.1.4 Estimation of Pump Pressure Considering Enlargement and Contraction Correction

Add to drillstring friction pressure losses calculated (with any correction) the pressure losses caused by enlargement and contraction of each tool joint. Do the same for the annulus friction pressure losses.

$$\Delta p_p = \Delta p_s + [\Delta p_{ds} + (\Delta p_e + \Delta p_c) N_{TJ}] + [\Delta p_a + (\Delta p_e + \Delta p_c) N_{TJ}] + \Delta p_b. \quad (7.9)$$

7.2 Equivalent Diameter

Equivalent diameter is a technique that makes an adjustment between two diameters. Consider internal drillpipe and tool joint diameters to estimate pressure drop calculation in the drillstring and external drill pipe and tool joint diameters for the annulus.

Use the following equation to estimate equivalent diameter[§], D_e , in drillstring (between inside pipe and tool joint diameters).

$$De_p = \left[\frac{L_2 d_{TJ}^4 D_p^4}{L_1 D_p^4 + (L_1 - L_2) d_{TJ}^4} \right]^{1/4} \cdot \dots\dots\dots (7.10)$$

Use Eq. 7.11 to estimate equivalent diameter in the annulus (between outside pipe and tool joint diameters).

$$De_a = \left[\frac{L_2 D_{TJ}^4 D_1^4}{L_1 D_1^4 + (L_1 - L_2) D_{TJ}^4} \right]^{1/4} \cdot \dots\dots\dots (7.11)$$

Finally, calculate friction pressure losses in the drillstring and annulus as do normally but use equivalent diameter in the calculation of frictional pressure drop.

$$\Delta p_p = \Delta p_s + \Delta p_{ds} + \Delta p_a + \Delta p_b. \dots\dots\dots (5.2)$$

7.3 Two Different IDs

This approach proposes to estimate the frictional pressure drop in the annulus and in the drillstring considering the actual pipe/tool joint length and diameter in the calculation.

[§]Personal communication, C.Brian. Grant Prideco, USA, TX. Oct. 2005.

- Pipe:

a. Estimation of total drillstring length, $L_{\text{total } dp}$:

$$L_{\text{total } dp} = (L_2 N_{DP} - L_1 N_{TJ}). \quad \dots\dots\dots(7.12)$$

b. Use the ID of the drillstring to estimate the frictional pressure drop, Δp_{ds} :

$$\Delta p_{ds} = (dp/dL)_{ds} L_{\text{total } dp}. \quad \dots\dots\dots(7.13)$$

c. Estimation of total tool joint length, $L_{\text{total } TJ}$:

$$L_{\text{total } TJ} = (L_1 N_{TJ}). \quad \dots\dots\dots(7.14)$$

d. Use ID of tool joint and respective length to calculate its contribution to the pressure loss to the drillstring, Δp_{TJ} .

$$\Delta p_{TJ} = (dp/dL)_{TJ} L_{\text{total } TJ}. \quad \dots\dots\dots(7.15)$$

e. Add drillstring and tool joint frictional pressure drop to estimate the total drillstring friction pressure losses.

$$(\Delta p_{\text{total } 2IDs})_{ds} = \Delta p_{ds} + \Delta p_{TJ}. \quad \dots\dots\dots(7.16)$$

- Annulus:

Use the same procedure to estimate the total frictional pressure drop in the annulus, $(\Delta p_{\text{total } 2IDs})_a$, followed in the pipe section, but use the annulus data.

Finally,

$$\Delta p_p = \Delta p_s + (\Delta p_{\text{Total } 2IDs})_{ds} + (\Delta p_{\text{Total } 2IDs})_a + \Delta p_b. \quad \dots\dots\dots(7.17)$$

7.4 Enlargement and Contraction Plus Equivalent Diameter

The main idea in this approach is to combine the first two methods to correct frictional pressure drop together. To reach this objective, use the following procedure:

- a. Estimate the contribution to frictional pressure drop in the drillstring and in the annulus by enlargement and contraction. See Section 7.1.
- b. Calculate the frictional pressure drop in the drillstring and in the annulus as shown in Section 7.2.
- c. Add the enlargement and contraction contribution to frictional pressure drop in the drillstring and in the annulus already corrected by equivalent diameter.

7.5 Enlargement and Contraction Plus Two Different IDs

In this case we evaluate two approaches together one more time. To achieve this goal apply the following steps:

- a. Estimate the contribution to frictional pressure drop in the drillstring and in the annulus by enlargement and contraction. See Section 7.1
- b. Calculate the frictional pressure drop in the drillstring and in the annulus as shown in Section 7.3.
- c. Add the enlargement and contraction contribution to frictional pressure drop in the drillstring and in the annulus already corrected by two different IDs.

CHAPTER VIII

DATA USED TO VALIDATE THE NEW APPROACHES

Accurate downhole and surface measurements of a synthetic-based drilling fluid were taken in a Gulf of Mexico well to determine variances between actual and calculated pump pressure.

A special team headed by Marathon Oil Co. successfully instrumented and collected a very large volume of hydraulics data on a well in the Gulf on Mexico at 12,710 ft measured depth. Using multiple sensor packages, accurate measurement of downhole dynamic pressure (hydraulic data) were obtained.⁹

The well selected for the test was in 420 ft of water in Block 89, South Pass, Gulf of Mexico. Testing was conducted after running and cementing a single-weight intermediate string of 11 7/8-in. casing to 12,710 ft. **Fig. 8.1** shows the well profile at the time of the test with the 5-in. drillstring run to 12,439 ft measured depth. Drillstring details also are given in **Fig. 8.1**.

The mud was the same 11.5 lbm/gal polyalphaolefin (PAO)-based synthetic drilling fluid used to drill the long, intermediate casing interval. A single mud pit was isolated to limit surface volume to about 220 bbl and to minimize circulating time for conditioning mud. This also reduces temperature variations while the mud was on the surface. The temperature seems to be constant during the test and it is approximate to 150°F.

In addition to conventional rheological measurements, HPHT properties were taken using a Fann Model 70 viscometer.

Table 4.1 shows the data obtained from White and Zamora⁹ used in the project.

Table 4.1—Data From Fann 70 (from White and Zamora⁹)

RPM	Reading
600	92
300	58
200	46
100	32
6	10
3	8

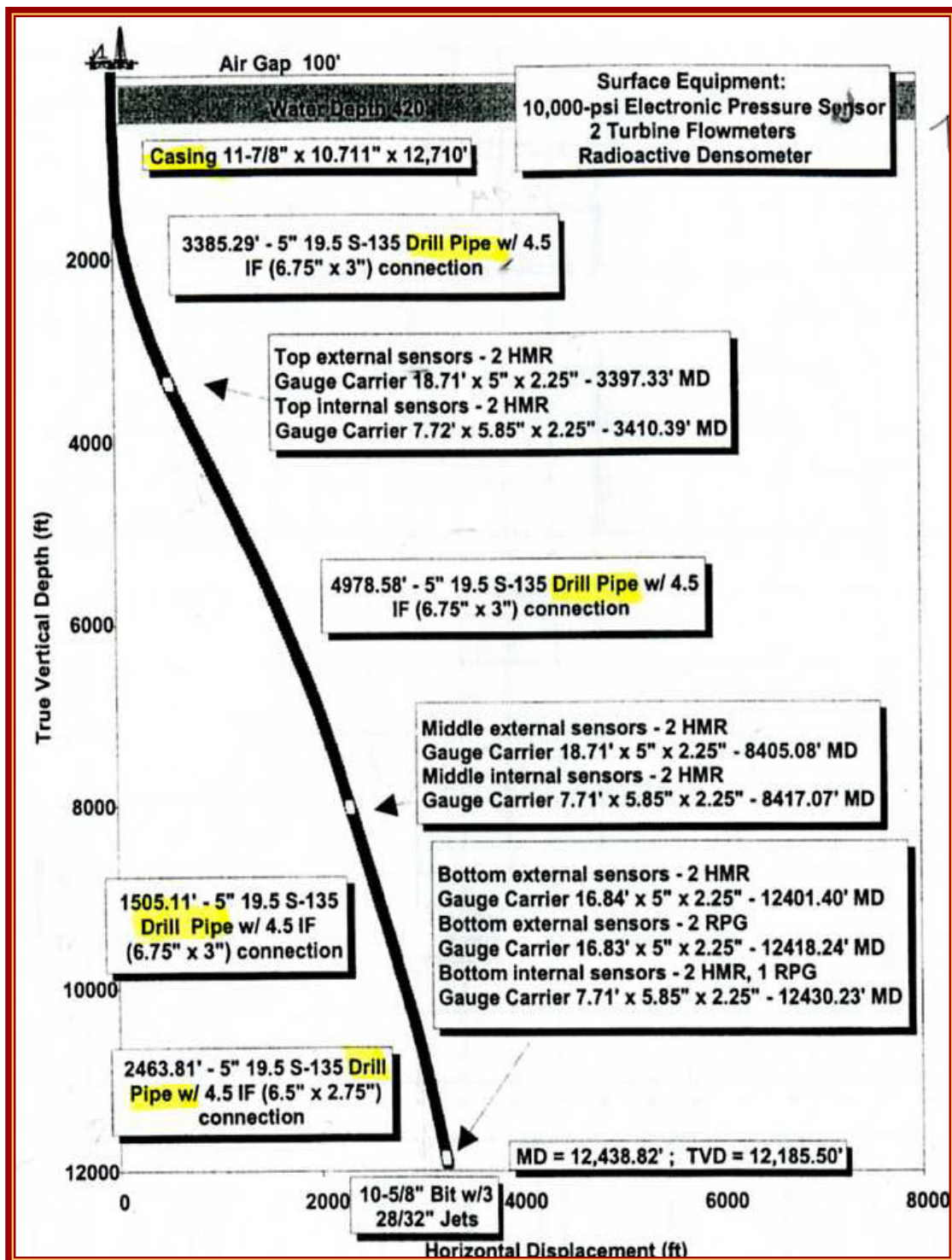


Fig. 8.1— Schematic of well and instrumentation for hydraulics study.⁹

CHAPTER IX

RESULTS ANALYSIS

One set of data of non-Newtonian drilling fluid has been used to illustrate the accuracy of this approach for selecting the best rheological model, one with the lowest E_{AAP} value. The physical properties of this fluid are given in **Table 4.1**, and the values for the absolute average percent error are given for each model in **Table 9.1**.

Table 9.1— E_{AAP} Value for Rheological Models

Rheological Model	E_{AAP}
API	1.510
Herschel & Bulkley	2.898
Robertson & Stiff	2.914
Unified	3.952
Casson	4.667
Power Law	6.887
Bingham	24.261
Newtonian	46.538

Table 9.1 shows that the API RP13D model was the best model to represent the rheological properties for this non-Newtonian fluid. However, it was close followed by Herschel-Bulkley, Casson, Robertson and Stiff, and Unified.

The Newtonian and Bingham models gave high values of E_{AAP} for the fluid, and therefore they are not recommended for use in pressure drop and hydraulics calculations. See appendix D.

Drilling fluid viscosity has a significant impact on circulating pressure losses and solid suspension characteristics of the fluid.

On the other hand, we used five tool joint corrections for this set of data for all rheological models. The data used consisted of rheological and pressure friction loss in the drillstring and annulus, and pump pressure. We compared the calculated drillstring, annulus, and pump pressures, which were corrected, with the drillstring, annulus and pump pressure measured by White and Zamora.⁹

The eight rheological models gave better idea of how the correction by the presence of tool joints can influence the pump pressure for each one.

Fig. 9.1 shows the data of pump pressure vs. measured and calculated flow rates. Note that the calculated pump pressure is derived without any tool joint corrections.

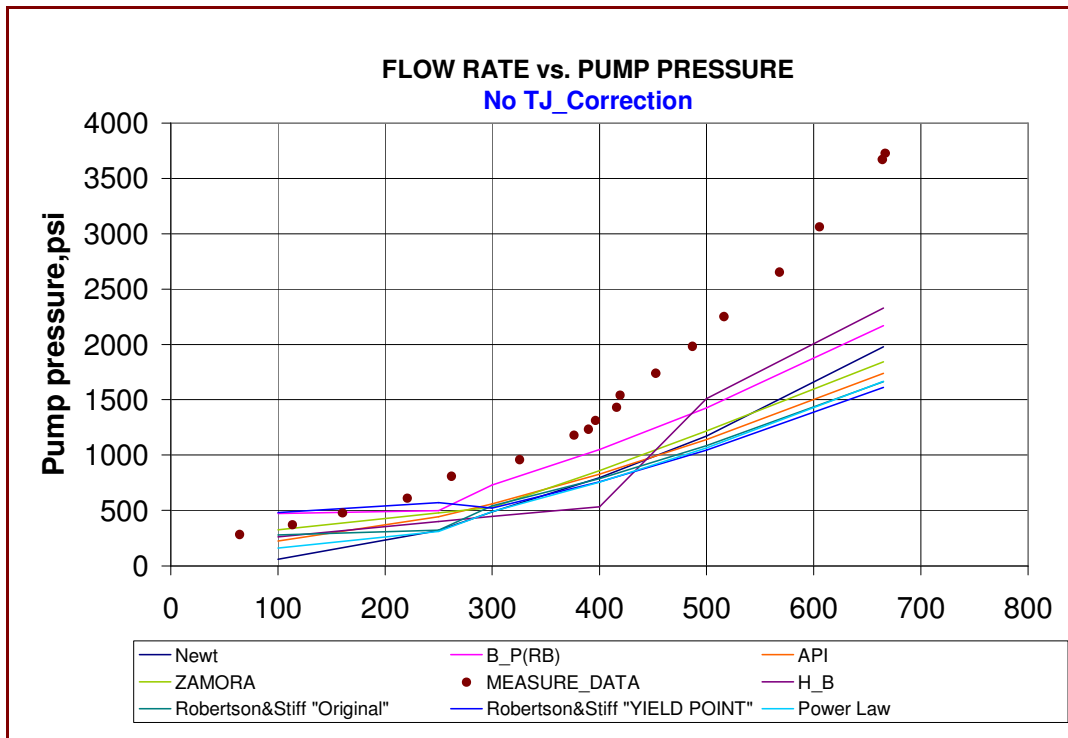


Fig. 9.1— Flow rate vs. pump pressure for eight rheological models at 150°F.

For this case, with the API RP 13D we found a relative error of 42 % between the measured and calculated pump pressure. Also, the best approximation was for the Bingham plastic model with 28%.

Now, let's consider the first approach, correction by enlargement and contraction, in the analysis. **Fig. 9.2** shows how the calculated pump pressure matches the measured data. API RP 13D presents a good fit with 10% relative error. However, the best match can be achieved with the unified model (6%). Note that the relative error consideration of enlargement and contraction significantly reduces the relative error.

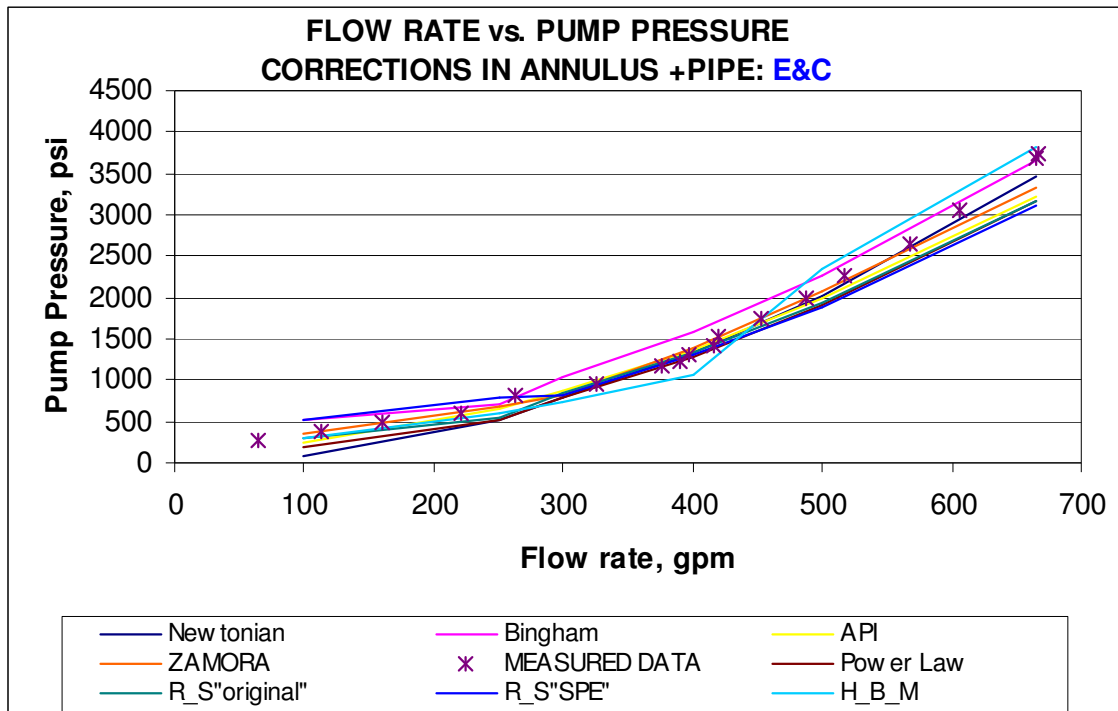


Fig. 9.2— Flow rate vs. pump pressure with E&C correction.

Fig. 9.3 shows that the match between pump calculated and measured pump pressure is not as good as the first approach when corrections depend on equivalent diameter. However, the improvement over uncorrected approaches is clear. All models except for Robertson and Stiff (original and yield point) present a good match; relative errors for this case are in a range of 54 to 62%.

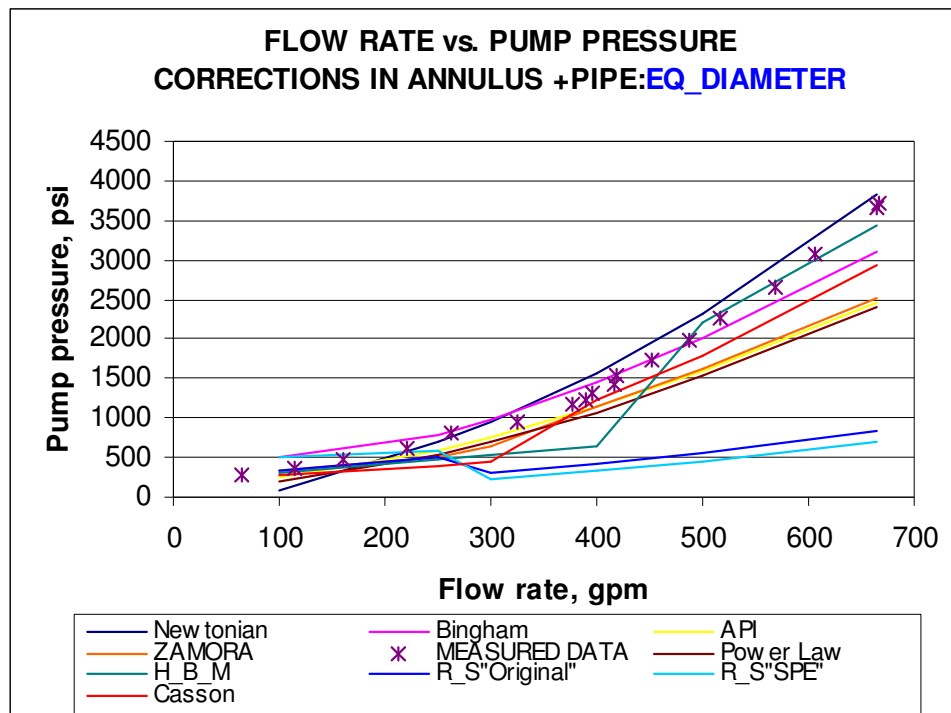


Fig. 9.3— Flow rate vs. pump pressure with ED correction.

Fig. 9.4 shows that the match between calculated and measured pump pressure is not as good as the first and the second approaches when two different IDs are considered. However, progress is obvious. The Casson model presents the best adjustment.

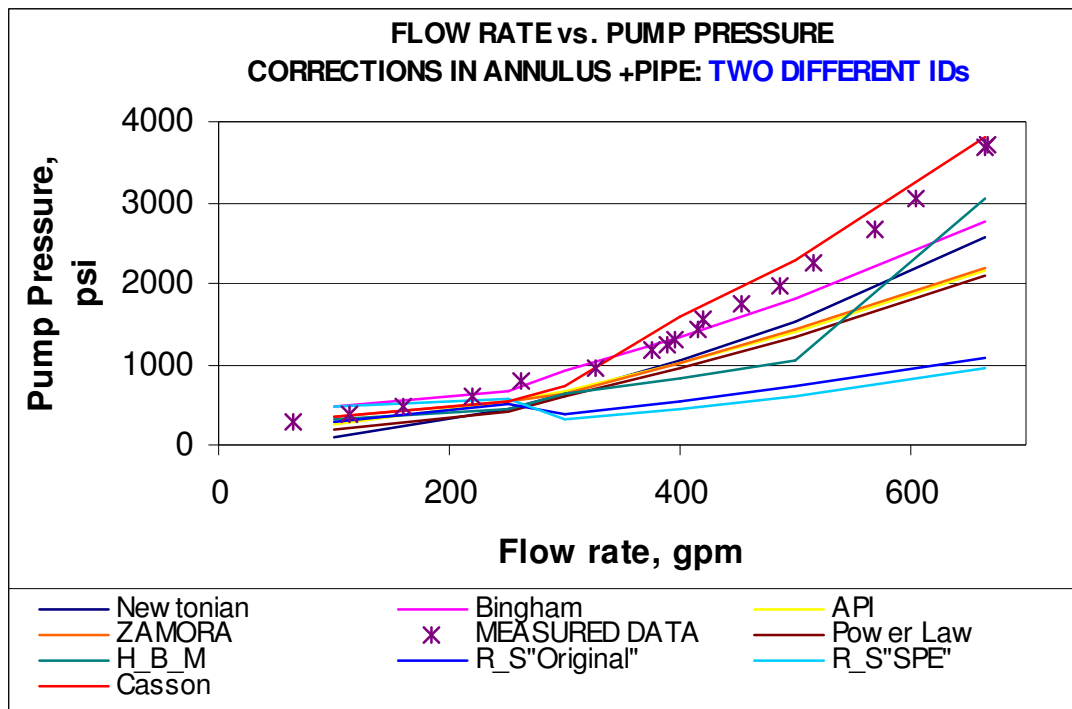


Fig. 9.4— Flow rate vs. pump pressure with correction for 2IDs

Now, let's consider the fourth approach, correction by enlargement and contraction plus equivalent diameter, in the analysis. **Fig. 9.5** shows how the calculated pump pressured matches the measured data. The API model presents a good fit with 15% relative error. However the best match can be achieved with the Unified model (12%).

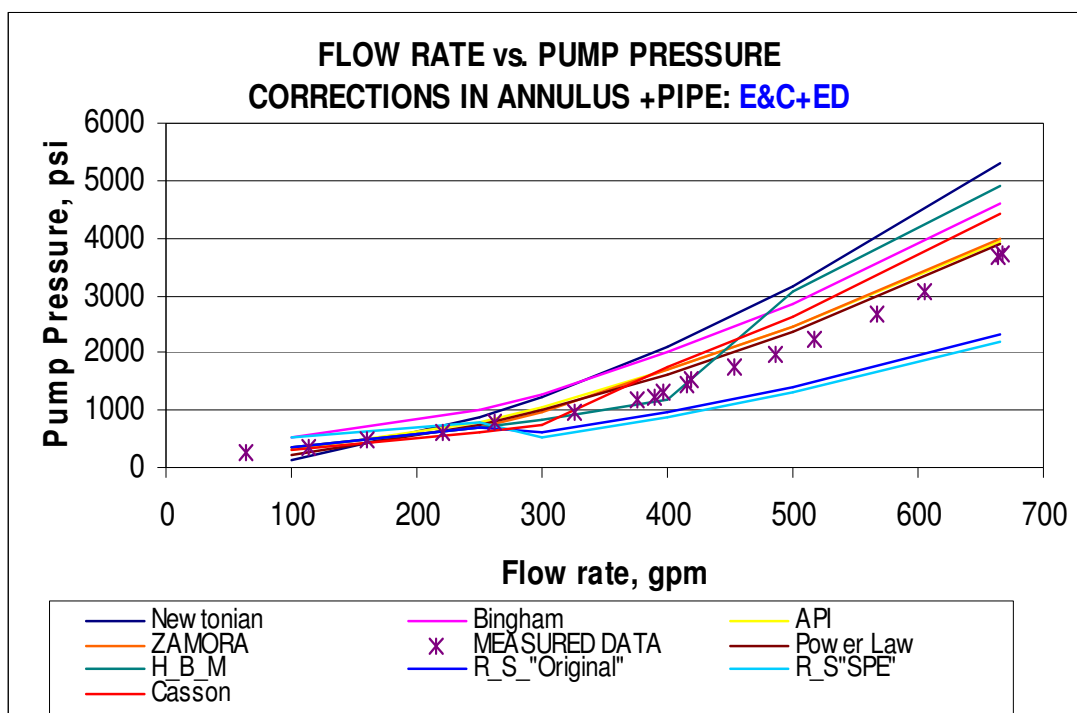


Fig. 9.5— Flow rate vs. pump pressure with correction for E&C+ ED.

Considering enlargement and contraction plus two different IDs in the fifth approach (**Fig. 9.6**), the match between calculated and measured pump pressure is really good. Also, this approach gives the best adjustment in comparison with the earlier approaches. The best rheological model that matches with the measured data are the API model with 9% relative error, the Unified model with 7% relative error and Herschel-Bulkley model with 8% relative error.

Table 9.2 shows more details.

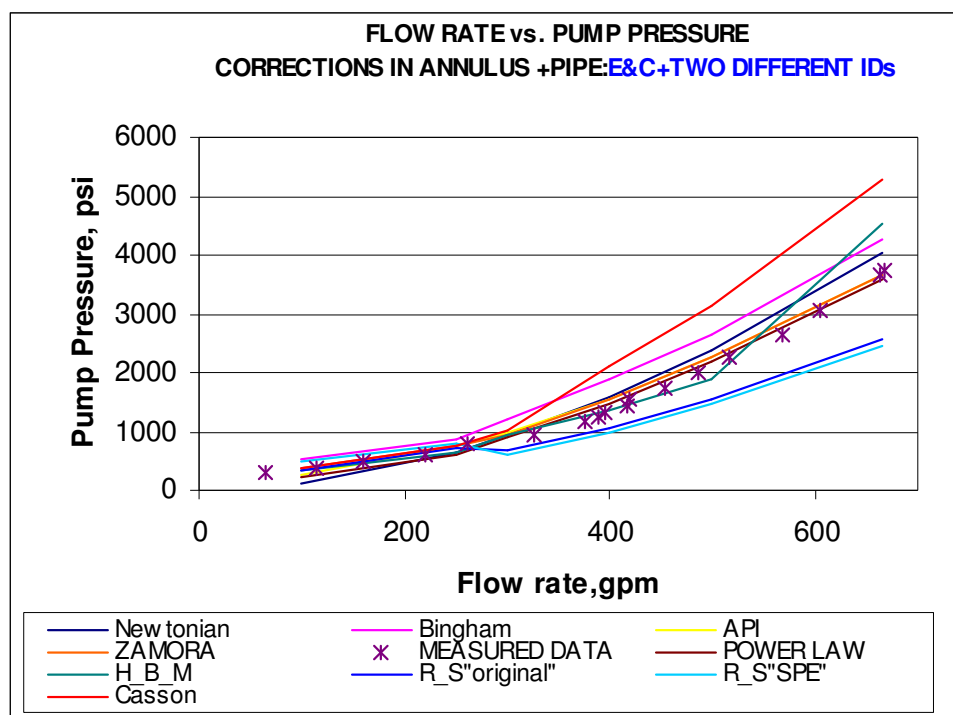


Fig. 9.6— Flow rate vs. pump pressure with correction for E&C+2IDs.

Table 9.2— Analysis of Five Corrections for Eight Rheological Models

RHEOLOGICAL MODELS, T=150 F	N C	E&C	TWO_ID	EQ_DIAM	E&C+TWO_ID	E&C+EQ_DIAM
NEWTONIAN MODEL	52	20	37	21	21	47
BINGHAM PLASTIC MODEL	28	17	16	23	31	55
POWER LAW MODEL	51	18	39	29	13	15
API MODEL	42	10	30	22	9	15
UNIFIED ZAMORA MODEL	35	6	25	22	7	12
HERSCHEL & BULKLEY MODEL	41	14	32	25	9	18
ROBERTSON &STIFF"original"	43	11	50	54	18	23
ROBERTSON &STIFF"yield point"	42	15	56	62	29	36
CASSON MODEL	40	8	14	15	29	21

Let's analyze what happened in the annulus. Inside the annulus, the velocity is lower if we compare it with the drillstring; as a consequence, the shear rate is reduced and the viscosity is increased.

Most of the cases, the drilling fluid inside the annulus behaves as shear-thinning fluid presenting a yield stress as a viscoplastic fluid does. This is the reason why the rheological models that can be simulated as shear-thinning with yield point have better results.

This is the case the shear-thinning Power Law model gives the best approximation. See Appendix E for more details.

CHAPTER X

CONCLUSIONS AND RECOMMENDATIONS

10.1 Conclusions

- The rheological models, Bingham, Power-law, API RP 13D, Herschel-Bulkley, Unified, Robertson and Stiff, and Casson have been evaluated for accurate representation of the wide range of shear stress/shear rate data. These models are confirmed to describe sufficiently the rheology of most non-Newtonian fluids.
- Selection of the best rheological model is of great importance in obtaining correct results for pressure drop and hydraulics. A simple and direct approach has been presented for selecting the best rheological model for any non-Newtonian fluid according to the lowest E_{AAP} criteria.
- The Casson model can be applied with high confidence to predict rheological properties and hydraulics calculations in oil-based mud. Also, this model can fit adequately many real yield stress fluids, with simply two parameters.
- The API model provides the best general prediction of rheological behavior for the mud samples studied. It was followed by Herschel-Bulkley, Robertson and Stiff, and Unified models. Correct pressure drop calculations can be achieved by using the E_{AAP} approach, since these calculations depend mainly on the selected model.
- A tool joint can increase pressure losses in the annulus and in the drillstring due to geometry effects of contraction and expansion. Current

API recommended drilling hydraulics calculation techniques (from RP 13D) do not include tool-joint parameters; the API calculations are not accurate. To dramatically reduce errors, practical methods have been developed to correct the pump pressure friction losses including the by tool joint effect.

- The proposed methods for predicting pressure losses by correcting for tool joint effects using Herschel-Bulkley, Unified, Casson and Robertson and Stiff models work well. The results were more accurate than those obtained with standards method using Bingham plastic and Power-law models.
- For mud samples studied, the E&C+2IDs and Unified model (after correction), followed by Herschel-Bulkley and API, and give the best approximation to measured pump pressure.

10.2 Recommendations

Considering other data sets is important because it gives us a major range to evaluate the rheological models as well as tool-joint corrections. Also, it gives as a result, a better interpretation and validation the study proposed for this research.

NOMENCLATURE

a	=	frictional fractions parameters, dimensionless.
a_1	=	transversal area of tool joint, in ² .
a_2	=	transversal area of pipe, in ² .
A	=	Robertson and Stiff model parameter similar to k , lbf.sec ^{B} /100 ft ² or dyne.sec ^{B} /100 cm ²
b	=	frictional fractions parameters, dimensionless
B	=	Robertson and Stiff model parameter similar to n , dimensionless
C	=	Robertson and Stiff model correction factor, 1/sec ^{B}
C_a	=	Casson number, dimensionless
C_c	=	Herschel-Bulkley model parameter, dimensionless
C_a^*	=	Herschel-Bulkley model parameter, dimensionless
d	=	internal diameter of wide pipe, in.
d_{ou}	=	internal Diameter of narrow pipe, in.
d_{TJ}	=	internal diameter of tool joint, in.
(dp/dL)	=	gradient pressure, psi/ft
$(dp/dL)_{ds}$	=	gradient pressure in drill string, psi/ft
$(dp/dL)_{TJ}$	=	gradient pressure in tool joint, psi/ft
D_e	=	equivalent Diameter, in.
D_{ea}	=	equivalent diameter between two annuli, in.
D_{ep}	=	equivalent diameter between two inside pipe diameter, in.
D_N	=	nozzle diameter, in.
D_p	=	inside pipe Diameter, in.
D_{TJ}	=	outside diameter of tool joint, in.
D_1	=	outside pipe diameter, in.
D_2	=	inside casing diameter, in.
E_{AAP}	=	absolute average percent error, %

f	=	friction factor, dimensionless
f_a	=	friction factor to the annulus, dimensionless
f_{laminar}	=	friction factor to laminar flow, dimensionless
f_p	=	friction factor to the pipe, dimensionless
f_{partial}	=	Intermediate friction factor (transient and turbulent), dimensionless
$f_{\text{transient}}$	=	friction factor to transient flow, dimensionless
$f_{\text{turbulent}}$	=	friction factor to turbulent flow, dimensionless
F_c	=	contraction mechanical energy loss, lbf ft/lbm
F_e	=	enlargement mechanical energy loss, lbf ft/lbm
g_c	=	conversion factor, 32.174 lbf ft/lbm sec ²
G	=	unified model parameter, dimensionless
k	=	consistence index, lbf.sec ^{n} /100ft ² or dyne.sec ^{n} /100cm ²
k_a	=	consistence index in the annulus, lbf.sec ^{n} /100ft ² or dyne.sec ^{n} /100cm ²
k_p	=	consistence index in the pipe, lbf.sec ^{n} /100ft ² or dyne.sec ^{n} /100cm ²
K_e	=	enlargement coefficient, dimensionless
K_c	=	contraction coefficient, dimensionless
m	=	slope
L	=	length, ft
$L_{\text{total dp}}$	=	total drillpipe length, ft
$L_{\text{total TJ}}$	=	total tool joint length, ft.
L_1	=	length of one tool joint (i.e. pin + box tong length), in
L_2	=	length of one drillpipe (without tool joint length), in
n	=	flow behavior index, dimensionless
n_a	=	flow behavior index in the annulus, dimensionless
n_p	=	flow behavior index in the pipe, dimensionless
N	=	number of shear rate/shear stress data

N_{DP}	=	numbers of drillpipe
N_{He}	=	Hedstrom number, dimensionless
N_{Re}	=	Reynolds number, dimensionless
N_{Rec}	=	critical value of Reynolds number, dimensionless
N_{TJ}	=	number of tool joints, total pipe length/30 ft
p	=	Pressure, psi
p_p	=	pump pressure, psi
q	=	flow rate, gallon/min
q_1	=	low flow rate to work for examples, gallon/min
q_2	=	high flow rate to work for examples, gallon/min
R	=	reading from rheometer
R_3	=	reading from rheometer at 3RPM
R_6	=	reading from rheometer at 6RPM
R_{600}	=	reading from rheometer at 600RPM
R_{300}	=	reading from rheometer at 300RPM
v	=	average velocity, ft/sec
v_a	=	annular average velocity, ft/sec
v_p	=	pipe average velocity, ft/sec
V	=	velocity from rheometer, RPM
y	=	Herschel & Bulkley model parameter, dimensionless
z	=	Herschel & Bulkley model parameter, dimensionless
β	=	ratio of diameters of small to large pipes, dimensionless
γ	=	shear rate, 1/sec
γ_w	=	wall shear rate, 1/sec
γ^*	=	shear rate value corresponding to the geometric mean of the shear stress, τ^*
γ_{min}	=	minimum shear stress value of data
γ_{max}	=	maximum shear stress value of data

ΔL	=	change in length, ft
Δp	=	pressure loss, psi
Δp_a	=	frictional pressure drop in the annulus, psi
Δp_b	=	frictional pressure loss across the bit, psi
Δp_{dc}	=	frictional pressure loss inside the drill collars, psi
Δp_{dp}	=	frictional pressure loss inside the drillpipe, psi
Δp_{ds}	=	frictional pressure loss inside the drill string, psi
Δp_s	=	frictional pressure loss in the surface equipment, psi
Δp_{TJ}	=	tool joint pressure loss, psi
Δp_p	=	pump pressure loss, psi
$(\Delta p_{\text{Total/2IDs}})_{ds}$	=	total pressure drop in the drillstring after 2IDs correction, psi
$(\Delta p_{\text{Total 2IDs}})_a$	=	total pressure drop in the annulus after 2IDs correction, psi
θ	=	angle of divergence on convergence, degrees
λ	=	Robertson and Stiff model parameter, in.
μ	=	viscosity, cp
μ_p	=	plastic viscosity, cp
μ_a	=	apparent viscosity for Newtonian fluid at 300 R ₃₀₀ , cp
μ_e	=	equivalent viscosity, cp
μ_c	=	Casson plastic viscosity, lbf.sec/100 ft ²
ρ	=	density, Lbm/gal
τ	=	shear stress, lbf/100 ft ²
τ_c	=	Casson yield stress, lbf/100 ft ²
$\tau_{\text{calculated}}$	=	calculated shear stress, lbf/100 ft ²
τ_{max}	=	Maximum shear stress value of data, lbf/100 ft ²

τ_{measured}	=	measured shear stress, lbf/100 ft ²
τ_{min}	=	Minimum shear stress value of data, lbf/100 ft ²
τ_w	=	wall shear stress, lbf/100 ft ²
τ_y	=	yield point, lbf/100 ft ²
τ_{yL}	=	lower shear yield point, lbf/100ft ²
τ_o	=	yield stress, lbf/100 ft ²
τ^*	=	shear stress value corresponding to the geometric mean of the shear rate, $\dot{\gamma}^*$

REFERENCES

- 1 "Recommended Practice on the Rheology and Hydraulics of Oil-Well Drilling Fluids, API RP 13D", Fourth Edition. American Petroleum Institute, (June 1995).
- 2 Zamora, M. and Power, D.: "Making a Case for AADE Hydraulics and the Unified Rheological Model," paper AADE-02-DFWM-HO-13 presented at the 2002 AADE Technical Conference, Houston, 2-3 April.
- 3 Thivolle, S.: "A New Practical Rheology Model for HPHT Fluid," paper presented for M. Eng. degree Texas A&M University. College Station, Texas (2004).
- 4 Herzhaft, B., Rousseau, L., Neau, L., Moan, M. and Bossard, F.: "Influence of Temperature and Clays/Emulsion Microstructure on Oil-Based Mud Low Shear Rate Rheology," paper SPE 86197 presented at the 2002 SPE Annual Technical Conference and Exhibition, San Antonio, 29 September-2 October.
- 5 Power, D. and Zamora, M.: "Drilling Fluid Yield Stress: Measurement Techniques for Improved Understanding of Critical Drilling Fluid Parameters," paper AADE-03-NTCE-35 presented at the 2003 AADE Technical Conference, Houston, 1-3 April.
- 6 Politte, M.D.: "Invert Oil Mud Rheology as a Function of Temperature," paper SPE 13458 presented at the 1985 SPE/IADC, New Orleans, 6-8 March.
- 7 Davison, J.M., Clary, S., Saasen, A., Allouche, M., Bodin, D. *et al.*: "Rheology of Various Drilling Fluid Systems Under Deepwater Drilling Conditions and the Importance of Accurate Predictions of Downhole Fluid Hydraulics," paper SPE 56632 presented at the 1999 SPE Annual Technical Conference, Houston, 3-6 October.

- 8 Adamson, K., Birch, G., Gao, E., Hand, S., Macdonald, C. *et al.*: "High Pressure, High Temperature Well Construction," *Oilfield Review* (Summer 1998) 36.
- 9 White, W. and Zamora, M.: "Downhole Measurements of Synthetic-Based Drilling Fluid in an Offshore Well Quantify Dynamic Pressure and Temperature Distributions," paper SPE 35057 presented at the 1997 SPE Drilling Conference, New Orleans, 12-15 March.
- 10 Denison, E.: "Pressure Losses Inside Tool Joints Can Alter Drilling Hydraulics," paper presented at the 1977 Energy Technology Conference and Exhibitions, Houston, 18-22 September.
- 11 Yeon-Tae, J. and Subhash, S.: "Analysis of Tool Joint Effects for Accurate Friction Pressure Loss Calculations," paper SPE 87182 presented at the 2004 SPE Drilling Conference, Dallas, 2-4 March.
- 12 Barnes, H.A., Hutton, J.F. and Walters, K.: *An Introduction to Rheology*, Elsevier, Amsterdam,(1989).
- 13 Macosko, C.W.: *Rheology: Principles, Measurements, and Applications*, Wiley-VCH, New York (1994).
- 14 Bourgoyne, A.T., Chenevert, M.E., Millheim, K.K. and Young, F.S.: *Applied Drilling Engineering*, SPE, Richardson, Texas (1991) 2.
- 15 Lummus, J. and Azar, J.J.: *Drilling Fluids Optimization*; Penn Well Publishing Company, Tulsa, Oklahoma (1986).
- 16 Lima, H.: "A Dynamic Model of Well Hydraulics in Deepwater Riserless Drilling Operations Using Synthetic-Based Drilling Fluid," Ph.D. dissertation, Texas A&M University, College Station, 1998.
- 17 Zamora, M. and Sanjit, R.: "Using True Real-Time Data Interpretation to Facilitate Deepwater Drilling," paper AADE 01-NC-HO-09 presented at 2001 AADE National Drilling Conference, Houston, 27-29 March.
- 18 Becker, R.G.,Morgan, W.C, Chin, J.E. and Griffith, J.: "Improved Rheology Model and Hydraulics Analysis for Tomorrow's Wellbore Fluid

- Applications,” paper SPE 82415 presented at the 2003 Production and Operations Symposium, Tulsa, Oklahoma, 22-25 March.
- 19 Lauzon, R.V and Reid, K.I.G.: “New Rheological Model Offers Field Alternative,” *Oil and Gas Journal*, (May 1979) 51.
 - 20 Versan, M. and Tolga, A.: “Effect of Polymers on the Rheological properties of KCl/Polymer Type Drilling Fluid,” *Energy Sources*, (2005) **27**,405.
 - 21 Robertson, R.E. and Stiff, H.A.: “An Improved Mathematical Model for Relating Shear Stress to Shear Rate in Drilling Fluid and Cement Slurries,” *Trans, AIME*, (1976). **26**,31.
 - 22 Ohen, H.A. and Blick, E.F.: “Golden Section Search Method for Determining Parameters in Robertson-Stiff non-Newtonian fluid Model,” *J. Petroleum Science and Engineering*, (1990) **4**, 309.
 - 23 Merlo, A., Maglione, R., and Piatti, C.: “An Innovative Model for Drilling Fluid Hydraulics,” paper SPE 29259 presented at 1995 SPE Oil and Gas Conference, Kuala Lumpur, 20-22 March.
 - 24 Zamora, M., Roy, S. and Slater, K.: “Comparing a Basic Set of Drilling Fluid Pressure-Loss Relationships to Flow-Loop and Field Data,” paper AADE-05-NTCE-27 presented at the AADE 2005 National Technical Conference and Exhibition, Houston, 5-7 April.
 - 25 Mojisola, E.: “Development and Evaluation of Various Drilling Fluids for Slim Hole Wells,” M.S. thesis, The University of Oklahoma, Norman, 2005.
 - 26 Lenschow, J.: “Pressure Drop Calculations for Drilling Fluid,” paper SPE 25520 submitted to SPE for consideration for publication in one of its technical journals, 1992, 10 Aug.
 - 27 Ayeny, O.: “Evaluation of Commonly Used Fluid Rheological Models Using Developed Drilling Hydraulics Simulator,” presented at 2004 Canadian International Petroleum Conference, Calgary, 8-10 June.

- 28 Zeiad, A.: "New Monographs for Estimating Pressure Drop of Non-Newtonian Fluids Through Pipes and Annuli," *Polymer-Plastics Technology and Engineering*, (1996) **35**, 801.
- 29 Beirute, R. and Flumerfeldt, R.: "An Evaluation of the Robertson-Stiff Model Describing Rheological Properties of Drilling Fluids and Cement Slurries," *Society of Petroleum Engineers Journal*, April, (1976) 97.
- 30 Hanks, R.: "Laminar-Turbulent Transition in Pipeflow of Casson Model Fluids," *J. of Energy Resources Technology*, (1981) **103**, 318.
- 31 International Association of Drilling Contractors.: *Drilling Manual*, 9th Edition, Houston, Texas, June 1974.
- 32 Schlumberger Ltd.: *The Oilfield Glossary: Where the Oil Field Meets the Dictionary*, Available at: <http://glossary.oilfield.slb.com/> (accessed in August 2005)
- 33 "Flow of Fluid", Technical Paper 410, Crane Co., Chicago, (1988).
- 34 Gibson, A.H.: *Hydraulics and Its Applications*, Second Edition, Constable & C. Ltd. New York, (1922).

APPENDIX A

Table A1—Rheology and Hydraulics Equations for Newtonian Model.

Hydraulics Equations: NEWTONIAN MODEL, $\tau = \mu \dot{\gamma}$	
Pipe Flow	Annular Flow
$v_p = \frac{0.408 q}{D_p^2}$ <p style="text-align: right;">ft/sec</p>	$v_a = \frac{0.408 q}{D_2^2 - D_1^2}$ <p style="text-align: right;">ft/sec</p>
$\mu_a = R_{300}$ <p style="text-align: right;">cp</p>	
$N_{Re} = \frac{928 D_p v_p \rho}{\mu_a}$	$N_{Re} = \frac{757 (D_2 - D_1) v_a \rho}{\mu_a}$
Laminar ($N_{Re} < 2,100$) $f_p = \frac{16}{N_{Re}}$	Laminar ($N_{Re} < 2,100$) $f_a = \frac{16}{N_{Re}}$
Turbulent $f_p = \frac{0.0791}{N_{Re}^{0.25}}$	Turbulent $f_a = \frac{0.0791}{N_{Re}^{0.25}}$
$\left(\frac{dp}{dL} \right) = \frac{f_p v_p^2 \rho}{25.81 D_p}$ <p style="text-align: right;">psi/ft</p> $\Delta p = \left(\frac{dp}{dL} \right) \Delta L$ <p style="text-align: right;">psi</p>	$\left(\frac{dp}{dL} \right) = \frac{f_a v_a^2 \rho}{25.81 (D_2 - D_1)}$ <p style="text-align: right;">psi/ft</p> $\Delta p = \left(\frac{dp}{dL} \right) \Delta L$ <p style="text-align: right;">psi</p>
$\Delta p_{Nozzles}, psi = \frac{156 \rho q^2}{(D_{N1}^2 + D_{N2}^2 + D_{N3}^2)^2}$ <p style="text-align: right;">Marilyn Vilorio, April 2006</p>	

Table A2—Rheology and Hydraulics Equations for Bingham Plastics Model.

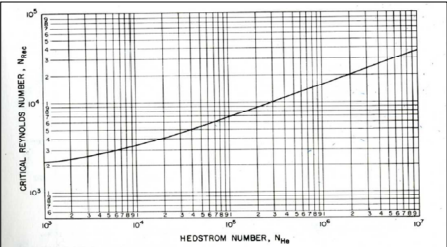
Hydraulics Equations: BINGHAM PLASTIC MODEL, $\tau = \tau_y + \mu_p \dot{\gamma}$	
Pipe Flow	Annular Flow
$v_p = \frac{0.408 q}{D_p^2}$ <p style="text-align: right;">ft/sec</p>	$v_a = \frac{0.408 q}{D_2^2 - D_1^2}$ <p style="text-align: right;">ft/sec</p>
$\mu_p = R_{600} - R_{300}$ <p style="text-align: right;">cp</p>	
$\tau_y = R_{300} - \mu_p$ <p style="text-align: right;">lbf/100 ft²</p>	
$\mu_a = \mu_p + \frac{5\tau_y D_p}{v_p}$ <p style="text-align: right;">cp</p>	$\mu_a = \mu_p + \frac{5\tau_y (D_2 - D_1)}{v_a}$ <p style="text-align: right;">cp</p>
Turbulence Criteria #1 $N_{Re} = \frac{928 D_p v_p \rho}{\mu_a}$ <p>($N_{Re} < 2,100$) → LAMINAR FLOW</p> $f_p = \frac{16}{N_{Re}}$	$N_{Re} = \frac{757 (D_2 - D_1) v_p \rho}{\mu_a}$ <p>($N_{Re} < 2,100$) → LAMINAR FLOW</p> $f_a = \frac{16}{N_{Re}}$
Turbulence Criteria #2 $He = \frac{37,100 \rho \tau_y D_p^2}{\mu_p^2}$ $N_{Re} = \frac{928 D_p v_p \rho}{\mu_p}$	$D_e = 0.816 (D_2 - D_1)$ $He = \frac{37,100 \rho \tau_y D_e^2}{\mu_p^2}$ $N_{Re} = \frac{928 D_e v_a \rho}{\mu_p}$
 <p>Critical Reynolds Numbers for Bingham Plastic Model</p>	<p>($N_{Re} < N_{Rec}$) LAMINAR FLOW. Use f as criteria #1</p> <p>($N_{Re} > N_{Rec}$) TURBULENT FLOW. Use the following equation:</p> $f_{p,a} = \frac{0.0791}{N_{Re}^{0.25}}$ <p>This friction equation is valid for both annular and pipe</p>
$\left(\frac{dp}{dL} \right) = \frac{f_p v_p^2 \rho}{25.81 D_p}$ <p style="text-align: right;">psi/ft</p> $\Delta p = \left(\frac{dp}{dL} \right) \Delta L$ <p style="text-align: right;">psi</p>	$\left(\frac{dp}{dL} \right) = \frac{f_a v_a^2 \rho}{25.81 (D_2 - D_1)}$ <p style="text-align: right;">psi/ft</p> $\Delta p = \left(\frac{dp}{dL} \right) \Delta L$ <p style="text-align: right;">psi</p>
$\Delta p_{Nozzles, psi} = \frac{156 \rho q^2}{(D_{N1}^2 + D_{N2}^2 + D_{N3}^2)^2}$ <p style="text-align: right;">Marilyn Viloria, June 2006</p>	

Table A3—Rheology and Hydraulics Equations for Power Law Model.

Hydraulics Equations: POWER LAW MODEL, $\tau = k \dot{\gamma}^n$	
Pipe Flow	Annular Flow
$n = 3.32 \log \left(\frac{R_{600}}{R_{300}} \right)$ $k = \frac{510 R_{300}}{511^n}$	
eq_cps=dyne sec ⁿ /100 cm ²	
$v_p = \frac{0.408 q}{D_p^2}$	$v_a = \frac{0.408 q}{D_2^2 - D_1^2}$
ft/sec	ft/sec
$N_{Re} = \frac{89100 \rho v_p^{2-n}}{k} \left(\frac{0.0416 D_p}{3 + \frac{1}{n}} \right)^n$	$N_{Re} = \frac{109000 \rho v_a^{2-n}}{k} \left[\frac{0.0208 (D_2 - D_1)}{2 + \frac{1}{n}} \right]^n$
Laminar $N_{Re} \leq 3470 - 1370 n$	
$\left(\frac{dp}{dL} \right) = \frac{k v_p^n \left(\frac{3 + 1/n}{0.0416} \right)^n}{144000 D_p^{1+n}}$	$\left(\frac{dp}{dL} \right) = \frac{k v_a^n \left(\frac{2 + 1/n}{0.0208} \right)^n}{144000 (D_2 - D_1)^{1+n}}$
Turbulent $N_{Re} \geq 4270 - 1370 n$	Turbulent $N_{Re} \geq 4270 - 1370 n$
$a = \frac{\log n + 3.93}{50}$	$b = \frac{1.75 - \log n}{7}$
$f_p = \frac{a}{N_{Re}^b}$	$f_a = \frac{a}{N_{Re}^b}$
$\left(\frac{dp}{dL} \right) = \frac{f_p v_p^2 \rho}{25.81 D_p}$	$\left(\frac{dp}{dL} \right) = \frac{f_a v_a^2 \rho}{25.81 (D_2 - D_1)}$
psi/ft	psi/ft
$\Delta p = \left(\frac{dp}{dL} \right) \Delta L$	$\Delta p = \left(\frac{dp}{dL} \right) \Delta L$
psi	psi
$\Delta p_{Nozzles} = \frac{156 \rho q^2}{(D_{N1}^2 + D_{N2}^2 + D_{N3}^2)^2}$	
psi	
Marilyn Viloria, June 2006	

Table A4—Rheology and Hydraulics Equations for API RP13D Model.

Hydraulics Equations: API RP 13D, $\tau = k \dot{\gamma}^n$	
Pipe Flow	Annular Flow
$n_p = 3.32 \log \left(\frac{R_{600}}{R_{300}} \right)$	$n_a = 0.657 \log \left(\frac{R_{100}}{R_3} \right)$
$k_p = \frac{5.11 R_{600}}{1,022^{n_p}}$ dyne sec ⁿ /cm ²	$k_a = \frac{5.11 R_{100}}{170.2^{n_a}}$ dyne sec ⁿ /cm ²
$v_p = \frac{0.408 q}{D_p^2}$ ft/sec	$v_a = \frac{0.408 q}{D_2^2 - D_1^2}$ ft/sec
$\mu_e = 100 k_p \left(\frac{96 v_p}{D_p} \right)^{n_p-1} \left(\frac{3 n_p + 1}{4 n_p} \right)^{n_p}$ cp	$\mu_e = 100 k_a \left(\frac{144 v_a}{D_2 - D_1} \right)^{n_a-1} \left(\frac{2 n_a + 1}{3 n_a} \right)^{n_a}$ cp
$N_{Re} = \frac{928 D v_p \rho}{\mu_e}$	$N_{Re} = \frac{928 (D_2 - D_1) v_a \rho}{\mu_e}$
Laminar (N_{Re} < 2,100) $f_p = \frac{16}{N_{Re}}$	Laminar (N_{Re} < 2,100) $f_a = \frac{24}{N_{Re}}$
Turbulent $\left. \begin{aligned} a &= \frac{\log n_p + 3.93}{50} \\ b &= \frac{1.75 - \log n_p}{7} \end{aligned} \right\} f_p = \frac{a}{N_{Re}^b}$	Turbulent $\left. \begin{aligned} a &= \frac{\log n_a + 3.93}{50} \\ b &= \frac{1.75 - \log n_a}{7} \end{aligned} \right\} f_a = \frac{a}{N_{Re}^b}$
$\left(\frac{dp}{dL} \right) = \frac{f_p v_p^2 \rho}{25.81 D_p}$ psi/ft $\Delta p = \left(\frac{dp}{dL} \right) \Delta L$ psi	$\left(\frac{dp}{dL} \right) = \frac{f_a v_a^2 \rho}{25.81 (D_2 - D_1)}$ psi/ft $\Delta p = \left(\frac{dp}{dL} \right) \Delta L$ psi
$\Delta p_{Nozzles} = \frac{156 \rho q^2}{(D_{N1}^2 + D_{N2}^2 + D_{N3}^2)^2}$	
psi	
HCJ May 30, 2002	

Table A5—Rheology and Hydraulics Equations for Herschel-Bulkley Model.

Hydraulics Equations: HERSCHEL-BULKLEY MODEL, $\tau = \tau_0 + k \dot{\gamma}^n$	
Pipe Flow	Annular Flow
$\tau_0 = \frac{\tau^{*2} - \tau_{\min} \tau_{\max}}{2\tau^* - \tau_{\min} - \tau_{\max}}$ <p style="text-align: right;">$\tau_0 = \text{lbf}/100\text{sq ft}$</p> <p>where τ^* is the shear stress value corresponding to the geometric mean of the shear rate, $\dot{\gamma}^*$</p> $\dot{\gamma}^* = \sqrt{\dot{\gamma}_{\min} \dot{\gamma}_{\max}}$ <p style="text-align: right;">$\dot{\gamma} = 1/\text{sec}$</p> $\log(\tau - \tau_0) = \log(k) + n \log(\dot{\gamma}) \quad \left\{ \begin{array}{l} n = \frac{\sum \log(\tau - \tau_0) \sum \log(\dot{\gamma}) - N \sum (\log(\tau - \tau_0) \log(\dot{\gamma}))}{(\sum \log \dot{\gamma})^2 - N \sum (\log \dot{\gamma})^2} \\ \log(k) = \frac{\sum \log(\tau - \tau_0) - n \sum \log(\dot{\gamma})}{N} \end{array} \right.$ <p style="text-align: right;">$n = \text{DIMENSIONLESS}$ N=data number $k = \text{lbf} \cdot \text{sec}^n / 100\text{sq ft}$</p>	
$v_p = \frac{0.408 q}{D_p^2}$	$v_a = \frac{0.408 q}{D_2^2 - D_1^2}$
ft/sec	ft/sec
$N_{Re} = \left[\frac{2(3n+1)}{n} \right] \left\{ \frac{\rho v_p^{(2-n)} \left(\frac{D_p}{2} \right)^n}{\tau_0 \left(\frac{D_p}{2v_p} \right)^n + k \left[\frac{(3n+1)}{nC_c} \right]^n} \right\}$	$N_{Re} = \left[\frac{4(2n+1)}{n} \right] \left\{ \frac{\rho v_a^{(2-n)} \left(\frac{D_2 - D_1}{2} \right)^n}{\tau_0 \left(\frac{D_2 - D_1}{2v_a} \right)^n + k \left[\frac{2(2n+1)}{nC_a^*} \right]^n} \right\}$
D=ft	D=ft
$\rho = \text{lbm}/\text{ft}^3$	$\rho = \text{lbm}/\text{ft}^3$
$N_{Re\ c} = \left[\frac{4(3n+1)}{ny} \right]^{\frac{1}{1-z}}$	$N_{Re\ c} = \left[\frac{8(2n+1)}{ny} \right]^{\frac{1}{1-z}}$
$y = \frac{\log n + 3.93}{50}$	$z = \frac{1.75 - \log n}{7}$
Laminar $N_{Re} < N_{Re\ c}$	
$\left(\frac{dp}{dL} \right) = \frac{4k}{14400D_p} \left\{ \left(\frac{\tau_0}{k} \right) + \left[\frac{(3n+1)}{nC_c} \left(\frac{8q}{\pi D_p^3} \right) \right]^n \right\}$	$\left(\frac{dp}{dL} \right) = \frac{4k}{14400(D_2 - D_1)} \left\{ \left(\frac{\tau_0}{k} \right) + \left[\frac{16(2n+1)}{nC_a^*(D_2 - D_1)} \left[\frac{q}{\pi(D_2^2 - D_1^2)} \right] \right]^n \right\}$
q= ft ³ /s	q= ft ³ /s
dp/dL=psi/ft	dp/dL=psi/ft
k=lbf*sec ⁿ /100ft ²	k=lbf*sec ⁿ /100ft ²
Turbulent $N_{Re} > N_{Re\ c}$	
$f_p = y(C_c N_{Re})^{-z}$	$f_a = y(C_a^* N_{Re})^{-z}$
$C_c = 1 - \left(\frac{1}{2n+1} \right) \frac{\tau_0}{\tau_0 + k \left[\frac{(3n+1)q}{n\pi(D_p/2)^3} \right]^n}$	$C_a^* = 1 - \left(\frac{1}{n+1} \right) \frac{\tau_0}{\tau_0 + k \left\{ \left[\frac{2(2n+1)}{n((D_2/2) - (D_1/2))} \right] \left[\frac{q}{\pi(D_2^2/2 - (D_1/2)^2)} \right] \right\}^n}$
$\left(\frac{dp}{dL} \right) = \frac{f_p q^2 \rho}{144 \pi^2 D_p^5}$	$\left(\frac{dp}{dL} \right) = \frac{f_a q^2 \rho}{144 \pi^2 (D_2 - D_1)(D_2^2 - D_1^2)^2}$
psi/ft	psi/ft
$\Delta p = \left(\frac{dp}{dL} \right) \Delta L$	$\Delta p = \left(\frac{dp}{dL} \right) \Delta L$
psi	psi
$\Delta p_{\text{Nozzles, psi}} = \frac{156 \rho q^2}{(D_{N1}^2 + D_{N2}^2 + D_{N3}^2)^2}$	
Marilyn Vilorio, June 2006	

Table A6—Rheology and Hydraulics Equations for Unified Model.

Hydraulics Equations: Unified Rheological Model, $\tau = \tau_o + k \dot{\gamma}^n$	
Pipe Flow	Annular Flow
$\mu_p = R_{600} - R_{300}$	$\tau_o = 1.066 (2 R_3 - R_6)$
$n_p = 3.32 \log \left(\frac{2\mu_p + \tau_y}{\mu_p + \tau_y} \right)$ $k_p = 1.066 \left(\frac{\mu_p + \tau_y}{511^{n_p}} \right)$	$n_a = 3.32 \log \left(\frac{2\mu_p + \tau_y - \tau_o}{\mu_p + \tau_y - \tau_o} \right)$ $k_a = 1.066 \left(\frac{\mu_p + \tau_y - \tau_o}{511^{n_a}} \right)$
$G = \left(\frac{(3-\alpha)n+1}{(4-\alpha)n} \right) \left(1 + \frac{\alpha}{2} \right)$	
$\alpha=1$ for annuli $\alpha=0$ for pipe	
$v_p = \frac{24.51 q}{D^2}$	$v_a = \frac{24.51 q}{D_2^2 - D_1^2}$
$\gamma_w = \frac{1.6 * G * v}{D_e}$	
$\tau_w = \left[\left(\frac{4-\alpha}{3-\alpha} \right)^n \tau_o + k \gamma_w^n \right]$	
$N_{Re_p} = \frac{\rho v_p^2}{19.36 \tau_w}$	$N_{Re_a} = \frac{\rho v_a^2}{19.36 \tau_w}$
Laminar: $f_{\text{laminar}} = \frac{16}{N_{Re}}$ Transient: $f_{\text{transient}} = \frac{16 N_{Re}}{(3470 - 1370 n_p)^2}$ Turbulent: $a = \frac{\log n + 3.93}{50}$ $b = \frac{1.75 - \log n}{7}$	Laminar: $f_{\text{laminar}} = \frac{24}{N_{Re}}$ Transient: $f_{\text{transient}} = \frac{16 N_{Re}}{(3470 - 1370 n_a)^2}$ Turbulent: $a = \frac{\log n + 3.93}{50}$ $b = \frac{1.75 - \log n}{7}$
$f_{\text{partial}} = (f_{\text{transient}}^{-8} + f_{\text{turbulent}}^{-8})^{-1/8}$	
$f_p = (f_{\text{partial}}^{12} + f_{\text{laminar}}^{12})^{1/12}$	$f_a = (f_{\text{partial}}^{12} + f_{\text{laminar}}^{12})^{1/12}$
$\left(\frac{dp}{dL} \right) = 1.076 \frac{f_p v_p^2 \rho}{10^5 D_p}$	$\left(\frac{dp}{dL} \right) = \frac{1.076 f_a v_a^2 \rho}{10^5 D_e}$
$\Delta p = \left(\frac{dp}{dL} \right) \Delta L$	$\Delta p = \left(\frac{dp}{dL} \right) \Delta L$
$\Delta p_{\text{Nozzles}} = \frac{156 \rho q^2}{(D_{N1}^2 + D_{N2}^2 + D_{N3}^2)^2}$	

Table A7—Rheology and Hydraulics Equations for Robertson and Stiff Model “Original”.

Hydraulics Equations: ROBERTSON AND STIFF MODEL "Original", $\tau = A(\dot{\gamma} + C)^B$	
Pipe Flow	Annular Flow
$C = \frac{\gamma_{\min} * \gamma_{\max} - \gamma^{*2}}{2\gamma^* - \gamma_{\min} - \gamma_{\max}}$ $\log(\tau) = \log(A) + B\log(\dot{\gamma}) \quad \left\{ \begin{array}{l} B = \frac{\sum \log \tau \cdot \sum \log(\dot{\gamma} + C) - N \cdot \sum (\log \tau \cdot \log(\dot{\gamma} + C))}{[\sum \log(\dot{\gamma} + C)^2 - N \cdot \sum \log(\dot{\gamma} + C)]^2} \\ \log(A) = \frac{\sum \log \tau - B \cdot \sum \log(\dot{\gamma} + C)}{N} \end{array} \right.$	
$\frac{1}{\text{sec}^B}$	DIMENSIONLESS
$v_p = \frac{0.408}{D_p^2} \frac{q}{\text{ft/sec}}$	$v_a = \frac{0.408}{D_2^2 - D_1^2} \frac{q}{\text{ft/sec}}$
$N_{RE} = \frac{89100}{A} \frac{\rho v_p^{2-B}}{D_p} \left(\frac{0.416 D_p}{3 + \frac{1}{B}} \right)^B$	$N_{RE} = \frac{109000}{A} \frac{\rho v_a^{2-B}}{D_2^2 - D_1^2} \left[\frac{0.0208 (D_2 - D_1)}{2 + \frac{1}{B}} \right]^B$
$v = \text{ft/sec}$	$v = \text{ft/sec}$
$A = \text{dyne sec}^B / 100 \text{cm}^2 = \text{eq cp}$	$A = \text{dyne sec}^B / 100 \text{cm}^2 = \text{eq cp}$
Laminar	Laminar
$N_{RE} \leq 3470 - 1370B$	$N_{RE} \leq 3470 - 1370B$
$\left(\frac{dp}{dL} \right) = 8.33E - 4 \times 2^{2+B} \times A \left\{ \left(\frac{1+3B}{B} \right) \left[\frac{0.2v_p + \frac{C}{6} D_p}{D_p^{\left(\frac{1+B}{B} \right)}} \right] \right\}^B$	$\left(\frac{dp}{dL} \right) = 8.33E - 4 \times 4^{1+B} \times A \left\{ \left(\frac{1+2B}{B} \right) \left[\frac{0.2v_a + \frac{C}{8} (D_2 - D_1)}{(D_2 - D_1)^{\left(\frac{1+B}{B} \right)}} \right] \right\}^B$
$\frac{dp}{dL} = \text{psi/ft}$	$\frac{dp}{dL} = \text{psi/ft}$
$D = \text{in}$	$D = \text{in}$
$v = \text{ft/min}$	$v = \text{ft/min}$
$A = \text{lb} \cdot \text{sec}^B / 100 \text{sq ft}$	$A = \text{lb} \cdot \text{sec}^B / 100 \text{sq ft}$
Turbulent	Turbulent
$N_{Re} \geq 4270 - 1370 B$	$N_{Re} \geq 4270 - 1370 B$
$a = \frac{\log B + 3.93}{50}$	$b = \frac{1.75 - \log B}{7}$
$f_p = \frac{a}{N_{Re}^b}$	$f_a = \frac{a}{N_{Re}^b}$
$\left(\frac{dp}{dL} \right) = \frac{f_p v_p^2 \rho}{25.81 D_p}$	$\left(\frac{dp}{dL} \right) = \frac{f_a v_a^2 \rho}{25.81 (D_2 - D_1)}$
$\Delta p = \left(\frac{dp}{dL} \right) \Delta L$	$\Delta p = \left(\frac{dp}{dL} \right) \Delta L$
$\Delta p = \text{psi}$	$\Delta p = \text{psi}$
$\Delta p_{\text{Nozzles}, \text{psi}} = \frac{156 \rho q^2}{(D_{N1}^2 + D_{N2}^2 + D_{N3}^2)^2}$	
Marilyn Vilorio, June 2006	

Table A8—Rheology and Hydraulics Equations for Robertson and Stiff Model “Yield Point”.

Hydraulics Equations: ROBERTSON-STIFF MODEL "YIELD POINT", $\tau = A(\dot{\gamma} + C)^B$	
Pipe Flow	Annular Flow
$C = \frac{\gamma_{\min}^* \gamma_{\max} - \gamma^{*2}}{2\gamma^* - \gamma_{\min} - \gamma_{\max}}$ $\log(\tau) = \log(A) + B \log(\dot{\gamma}) \quad \left\{ \begin{array}{l} B = \frac{\sum \log \tau \cdot \sum \log(\dot{\gamma} + C) - N \cdot \sum (\log \tau \cdot \log(\dot{\gamma} + C))}{[\sum \log(\dot{\gamma} + C)^2 - N \cdot \sum \log(\dot{\gamma} + C)]^2} \\ \log(A) = \frac{\sum \log \tau - B \cdot \sum \log(\dot{\gamma} + C)}{N} \end{array} \right.$	
$\frac{1}{\text{sec}^B}$	DIMENSIONLESS
$v_p = \frac{0.408 q}{D_p^2}$ ft/sec	$v_a = \frac{0.408 q}{D_2^2 - D_1^2}$ ft/sec
$N_{Re} = \frac{89100 \rho v_p^{2-B}}{A} \left(\frac{0.416 D_p}{3 + \frac{1}{B}} \right)^B$	$N_{Re} = \frac{109000 \rho v_a^{2-B}}{A} \left[\frac{0.0208 (D_2 - D_1)}{2 + \frac{1}{B}} \right]^B$ A=dyn sec ^B /100cm ² =eq cp
Laminar $N_{Re} \leq 3470 - 1370 B$	
$\lambda = \frac{2(AC^B)}{(dp/dL)}$ NOTE: that ÷ is greater than zero if the fluid has a yield point (÷0=AC ^B)	$\lambda = \frac{AC^B}{(dp/dL)}$ C=1/sec ^B dP/dL=lb/ft ² /ft A=lb·sec ^B /ft ²
<div style="border: 1px solid black; padding: 5px; width: fit-content;"> Use same equation for annular or pipe in laminar flow. D(ft)=D₂-D₁, annulus. D(ft)=D_p, pipe. </div> $q = \pi \left\{ \left[\frac{1}{2A} \left(\frac{dp}{dL} \right) \right]^{\frac{1}{B}} \left(\frac{B}{3B+1} \right) \left[\left(\frac{D}{2} \right)^{\frac{3B+1}{B}} - (\lambda)^{\frac{3B+1}{B}} \right] - \frac{1}{3} C \left[\left(\frac{D}{2} \right)^3 - (\lambda)^3 \right] \right\}$	$q = \text{ft}^3/\text{sec}$ $\div P/L = \text{lb/ft}^2/\text{ft}$ A=lb·sec ^B /sq ft
Turbulent $N_{Re} \geq 4270 - 1370 B$	
$a = \frac{\log B + 3.93}{50}$	$b = \frac{1.75 - \log B}{7}$
$f_p = \frac{a}{N_{Re}^b}$ $\left(\frac{dp}{dL} \right) = \frac{f_p v_p^2 \rho}{25.81 D}$ psi/ft	$f_a = \frac{a}{N_{Re}^b}$ $\left(\frac{dp}{dL} \right) = \frac{f_a v_a^2 \rho}{25.81 (D_2 - D_1)}$ psi/ft
$\Delta p = \left(\frac{dp}{dL} \right) \Delta L$ psi	$\Delta p = \left(\frac{dp}{dL} \right) \Delta L$ psi
$\Delta p_{Nozzles, psi} = \frac{156 \rho q^2}{(D_{N1}^2 + D_{N2}^2 + D_{N3}^2)^2}$	
Marilyn Vilorio, June 2006	

Table A9—Rheology and Hydraulics Equations for Casson.

Hydraulics Equations: CASSON MODEL, $\tau^{1/2} = \tau_c^{1/2} + \mu_c^{1/2} \dot{\gamma}^{1/2}$	
Pipe Flow	Annular Flow
$v_p = \frac{0.408 q}{D_p^2}$ ft/sec	$v_a = \frac{0.408 q}{D_2^2 - D_1^2}$ ft/sec
$\tau^{1/2} = \tau_c^{1/2} + \mu_c^{1/2} \dot{\gamma}^{1/2} \quad \left\{ \begin{array}{l} \mu_c^{1/2} = \frac{\sum \log(\tau^{1/2}) \sum \log(\dot{\gamma}^{1/2}) - N \sum (\log(\tau^{1/2}) \log(\dot{\gamma}^{1/2}))}{(\sum \log \dot{\gamma}^{1/2})^2 - N \sum (\log \dot{\gamma}^{1/2})^2} \\ \tau_c^{1/2} = \frac{\sum \log(\tau^{1/2}) - \mu_c^{1/2} \sum \log(\dot{\gamma}^{1/2})}{N} \end{array} \right.$	
$N_{Re} = \frac{928 D v_p \rho}{\mu_c}$	$N_{Re} = \frac{757 (D_2 - D_1) v_a \rho}{\mu_c}$
Turbulence Criteria 1.- Calculate the Casson number, for annulus and pipe. $Ca = \frac{D^2 \tau_c \rho}{32.174 \mu_c^2}$ 2.- Estimate from figure the N_{Re} critical, for annulus and pipe 3.- Compare N_{Re} critical with N_{Re} 4.- Use same equation for annular or pipe in laminar flow, Use: D=D2-D1, annulus D=Dp, pipe	Critical value of N_{Re} as function of Casson Number
Laminar $q = \frac{\pi D^3}{8 \mu_c} \left[\frac{D \left(\frac{dp}{dL} \right)}{16} - \frac{4}{7} \sqrt{\tau_c} \sqrt{\frac{(dp/dL) D}{4}} - \frac{64 \tau_c^4}{84 \left(\frac{dp}{dL} \right) D^3} + \frac{\tau_c}{3} \right]$ <p style="text-align: right;">dp/dL=lb/ft²/ft</p> <p style="text-align: center;">NOTE: Apply solve from EXCEL to find a solution for pressure loss</p>	
Turbulent $f_p = \frac{0.0791}{N_{Re}^{0.25}}$	Turbulent $f_a = \frac{0.0791}{N_{Re}^{0.25}}$
$\left(\frac{dp}{dL} \right) = \frac{f_p v_p^2 \rho}{25.81 D_p}$ <p style="text-align: right;">psi/ft</p> $\Delta p = \left(\frac{dp}{dL} \right) \Delta L$ <p style="text-align: right;">psi</p>	$\left(\frac{dp}{dL} \right) = \frac{f_a v_a^2 \rho}{25.81 (D_2 - D_1)}$ <p style="text-align: right;">psi/ft</p> $\Delta p = \left(\frac{dp}{dL} \right) \Delta L$ <p style="text-align: right;">psi</p>
$\Delta p_{Nozzles}, psi = \frac{156 \rho q^2}{(D_{N1}^2 + D_{N2}^2 + D_{N3}^2)^2}$ <p style="text-align: right;">Marilyn Viloria, June 2006</p>	

APPENDIX B

Example:

Drillpipe-5 in. 19.5 S-135 w/4.5 IF (6.75in.x 3in. connection): $D_1 = 5$ in, $D_p = 4.5$ in

Casing 11 7/8 in.x10.711 in., $D_2 = 10.711$ in.

Length of well= 12440 ft

Rheological data= same as in chapter IV

$q_1 = 100$ GPM, $q_2 = 665$ GPM

Density (ρ) = 11.55 lb/galm

Bit: 10 5/8 in. w/3: 28/32 in. jets

$\Delta p_s = 0$

B-1 NEWTONIAN FLUID

$q_1 = 100$ gallon/min

- Pipe Flow

$$v_p = \frac{0.408q}{D_p^2} = \frac{0.408 \times 100}{(4.5)^2} = 2.015 \text{ ft/sec}$$

$$\mu_a = R_{300} = 58 \text{ cp}$$

$$N_{Re} = \frac{928 D_p v_p \rho}{\mu_a} = \frac{928 \times 4.5 \times 2.015 \times 11.55}{58} = 1675.520$$

If $N_{Re} < N_{Rec} \rightarrow$ flow is laminar.

$$f = 16 / N_{Re} = 16 / 1675.52 = 0.00955$$

$$\left(\frac{dp}{dL} \right) = \frac{f v_p^2 \rho}{25.81 D_p} = \frac{0.00955 \times (2.0125)^2 \times 11.55}{25.81 \times 4.5} = 0.0039 \text{ psi/ft}$$

$$\Delta p_{ds} = \left(\frac{dp}{dL} \right) \Delta L = 0.0039 \times 12440 = 47.846 \text{ psi}$$

- Annular Flow

$$v_a = \frac{0.408q}{(D_2^2 - D_1^2)} = \frac{0.408 \times 100}{(10.711^2 - 5^2)} = 0.4547 \text{ ft/sec}$$

$$N_{Re} = \frac{757(D_2 - D_1)v_a\rho}{\mu_a} = \frac{757 \times (10.711 - 5) \times 0.4547 \times 11.55}{58} = 391.477$$

If $N_{Re} < N_{Rec} \rightarrow$ flow is laminar.

$$f = 16 / N_{Re} = 16 / 391.477 = 0.04087$$

$$\left(\frac{dp}{dL}\right) = \frac{fv_a^2\rho}{25.81(D_2 - D_1)} = \frac{0.04087 \times (0.4547)^2 \times 11.55}{25.81 \times (10.711 - 5)} = 0.00066 \text{ psi/ft}$$

$$\Delta p_a = \left(\frac{dp}{dL}\right)\Delta L = 0.00066 \times 12440 = 8.237 \text{ psi}$$

- Frictional pressure losses across the bit, Δp_b :

$$\Delta p_b = \frac{156\rho q^2}{(D_{N1}^2 + D_{N2}^2 + D_{N3}^2)^2} = \frac{156 \times 11.55 \times 100^2}{(28^2 + 28^2 + 28^2)^2} = 3.257 \text{ psi}$$

Finally, the pump pressure:

$$\Delta p_p = \Delta p_s + \Delta p_{ds} + \Delta p_b + \Delta p_a = 0 + 47.846 + 3.257 + 8.237 = 59.340 \text{ psi}$$

$q_2 = 665$ gallon/min

- Pipe Flow

$$v_p = \frac{0.408q}{D_p^2} = \frac{0.408 \times 665}{(4.5)^2} = 13.399 \text{ ft/sec}$$

$$\mu_a = 58 \text{ cp}$$

$$N_{Re} = \frac{928D_p v_p \rho}{\mu_a} = \frac{928 \times 4.5 \times 13.399 \times 11.55}{58} = 11142.208$$

If $N_{Re} > N_{Rec} \rightarrow$ flow is turbulent.

$$f = 0.0791 / N_{Re}^{0.25} = 0.0791 / (11142.208)^{0.25} = 0.00769$$

$$\left(\frac{dp}{dL}\right) = \frac{fv_p^2 \rho}{25.81 D_p} = \frac{0.00769 \times (13.399)^2 \times 11.55}{25.81 \times 4.5} = 0.1375 \text{ psi/ft}$$

$$\Delta p_{ds} = \left(\frac{dp}{dL}\right) \Delta L = 0.1375 \times 12440 = 1709.94 \text{ psi}$$

- Annular Flow

$$v_a = \frac{0.408q}{(D_2^2 - D_1^2)} = \frac{0.408 \times 665}{(10.711^2 - 5^2)} = 3.024 \text{ ft/sec}$$

$$N_{Re} = \frac{757(D_2 - D_1)v_a \rho}{\mu_a} = \frac{757 \times (10.711 - 5) \times 3.024 \times 11.55}{58} = 2603.322$$

If $N_{Re} > N_{Rec} \rightarrow$ flow is turbulent.

$$f = 0.0791 / N_{Re}^{0.25} = 0.0791 / (2603.322)^{0.25} = 0.01107$$

$$\left(\frac{dp}{dL}\right) = \frac{fv_a^2 \rho}{25.81(D_2 - D_1)} = \frac{0.01107 \times (3.024)^2 \times 11.55}{25.81 \times (10.711 - 5)} = 0.00793 \text{ psi/ft}$$

$$\Delta p_a = \left(\frac{dp}{dL}\right) \Delta L = 0.00793 \times 12440 = 98.710 \text{ psi}$$

- Frictional pressure losses across the bit, Δp_b :

$$\Delta p_b = \frac{156 \rho q^2}{(D_{N1}^2 + D_{N2}^2 + D_{N3}^2)^2} = \frac{156 \times 11.5 \times 665^2}{(28^2 + 28^2 + 28^2)^2} = 144.037 \text{ psi}$$

Finally, the pump pressure:

$$\Delta p_p = \Delta p_s + \Delta p_{ds} + \Delta p_b + \Delta p_a = 0 + 1709.94 + 144.037 + 98.710 = 1952.687 \text{ psi}$$

B-2 BINGHAM PLASTIC FLOW

$q_1 = 100$ gallon/min

- Pipe Flow

$$v_p = \frac{0.408q}{D_p^2} = \frac{0.408 \times 100}{(4.5)^2} = 2.015 \text{ ft/sec}$$

$$\mu_p = R_{600} - R_{300} = 92 - 58 = 34 \text{ cp}$$

$$\tau_y = R_{300} - \mu_p = 58 - 34 = 24 \text{ lbf/100 ft}^2$$

$$\mu_a = \mu_p + \frac{5\tau_y D_p}{v_p} = 34 + \frac{5 \times 24 \times 4.5}{2.015} = 301.990 \text{ cp}$$

$$N_{Re} = \frac{928 D_p v_p \rho}{\mu_p} = \frac{928 \times 4.5 \times 2.015 \times 11.55}{301.990} = 321.829$$

If $N_{Re} < N_{Rec} \rightarrow$ flow is laminar.

$$f = 16 / N_{Re} = 16 / 321.829 = 0.04972$$

$$\left(\frac{dp}{dL} \right) = \frac{f v_p^2 \rho}{25.81 D_p} = \frac{0.04972 \times (2.015)^2 \times 11.55}{25.81 \times 4.5} = 0.0195 \text{ psi/ft}$$

$$\Delta p_{ds} = \left(\frac{dp}{dL} \right) \Delta L = 0.0195 \times 12440 = 249.7 \text{ psi}$$

- Annular Flow

$$v_a = \frac{0.408 q}{(D_2^2 - D_1^2)} = \frac{0.408 \times 100}{(10.711^2 - 5^2)} = 0.4547 \text{ ft/sec}$$

$$\mu_a = \mu_p + \frac{5\tau_y (D_2 - D_1)}{v_a} = 34 + \frac{5 \times 24 \times (10.711 - 5)}{0.4547} = 1541.192 \text{ cp}$$

$$N_{Re} = \frac{757 (D_2 - D_1) v_a \rho}{\mu_a} = \frac{757 \times (10.711 - 5) \times 0.4547 \times 11.55}{1541.192} = 14.732$$

If $N_{Re} < N_{Rec} \rightarrow$ flow is laminar.

$$f = 16 / N_{Re} = 16 / 14.732 = 1.08608$$

$$\left(\frac{dp}{dL} \right) = \frac{f v_a^2 \rho}{25.81 (D_2 - D_1)} = \frac{1.08608 \times (0.4547)^2 \times 11.55}{25.81 \times (10.711 - 5)} = 0.01759 \text{ psi/ft}$$

$$\Delta p_a = \left(\frac{dp}{dL} \right) \Delta L = 0.01759 \times 12440 = 218.8839 \text{ psi}$$

- Frictional pressure losses across the bit, Δp_b :

$$\Delta p_b = \frac{156 \rho q^2}{(D_{N1}^2 + D_{N2}^2 + D_{N3}^2)^2} = \frac{156 \times 11.5 \times 100^2}{(28^2 + 28^2 + 28^2)^2} = 3.257 \text{ psi}$$

Finally, the pump pressure:

$$\Delta p_p = \Delta p_s + \Delta p_{ds} + \Delta p_b + \Delta p_a = 0 + 249.7 + 3.257 + 218.88 = 471.84 \text{ psi}$$

$q_2 = 665$ gallon/min

- Pipe Flow

$$v_p = \frac{0.408 q}{D_p^2} = \frac{0.408 \times 665}{(4.5)^2} = 13.399 \text{ ft/sec}$$

$$\mu_p = 34 \text{ cp}$$

$$\tau_y = 24 \text{ lbf/100 ft}^2$$

$$\mu_a = \mu_p + \frac{5 \tau_y D_p}{v_p} = 34 + \frac{5 \times 24 \times 4.5}{13.399} = 74.302 \text{ cp}$$

$$N_{Re} = \frac{928 D_p v_p \rho}{\mu_p} = \frac{928 \times 4.5 \times 13.399 \times 11.55}{74.302} = 8697.9956$$

If $N_{Re} > N_{Rec} \rightarrow$ flow is turbulent.

$$f = 0.0791 / N_{Re}^{0.25} = 0.0791 / (8697.9956)^{0.25} = 0.00819$$

$$\left(\frac{dp}{dL} \right) = \frac{f v_p^2 \rho}{25.81 D_p} = \frac{0.00819 \times (13.399)^2 \times 11.55}{25.81 \times 4.5} = 0.14623 \text{ psi/ft}$$

$$\Delta p_{ds} = \left(\frac{dp}{dL} \right) \Delta L = 0.14623 \times 12440 = 1819.15123 \text{ psi}$$

- Annular Flow

$$v_a = \frac{0.408 q}{(D_2^2 - D_1^2)} = \frac{0.408 \times 665}{(10.711^2 - 5^2)} = 3.024 \text{ ft/sec}$$

$$\mu_a = \mu_p + \frac{5\tau_y(D_2 - D_1)}{v_a} = 34 + \frac{5 \times 24 \times (10.711 - 5)}{3.024} = 260.627 \text{ cp}$$

$$N_{Re} = \frac{757(D_2 - D_1)v_a\rho}{\mu_a} = \frac{757 \times (10.711 - 5) \times 3.024 \times 11.55}{260.627} = 579.365$$

If $N_{Re} < N_{Rec} \rightarrow \text{flow is laminar.}$

$$f = 16 / N_{Re} = 16 / (579.365) = 0.02762$$

$$\left(\frac{dp}{dL}\right) = \frac{fv_a^2\rho}{25.81(D_2 - D_1)} = \frac{0.02762 \times (3.024)^2 \times 11.55}{25.81 \times (10.711 - 5)} = 0.01979 \text{ psi/ft}$$

$$\Delta p_a = \left(\frac{dp}{dL}\right)\Delta L = 0.01979 \times 12440 = 246.169 \text{ psi}$$

- Frictional pressure losses across the bit, Δp_b :

$$\Delta p_b = \frac{156\rho q^2}{(D_{N1}^2 + D_{N2}^2 + D_{N3}^2)^2} = \frac{156 \times 11.5 \times 665^2}{(28^2 + 28^2 + 28^2)^2} = 144.037 \text{ psi}$$

Finally, the pump pressure:

$$\Delta p_p = \Delta p_s + \Delta p_{ds} + \Delta p_b + \Delta p_a = 0 + 1819.15 + 144.037 + 246.169 = 2209.356 \text{ psi}$$

B-3 POWER LAW FLOW

$q_1 = 100$ gallon/min

- Pipe Flow

a. Velocity:

$$v_p = \frac{0.408q}{D_p^2} = \frac{0.408 \times 100}{(4.5)^2} = 2.015 \text{ ft/sec}$$

b. Reynolds number:

$$n = 3.32 \log\left(\frac{R_{600}}{R_{300}}\right) = 3.32 \log\left(\frac{92}{58}\right) = 0.6652$$

$$k = \frac{510R_{300}}{511^n} = \frac{510 \times 58}{511^{0.6652}} = 467.058 \quad \text{dyne.sec}^n/100\text{cm}^2$$

$$N_{\text{Re}} = \frac{89100v_p^{2-n}\rho}{k} \left(\frac{0.0416D_p}{3 + \frac{1}{n}} \right)^n$$

$$N_{\text{Re}} = \frac{89100 \times 2.015^{2-0.6652} \times 11.55}{467.068} \left(\frac{0.0416 \times 4.5}{3 + \frac{1}{0.6652}} \right)^{0.6652} = 676.774$$

c. For laminar flow, critical value

$$N_{\text{Rec}} = 3470 - 1370n = 3470 - 1370 \times 0.6652 = 2558.7$$

For turbulent flow, critical value

$$N_{\text{Rec}} = 4270 - 1370n = 4270 - 1370 \times 0.6652 = 3358.7$$

d. Regime flow determination:

Comparison between N_{Re} and N_{Rec}

If $N_{\text{Re}} < N_{\text{Rec}} \rightarrow$ flow is laminar.

Friction factor is included in Eq.5.21.

e. - Frictional pressure loss calculation inside drillstring:

Laminar:

$$\left(\frac{dp}{dL} \right) = \frac{k v_p^n \left(\frac{3 + 1/n}{0.0416} \right)^n}{144000 D_p^{1+n}} = \frac{467.058 \times 2.015^{0.6652} \times \left(\frac{3 + 1/0.6652}{0.0416} \right)^{0.6652}}{144000 \times 4.5^{1+0.6652}}$$

$$= 0.00953$$

$$\Delta p_{ds} = \left(\frac{dp}{dL} \right) \Delta L = 0.00953 \times 12440 = 118.53 \text{ psi}$$

- Annular Flow

a. Velocity:

$$v_a = \frac{0.408q}{(D_2^2 - D_1^2)} = \frac{0.408 \times 100}{(10.711^2 - 5^2)} = 0.4547 \text{ ft/sec}$$

b. Reynolds number:

$$N_{Re} = \frac{109000 v_a^{2-n} \rho}{k} \left(\frac{0.0208(D_2 - D_1)}{2 + \frac{1}{n}} \right)^n$$

$$N_{Re} = \frac{109000 \times 0.4547^{2-0.6652} \times 11.55}{467.058} \left(\frac{0.0208 \times (10.711 - 5)}{2 + \frac{1}{0.6652}} \right)^{0.6652} = 99.111$$

c. For laminar flow, critical value

$$N_{Rec} = 3470 - 1370n = 3470 - 1370 \times 0.6652 = 2558.7$$

For turbulent flow, critical value

$$N_{Rec} = 4270 - 1370n = 4270 - 1370 \times 0.6652 = 3358.7$$

d. Regime flow determination:

Comparison between N_{Re} and N_{Rec}

If $N_{Re} < N_{Rec} \rightarrow$ flow is laminar.

Friction factor is included in Eq. 5.23.

e. Frictional pressure loss calculation inside annulus:

Laminar:

$$\left(\frac{dp}{dL}\right) = \frac{kv_a^n \left(\frac{2+1/n}{0.0208}\right)^n}{144000(D_2 - D_1)^{1+n}} = \frac{467.058 \times 0.4547^{0.6652} \times \left(\frac{2+1/0.6652}{0.0208}\right)^{0.6652}}{144000 \times (10.711 - 5)^{1+0.6652}}$$

$$= 0.00319 \text{ psi/ft}$$

$$\Delta p_a = \left(\frac{dp}{dL}\right) \Delta L = 0.00319 \times 12440 = 39.727 \text{ psi}$$

Finally, the pump pressure:

$$\Delta p_p = \Delta p_s + \Delta p_{ds} + \Delta p_b + \Delta p_a = 0 + 118.53 + 3.257 + 39.727 = 161.51 \text{ psi}$$

$q_2 = 665$ gallon/min

- Pipe Flow

a. Velocity:

$$v_p = \frac{0.408q}{D_p^2} = \frac{0.408 \times 665}{(4.5)^2} = 13.399 \text{ ft/sec}$$

b. Reynolds number:

$$N_{Re} = \frac{89100 v_p^{2-n} \rho}{k} \left(\frac{0.0416 D_p}{3 + \frac{1}{n}} \right)^n$$

$$N_{Re} = \frac{89100 \times 13.399^{2-0.6652} \times 11.55}{467.058} \left(\frac{0.0416 \times 4.5}{3 + \frac{1}{0.6652}} \right)^{0.6652} = 8486.21$$

c. For laminar flow, critical value $N_{Rec} = 2558.7$

For turbulent flow, critical value $N_{Rec} = 3358.7$

d. Regime flow determination:

Comparison between N_{Re} and N_{Rec}

If $N_{Re} > N_{Rec} \rightarrow$ flow is turbulent.

$$a = \frac{\log n + 3.93}{50} = \frac{\log 0.6652 + 3.93}{50} = 0.075$$

$$b = \frac{1.75 - \log n}{7} = \frac{1.75 - \log 0.6652}{7} = 0.2753$$

$$f = \frac{a}{N_{Re}^b} = \frac{0.075}{8486.21^{0.2753}} = 0.00622$$

e. Frictional pressure loss calculation inside drillstring:

Turbulent:

$$\left(\frac{dp}{dL} \right) = \frac{f v_p^2 \rho}{25.81 D_p} = \frac{0.00622 \times 13.399^2 \times 11.55}{25.81 \times 4.5} = 0.11097 \text{ psi/ft}$$

$$\Delta p_{ds} = \left(\frac{dp}{dL} \right) \Delta L = 0.11097 \times 12440 = 1380.49 \text{ psi}$$

- Annular Flow

a. Velocity:

$$v_a = \frac{0.408q}{(D_2^2 - D_1^2)} = \frac{0.408 \times 665}{(10.711^2 - 5^2)} = 3.024 \text{ ft/sec}$$

b. Reynolds number:

$$N_{Re} = \frac{109000 \times 3.024^{2-0.6652} \times 11.55}{467.058} \left(\frac{0.0208 \times (10.711 - 5)}{2 + \frac{1}{0.6652}} \right)^{0.6652} = 1243.003$$

c. For laminar flow, critical value $N_{Rec} = 2558.7$

For turbulent flow, critical value $N_{Rec} = 3358.7$

d. Regime flow determination:

Comparison between N_{Re} and N_{Rec}

If $N_{Re} < N_{Rec} \rightarrow$ flow is laminar.

Friction factor is included in Eq. 5.23.

e. Frictional pressure loss calculation inside annulus:

Laminar:

$$\left(\frac{dp}{dL}\right) = \frac{kv_a^n \left(\frac{2+1/n}{0.0208}\right)^n}{144000(D_2 - D_1)^{1+n}}$$

$$= \frac{467.058 \times 3.027^{0.6652} \times \left(\frac{2+1/0.6652}{0.0208}\right)^{0.6652}}{144000 \times (10.711 - 5)^{1+0.6652}} = 0.01127 \text{ psi/ft}$$

$$\Delta p = \left(\frac{dp}{dL}\right) \times 12440 = 140.195 \text{ psi}$$

Finally, the pump pressure:

$$\Delta p_p = \Delta p_s + \Delta p_{ds} + \Delta p_b + \Delta p_a = 0 + 1380.49 + 144.04 + 140.195 = 1664.725 \text{ psi}$$

B-4 API FLOW

$q_1 = 100$ gallon/min

- Pipe Flow

a. *Velocity:*

$$v_p = \frac{0.408q}{D_p^2} = \frac{0.408 \times 100}{(4.5)^2} = 2.015 \text{ ft/sec}$$

b. Reynolds number:

$$n = 3.32 \log \left(\frac{R_{600}}{R_{300}} \right) = 3.32 \log \left(\frac{92}{58} \right) = 0.6652$$

$$k = \frac{5.10R_{600}}{1022^n} = \frac{5.10 \times 92}{1022^{0.6651}} = 4.6718 \text{ dyne.sec}^n/\text{ft}^2$$

$$\mu_e = 100k \left(\frac{96v_p}{D_p} \right)^{n-1} \left(\frac{3n+1}{4n} \right)^n$$

$$\mu_e = 100 \times 4.6718 \left(\frac{96 \times 2.015}{4.5} \right)^{0.6652-1} \left(\frac{3 \times 0.6652 + 1}{4 \times 0.6652} \right)^{0.6652} = 143.510 \text{ cp}$$

$$N_{Re} = \frac{928v_p \rho D_p}{\mu_e} = \frac{928 \times 2.015 \times 11.55 \times 4.5}{143.510} = 677.229$$

c. Critical value $N_{Rec} = 2100$.

d. Regime flow determination:

Comparison between N_{Re} and N_{Rec}

If $N_{Re} < N_{Rec} \rightarrow$ flow is laminar.

$$f = 16 / N_{Re} = 16 / 677.229 = 0.02363$$

e. Frictional pressure loss calculation inside drillstring:

$$\left(\frac{dp}{dL} \right) = \frac{fv_p^2 \rho}{25.81D_p} = \frac{0.02363 \times 2.015^2 \times 11.55}{25.81 \times 4.5} = 0.00954 \text{ psi/ft}$$

$$\Delta p_{ds} = \left(\frac{dp}{dL} \right) \Delta L = 0.00954 \times 12440 = 118.669 \text{ psi}$$

- *Annular Flow*

a. Velocity:

$$v_a = \frac{0.408q}{(D_2^2 - D_1^2)} = \frac{0.408 \times 100}{(10.711^2 - 5^2)} = 0.4547 \text{ ft/sec}$$

b. Reynolds number:

$$n = 0.657 \log\left(\frac{R_{100}}{R_3}\right) = 0.657 \log\left(\frac{32}{8}\right) = 0.3955$$

$$k = \frac{5.10 R_{100}}{170.2^n} = \frac{5.10 \times 32}{170.2^{0.3955}} = 21.43 \text{ dyne.sec}^n/\text{ft}^2$$

$$\begin{aligned} \mu_e &= 100k \left(\frac{144v}{D_2 - D_1} \right)^{n-1} \left(\frac{2n+1}{3n} \right)^n \\ &= 100 \times 21.43 \left(\frac{144 \times 0.4547}{10.711 - 5} \right)^{0.3955-1} \left(\frac{2 \times 0.3955 + 1}{3 \times 0.3955} \right)^{0.3955} = 577.239 \text{ cp} \end{aligned}$$

$$N_{Re} = \frac{928 v_a \rho (D_2 - D_1)}{\mu_e} = \frac{928 \times 0.4547 \times 11.55 \times (10.711 - 5)}{577.239} = 48.205$$

c. Critical value $N_{Rec} = 2100$.

d. Regime flow determination:

Comparison between N_{Re} and N_{Rec}

If $N_{Re} < N_{Rec} \rightarrow$ flow is laminar.

$$f_a = 24 / 48.205 = 0.49788$$

e. Frictional pressure loss calculation inside annulus:

$$\left(\frac{dp}{dL} \right) = \frac{f v_a^2 \rho}{25.81(D_2 - D_1)} = \frac{0.49788 \times 0.4547^2 \times 11.55}{25.81 \times (10.711 - 5)} = 0.008066 \text{ psi/ft}$$

$$\Delta p_a = \left(\frac{dp}{dL} \right) \Delta L = 0.008066 \times 12440 = 100.339 \text{ psi}$$

Finally, the pump pressure:

$$\Delta p_p = \Delta p_s + \Delta p_{ds} + \Delta p_b + \Delta p_a = 0 + 118.669 + 3.257 + 100.339 = 222.25 \text{ psi}$$

$q_2=665$ gallon/min

- Pipe Flow

a. Velocity:

$$v_p = \frac{0.408q}{D_p^2} = \frac{0.408 \times 665}{(4.5)^2} = 13.399 \text{ ft/sec}$$

b. Reynolds number:

$$n = 3.32 \log \left(\frac{R_{600}}{R_{300}} \right) = 3.32 \log \left(\frac{92}{58} \right) = 0.6651$$

$$k = \frac{5.10 R_{600}}{1022^n} = \frac{5.10 \times 92}{1022^{0.6651}} = 4.6718 \text{ dyne.sec}^n/\text{ft}^2$$

$$\mu_e = 100k \left(\frac{96v_p}{D_p} \right)^{n-1} \left(\frac{3n+1}{4n} \right)^n$$

$$\mu_e = 100 \times 4.6718 \left(\frac{96 \times 13.399}{4.5} \right)^{0.6651-1} \left(\frac{3 \times 0.6651 + 1}{4 \times 0.6651} \right)^{0.6651} = 76.063 \text{ cp}$$

$$N_{Re} = \frac{928 v_p \rho D_p}{\mu_e} = \frac{928 \times 13.399 \times 11.55 \times 4.5}{76.063} = 8496.512$$

c. Critical value $N_{Rec} = 2100$.

d. Regime flow determination:

Comparison between N_{Re} and N_{Rec}

If $N_{Re} > N_{Rec} \rightarrow$ flow is turbulent.

$$a = \frac{\log 0.6651 + 3.93}{50} = 0.075$$

$$b = \frac{1.75 - \log 0.6651}{7} = 0.2753$$

$$f = \frac{a}{N_{Re}^b} = \frac{0.075}{8496.512^{0.2753}} = 0.00621$$

e. Frictional pressure loss calculation inside drillstring:

$$\left(\frac{dp}{dL}\right) = \frac{fv_p^2 \rho}{25.81 D_p} = \frac{0.00621 \times 13.399^2 \times 11.55}{25.81 \times 4.5} = 0.11093 \text{ psi/ft}$$

$$\Delta p_{ds} = \left(\frac{dp}{dL}\right) \Delta L = 0.11093 \times 12440 = 1380.028 \text{ psi}$$

- Annular Flow

a. Velocity:

$$v_a = \frac{0.408q}{(D_2^2 - D_1^2)} = \frac{0.408 \times 665}{(10.711^2 - 5^2)} = 3.024 \text{ ft/sec}$$

b. Reynolds number:

$$n = 0.657 \log\left(\frac{R_{100}}{R_3}\right) = 0.657 \log\left(\frac{32}{8}\right) = 0.3955$$

$$k = \frac{5.10 R_{100}}{170.2^n} = \frac{5.10 \times 32}{170.2^{0.3955}} = 21.43 \text{ dyne.sec}^n/\text{ft}^2$$

$$\begin{aligned} \mu_e &= 100k \left(\frac{144v}{D_2 - D_1}\right)^{n-1} \left(\frac{2n+1}{3n}\right)^n \\ &= 100k \left(\frac{144 \times 3.024}{10.711 - 5}\right)^{0.3955-1} \left(\frac{2 \times 0.3955 + 1}{3 \times 0.3955}\right)^{0.3955} = 183.7093 \text{ cp} \end{aligned}$$

$$N_{Re} = \frac{928 v_a \rho (D_2 - D_1)}{\mu_e} = \frac{928 \times 3.024 \times 11.55 \times (10.711 - 5)}{183.7093} = 1007.57$$

c. Critical value $N_{Rec} = 2100$.

d. Regime flow determination:

Comparison between N_{Re} and N_{Rec}

$N_{Re} < N_{Rec} \rightarrow$ flow is laminar.

$$f = 24 / N_{Re} = 24 / 1007.57 = 0.02382$$

e. Frictional pressure loss calculation inside annulus:

$$\left(\frac{dp}{dL}\right) = \frac{fv_a^2 \rho}{25.81(D_2 - D_1)} = \frac{0.02382 \times 0.4547^2 \times 11.55}{25.81 \times (10.711 - 5)} = 0.017 \text{ psi/ft}$$

$$\Delta p_a = \left(\frac{dp}{dL}\right) \Delta L = 0.017 \times 12440 = 212.28 \text{ psi}$$

Finally, the pump pressure:

$$\Delta p_p = \Delta p_s + \Delta p_{ds} + \Delta p_b + \Delta p_a = 0 + 1380.028 + 144.04 + 212.28 = 1736.35 \text{ psi}$$

B-5 HERSCHEL-BULKLEY FLOW

$q_1 = 100 \text{ gallon/min}$

- Pipe Flow

a. Velocity:

$$v_p = \frac{0.408q}{D_p^2} = \frac{0.408 \times 100}{(4.5)^2} = 2.015 \text{ ft/sec}$$

b. Reynolds number:

$$C_c = 1 - \left(\frac{1}{2n+1} \right) \frac{\tau_0}{\tau_0 + k \left[\frac{(3n+1)q}{n\pi(D_p/2)^3} \right]^n}$$

Where:

$$D_p = 4.5/12 = 0.375 \text{ ft}$$

$$q = 100 \times 0.002228 = 0.2228 \text{ ft}^3/\text{sec}$$

$n = 0.7129$, from Herschel-Bulkley model, Chapter IV

$k = 0.6686 \text{ lbf} \cdot \text{sec}^n / 100 \text{ ft}^2$, from Herschel-Bulkley model, Chapter IV

$\tau_0 = 6.6582 \text{ lb} / 100 \text{ ft}^2$, from Herschel-Bulkley Model, Chapter IV

$$C_c = 1 - \left(\frac{1}{2 \times 0.7129 + 1} \right) \frac{6.6582}{6.6582 + 0.6686 \left[\frac{(3 \times 0.7129 + 1) \times 0.2228}{0.7129 \times \pi (0.375/2)^3} \right]^{0.7129}}$$

$$C_c = 0.8396$$

$$N_{Re} = \frac{2(3n+1)}{n} \left[\frac{\rho v_p^{(2-n)} \left(\frac{D_p}{2} \right)^n}{\tau_0 \left(\frac{D_p}{2v_p} \right)^n + k \left(\frac{3n+1}{nC_c} \right)^n} \right]$$

Where:

$$\rho = 11.55 \times 7.48 = 86.394 \text{ lbm/ft}^3$$

$$N_{Re} = \frac{2(3 \times 0.7129 + 1)}{0.7129} \left[\frac{86.394 \times 2.015^{(2-0.7129)} \times \left(\frac{0.375}{2} \right)^{0.7129}}{6.6582 \left(\frac{0.375}{2 \times 2.015} \right)^{0.7129} + 0.6686 \left(\frac{3 \times 0.7129 + 1}{0.7129 \times 0.8396} \right)^{0.7129}} \right]$$

$$N_{Re} = 166.96487$$

c. Critical value N_{Rec}

$$y = \frac{\log(n) + 3.93}{50} = \frac{\log(0.7129) + 3.93}{50} = 0.07566$$

$$z = \frac{1.75 - \log(n)}{7} = \frac{1.75 - \log(0.7129)}{7} = 0.27099$$

$$N_{Rec} = \left[\frac{4(3n+1)}{ny} \right]^{\frac{1}{1-z}} = \left[\frac{4(3 \times 0.7129 + 1)}{0.7129 \times 0.07566} \right]^{\frac{1}{1-0.27099}} = 1765.031$$

d. Regime flow determination:

Comparison between N_{Re} and N_{Rec}

If $N_{Re} < N_{Rec} \rightarrow$ flow is laminar.

Friction factor is included in Eq. 5.34

e. - Frictional pressure loss calculation inside drillstring:

Laminar:

$$\left(\frac{dp}{dL}\right) = \frac{4k}{14400D_p} \left\{ \left(\frac{\tau_0}{k}\right) + \left[\left(\frac{3n+1}{nC_c}\right) \left(\frac{8q}{\pi D_p^3}\right) \right]^n \right\}$$

$$\left(\frac{dp}{dL}\right) = \frac{4 \times 0.6686}{14400 \times 0.375} \left\{ \left(\frac{6.6582}{0.6686}\right) + \left[\left(\frac{3 \times 0.7129 + 1}{0.7129 \times 0.8396}\right) \left(\frac{8 \times 0.2228}{\pi \times 0.375^3}\right) \right]^{0.7129} \right\}$$

$$= 0.01371 \text{ psi/ft}$$

$$\Delta p_{ds} = \left(\frac{dp}{dL}\right) \Delta L = 0.01371 \times 12440 = 170.556 \text{ psi}$$

- Annular Flow

a. Velocity:

$$v_a = \frac{0.408q}{(D_2^2 - D_1^2)} = \frac{0.408 \times 100}{(10.711^2 - 5^2)} = 0.4547 \text{ ft/sec}$$

b. Reynolds number:

$$C_a^* = 1 - \left(\frac{1}{n+1}\right) \frac{\tau_0}{\tau_0 + k \left\{ \left[\frac{2(2n+1)}{n((D_2/2) - (D_1/2))} \right] \left[\frac{q}{\pi((D_2/2)^2 - (D_1/2)^2)} \right]^n \right\}}$$

$$C_a^* = 1 - \left(\frac{1}{0.7129 + 1}\right) \times$$

$$\frac{6.6582}{6.6582 + 0.6686 \left\{ \left[\frac{2(2 \times 0.7129 + 1)}{0.7129[(10.711/(2 \times 12)) - (5/(2 \times 12))]} \right] \left[\frac{0.2228}{\pi[(10.711/(2 \times 12))^2 - (5/(2 \times 12))^2]} \right]^{0.7129} \right\}}$$

$$C_a^* = 0.64091$$

$$N_{Re} = \frac{4(2n+1)}{n} \left\{ \frac{\rho v_a^{2-n} \left(\frac{D_2 - D_1}{2} \right)^n}{\tau_0 \left(\frac{D_2 - D_1}{2v_a} \right)^n + k \left[\frac{2(2n+1)}{nC_a^*} \right]^n} \right\}$$

$$N_{Re} = \frac{4(2 \times 0.7129 + 1)}{0.7129} \times$$

$$\left[\frac{86.394 \times 0.4547^{(2-0.7129)} \times \left(\frac{(10.711/12) - (5/12)}{2} \right)^{0.7129}}{6.6582 \left(\frac{(10.711/12) - (5/12)}{2 \times 0.4547} \right)^{0.7129} + 0.6686 \left(\frac{2(2 \times 0.7129 + 1)}{0.7129 \times 0.64091} \right)^{0.7129}} \right]$$

$$N_{Re}=19.64$$

c. Critical value N_{Rec}

$$y = \frac{\log(n) + 3.93}{50} = \frac{\log(0.7129) + 3.93}{50} = 0.07566$$

$$z = \frac{1.75 - \log(n)}{7} = \frac{1.75 - \log(0.7129)}{7} = 0.27099$$

$$N_{Rec} = \left[\frac{8(2n+1)}{ny} \right]^{\frac{1}{1-z}} = \left[\frac{8(2 \times 0.7129 + 1)}{0.7129 \times 0.07566} \right]^{\frac{1}{1-0.27099}} = 3207.697$$

d. Regime flow determination:

Comparison between N_{Re} and N_{Rec}

If $N_{Re} < N_{Rec} \rightarrow$ flow is laminar.

Friction factor is included in Eq. 5.40

e. Frictional pressure loss calculation inside annulus:

$$\left(\frac{dp}{dL}\right) = \frac{4k}{14400(D_2 - D_1)} \left\{ \left(\frac{\tau_0}{k}\right) + \left[\left(\frac{16(2n+1)}{nC_a^*(D_2 - D_1)} \right) \left(\frac{q}{\pi(D_2^2 - D_1^2)} \right) \right]^n \right\}$$

$$\left(\frac{dp}{dL}\right) = \frac{4 \times 0.6686}{14400(10.711/12 - 5/12)} \left\{ \left(\frac{6.6582}{0.6686}\right) + \left[\left(\frac{16(2 \times 0.7129 + 1)}{0.7129 \times 0.64091(10.711/12 - 5/12)} \right) \left(\frac{0.2228}{\pi((10.711/12)^2 - (5/12)^2)} \right) \right]^{0.7129} \right\}$$

$$(dp/dL) = 0.007625 \text{ psi/ft}$$

$$\Delta p_a = \left(\frac{dp}{dL}\right) \Delta L = 0.007625 \times 12440 = 94.849 \text{ psi}$$

Finally:

$$\Delta p_p = \Delta p_s + \Delta p_{ds} + \Delta p_b + \Delta p_a = 0 + 170.556 + 3.257 + 94.849 = 268.661 \text{ psi}$$

$q_2 = 665 \text{ gallon/min}$

- Pipe Flow

a. Velocity:

$$v_p = \frac{0.408q}{D_p^2} = \frac{0.408 \times 665}{(4.5)^2} = 13.399 \text{ ft/sec}$$

b. Reynolds number:

$$C_c = 1 - \left(\frac{1}{2n+1} \right) \frac{\tau_0}{\tau_0 + k \left[\frac{(3n+1)q}{n\pi(D_p/2)^3} \right]^n}$$

Where:

$$D_p = 4.5/12 = 0.375 \text{ ft}$$

$$q = 665 \times 0.002228 = 1.48162 \text{ ft}^3/\text{sec}$$

$n = 0.7129$, from Herschel-Bulkley model, Chapter IV

$k = 0.6686 \text{ lbf} \cdot \text{sec}^n / 100 \text{ ft}^2$, from Herschel-Bulkley model, Chapter IV

$\tau_0 = 6.6582 \text{ lb/100 ft}^2$, from Herschel-Bulkley Model, Chapter IV

$$C_c = 1 - \left(\frac{1}{2 \times 0.7129 + 1} \right) \frac{6.6582}{6.6582 + 0.6686 \left[\frac{(3 \times 0.7129 + 1) \times 1.48162}{0.7129 \times \pi (0.375/2)^3} \right]^{0.7129}}$$

$$C_c = 0.9417$$

$$N_{Re} = \frac{2(3n+1)}{n} \left[\frac{\rho v_p^{(2-n)} \left(\frac{D_p}{2} \right)^n}{\tau_0 \left(\frac{D_p}{2v_p} \right)^n + k \left(\frac{3n+1}{nC_c} \right)^n} \right]$$

Where:

$$\rho = 11.55 \times 7.48 = 86.394 \text{ lbm/ft}^3$$

$$N_{Re} = \frac{2(3 \times 0.7129 + 1)}{0.7129} \left[\frac{86.394 \times 13.399^{(2-0.7129)} \times \left(\frac{0.375}{2} \right)^{0.7129}}{6.6582 \left(\frac{0.375}{2 \times 13.399} \right)^{0.7129} + 0.6686 \left(\frac{3 \times 0.7129 + 1}{0.7129 \times 0.9417} \right)^{0.7129}} \right]$$

$$N_{Re} = 2800.24$$

c. Critical value N_{Rec}

$$y = \frac{\log(n) + 3.93}{50} = \frac{\log(0.7129) + 3.93}{50} = 0.07566$$

$$z = \frac{1.75 - \log(n)}{7} = \frac{1.75 - \log(0.7129)}{7} = 0.27099$$

$$N_{Rec} = \left[\frac{4(3n+1)}{ny} \right]^{\frac{1}{1-z}} = \left[\frac{4(3 \times 0.7129 + 1)}{0.7129 \times 0.07566} \right]^{\frac{1}{1-0.27099}} = 1765.031$$

$$N_{Rec} = 1765.031$$

d. Regime flow determination:

Comparison between N_{Re} and N_{Rec}

If $N_{Re} > N_{Rec} \rightarrow$ flow is turbulent.

$$f = y(C_c N_{Re})^{-z} = 0.07566(0.9417 \times 2800.24)^{-0.27099} = 0.00895$$

e. Frictional pressure loss calculation inside drillstring:

$$\left(\frac{dp}{dL}\right) = \frac{fq^2 \rho}{144 \times \pi^2 \times D_p^5} = \frac{0.00895 \times 1.48162^2 \times 86.394}{1421.22(4.5/12)^5} = 0.161033 \text{ psi/ft}$$

$$\Delta p_{ds} = \left(\frac{dp}{dL}\right) \Delta L = 0.161033 \times 12440 = 2003.254 \text{ psi}$$

- Annular Flow

a. Velocity:

$$v_a = \frac{0.408q}{(D_2^2 - D_1^2)} = \frac{0.408 \times 665}{(10.711^2 - 5^2)} = 3.024 \text{ ft/sec}$$

b. Reynolds number:

$$C_a^* = 1 - \left(\frac{1}{n+1}\right) \frac{\tau_0}{\tau_0 + k \left\{ \left[\frac{2(2n+1)}{n((D_2/2) - (D_1/2))} \right] \left[\frac{q}{\pi((D_2/2)^2 - (D_1/2)^2)} \right] \right\}^n}$$

$$C_a^* = 1 - \left(\frac{1}{0.7129+1}\right) \times$$

$$\frac{6.6582}{6.6582 + 0.6686 \left\{ \left[\frac{2(2 \times 0.7129 + 1)}{0.7129[(10.711/(2 \times 12)) - (5/(2 \times 12))]} \right] \left[\frac{1.48162}{\pi[(10.711/(2 \times 12))^2 - (5/(2 \times 12))^2]} \right] \right\}^{0.7129}}$$

$$C_a^* = 0.8291$$

$$N_{Re} = \frac{4(2n+1)}{n} \left\{ \frac{\rho v_a^{2-n} \left(\frac{D_2 - D_1}{2} \right)^n}{\tau_0 \left(\frac{D_2 - D_1}{2v_a} \right)^n + k \left[\frac{2(2n+1)}{nC_a^*} \right]^n} \right\}$$

$$N_{Re} = \frac{4(2 \times 0.7129 + 1)}{0.7129} \times \left[\frac{86.394 \times 3.024^{(2-0.7129)} \times \left(\frac{(10.711/12) - (5/12)}{2} \right)^{0.7129}}{6.6582 \left(\frac{(10.711/12) - (5/12)}{2 \times 3.024} \right)^{0.7129} + 0.6686 \left(\frac{2(2 \times 0.7129 + 1)}{0.7129 \times 0.8291} \right)^{0.7129}} \right]$$

$$N_{Re} = 429.6$$

c. Critical value N_{Rec}

$$y = \frac{\log(n) + 3.93}{50} = \frac{\log(0.7129) + 3.93}{50} = 0.07566$$

$$z = \frac{1.75 - \log(n)}{7} = \frac{1.75 - \log(0.7129)}{7} = 0.27099$$

$$N_{Rec} = \left[\frac{8(2n+1)}{ny} \right]^{\frac{1}{1-z}} = \left[\frac{8(2 \times 0.7129 + 1)}{0.7129 \times 0.07566} \right]^{\frac{1}{1-0.27099}} = 3207.697$$

d. Regime flow determination:

Comparison between N_{Re} and N_{Rec}

If $N_{Re} < N_{Rec} \rightarrow$ flow is laminar.

Friction factor is included in Eq. 5.40

e. Frictional pressure loss calculation inside annulus:

$$\left(\frac{dp}{dL}\right) = \frac{4k}{14400(D_2 - D_1)} \left\{ \left(\frac{\tau_0}{k}\right) + \left[\left(\frac{16(2n+1)}{n^* C_a^* (D_2 - D_1)} \right) \left(\frac{q}{\pi(D_2^2 - D_1^2)} \right) \right]^n \right\}$$

$$\left(\frac{dp}{dL}\right) = \frac{4 \times 0.6686}{14400(10.711/12 - 5/12)} \left\{ \left(\frac{6.6582}{0.6686}\right) + \left[\left(\frac{16(2 \times 0.7129 + 1)}{0.7129 \times 0.8291 \times (10.711/12 - 5/12)} \right) \left(\frac{1.48162}{\pi((10.711/12)^2 - (5/12)^2)} \right) \right]^{0.7129} \right\}$$

$$(dp/dL) = 0.014614 \text{ psi/ft}$$

$$\Delta p_a = \left(\frac{dp}{dL}\right) \Delta L = 0.014614 \times 12440 = 181.79 \text{ psi}$$

Finally:

$$\Delta p_p = \Delta p_s + \Delta p_{ds} + \Delta p_b + \Delta p_a = 0 + 2003.254 + 144.04 + 181.79 = 2329.084 \text{ psi}$$

B-6 UNIFIED FLOW

$q_1 = 100$ gallon/min

- Pipe Flow

a. Velocity:

$$v_p = \frac{24.5q}{D_p^2} = \frac{24.5 \times 100}{4.5^2} = 121.988 \text{ ft/min}$$

b. Number of Reynolds:

$$\mu_p = R_{600} - R_{300} = 92 - 58 = 34 \text{ cp}$$

$$\tau_y = R_{300} - \mu_p = 58 - 34 = 24 \text{ lbf/100 ft}^2$$

$$n_p = 3.32 \log \left(\frac{2\mu_p + \tau_y}{\mu_p + \tau_y} \right) = 3.32 \log \left(\frac{2 \times 34 + 24}{34 + 24} \right) = 0.665.$$

$$k_p = 1.066 \left(\frac{\mu_p + \tau_y}{511^{n_p}} \right) = 1.066 \left(\frac{34 + 24}{511^{0.665}} \right) = 0.971 \text{ lbf} \cdot \text{sec}^n / 100 \text{ ft}^2.$$

$$\tau_{yL} = (2R_3 - R_6) 1.066 = (2 \times 8 - 10) \times 1.066 = 6.396 \text{ lbf/100 ft}^2$$

$$G = \frac{3n+1}{4n} = \frac{3 \times 0.665 + 1}{4 \times 0.665} = 1.126$$

$$\gamma_w = \frac{1.6Gv_p}{D_p} = \frac{1.6 \times 1.126 \times 121.988}{4.5} = 48.836 \text{ 1/sec}$$

$$\tau_w = \left(\frac{4}{3}\right)^n \tau_0 + k\gamma_w^n = \left(\frac{4}{3}\right)^{0.665} \times 6.394 + 0.971 \times 48.836^{0.665} = 20.634 \text{ lbf/100 ft}^2$$

$$N_{Re} = \frac{\rho v_p^2}{19.36\tau_w} = \frac{11.55 \times 121.988^2}{19.36 \times 20.634} = 430.26$$

c. Friction factor determination for any flow regime:

$$f_{\text{laminar}} = 16 / N_{Re} = 16 / 430.26 = 0.03719$$

$$f_{\text{transient}} = \frac{16N_{Re}}{(3470 - 1370n)^2} = \frac{16 \times 430.26}{(3470 - 1370 \times 0.665)^2} = 0.00105$$

$$a = \frac{\log(0.665) + 3.93}{50} = 0.076$$

$$b = \frac{1.75 - \log(0.665)}{7} = 0.275$$

$$f_{\text{turbulent}} = \frac{a}{N_{Re}^b} = \frac{0.076}{430.26^{0.275}} = 0.01433$$

$$f_{\text{partial}} = (f_{\text{transient}}^{-8} + f_{\text{turbulent}}^{-8})^{-1/8} = (0.00105^{-8} + 0.01433^{-8})^{-1/8} = 0.00105$$

$$f = (f_{\text{partial}}^{12} + f_{\text{laminar}}^{12})^{1/12} = (0.00105^{12} + 0.03719^{12})^{1/12} = 0.03719$$

d. Frictional pressure loss calculation inside drillstring:

$$\left(\frac{dp}{dL}\right) = \frac{1.076 f v_p^2 \rho}{10^5 D_p} = \frac{1.076 \times 0.03719 \times 121.988^2 \times 11.55}{10^5 \times 4.5} = 0.01529 \text{ psi/ft}$$

$$\Delta p = \left(\frac{dp}{dL}\right) \Delta L = 0.01529 \times 12440 = 190.14 \text{ psi}$$

- Annular Flow

a. Velocity:

$$v_a = \frac{24.5q}{D_2^2 - D_1^2} = \frac{24.5 \times 100}{10.711^2 - 5^2} = 27.306 \text{ ft/min}$$

b. Reynolds number:

$$n_a = 3.32 \log \left(\frac{2\mu_p + \tau_y - \tau_o}{\mu_p + \tau_y - \tau_o} \right) = 3.32 \log \left(\frac{2 \times 34 + 24 - 6.396}{34 + 24 - 6.396} \right) = 0.729$$

$$k_a = 1.066 \left(\frac{\mu_p + \tau_y - \tau_o}{511^{n_a}} \right) = 1.066 \left(\frac{34 + 24 - 6.396}{511^{0.73}} \right) = 0.577 \text{ lbf} \cdot \text{sec}^n / 100 \text{ ft}^2$$

$$G = \left(\frac{2n+1}{3n} \right) \times 1.5 = \left(\frac{2 \times 0.729 + 1}{3 \times 0.729} \right) \times 1.5 = 1.68$$

$$\gamma_w = \frac{1.6 \times G \times v}{D_2 - D_1} = \frac{1.6 \times 1.68 \times 27.306}{10.711 - 5} = 12.89 \text{ 1/sec}$$

$$\tau_w = \left(\frac{3}{2} \right)^n \tau_o + k \gamma_w^n = \left(\frac{3}{2} \right)^{0.729} \times 6.396 + 0.577 \times 12.89^{0.729} = 12.33 \text{ Lbf/100 ft}^2$$

$$N_{Re} = \frac{\rho \times v^2}{19.36 \times \tau_w} = \frac{11.55 \times 27.306^2}{19.36 \times 12.33} = 36.08$$

c. Friction factor determination for any flow regime:

$$f_{laminar} = 24 / N_{Re} = 24 / 36.08 = 0.6652$$

$$f_{transient} = \frac{16 \times N_{Re}}{(3470 - 1370n)^2} = \frac{16 \times 36.08}{(3470 - 1370 \times 0.729)^2} = 0.000095$$

$$a = \frac{\log(0.729) + 3.93}{50} = 0.076$$

$$b = \frac{1.75 - \log(0.729)}{7} = 0.269$$

$$f_{\text{turbulent}} = \frac{a}{N_{\text{Re}}^b} = \frac{0.076}{36.08^{0.269}} = 0.0289$$

$$f_{\text{partial}} = \left(f_{\text{transient}}^{-8} + f_{\text{turbulent}}^{-8} \right)^{-1/8} = \left(0.000095^{-8} + 0.0289^{-8} \right)^{-1/8} = 0.000095$$

$$f_a = \left(f_{\text{partial}}^{12} + f_{\text{laminar}}^{12} \right)^{1/12} = \left(0.000095^{12} + 0.6652^{12} \right)^{1/12} = 0.6652$$

d. Frictional pressure loss calculation inside annulus:

$$\left(\frac{dP}{dL} \right) = \frac{1.076 \times f_a \times v^2 \times \rho}{10^5 (D_2 - D_1)} = \frac{1.076 \times 0.6652 \times 27.306^2 \times 11.55}{10^5 (10.711 - 5)} = 0.0108 \text{ psi/ft}$$

$$\Delta p = \left(\frac{dp}{dL} \right) \Delta L = 0.0108 \times 12440 = 134.26 \text{ psi}$$

Finally:

$$\Delta p_p = \Delta p_s + \Delta p_{ds} + \Delta p_b + \Delta p_a = 0 + 190.14 + 3.257 + 134.96 = 327.66 \text{ psi}$$

$q_2 = 665$ gallon/min

- Pipe Flow

a. Velocity:

$$v_p = \frac{24.5q}{D_p^2} = \frac{24.5 \times 665}{4.5^2} = 804.568 \text{ ft/min}$$

b. Number of Reynolds:

$$\mu_p = R_{600} - R_{300} = 92 - 58 = 34 \text{ cp}$$

$$\tau_y = R_{300} - \mu_p = 58 - 34 = 24 \text{ lbf/100 ft}^2$$

$$n_p = 3.32 \log \left(\frac{2\mu_p + \tau_y}{\mu_p + \tau_y} \right) = 3.32 \log \left(\frac{2 \times 34 + 24}{34 + 24} \right) = 0.665.$$

$$k_p = 1.066 \left(\frac{\mu_p + \tau_y}{511^{n_p}} \right) = 1.066 \left(\frac{34 + 24}{511^{0.665}} \right) = 0.971 \text{ lbf} \cdot \text{sec}^n / 100 \text{ ft}^2.$$

$$\tau_{yL} = (2R_3 - R_6)1.066 = (2 \times 8 - 10) \times 1.066 = 6.396 \text{ lbf/100ft}^2$$

$$G = \frac{3n+1}{4n} = \frac{3 \times 0.665 + 1}{4 \times 0.665} = 1.126$$

$$\gamma_w = \frac{1.6Gv_p}{D_p} = \frac{1.6 \times 1.126 \times 804.568}{4.5} = 322.11 \text{ 1/sec}$$

$$\tau_w = \left(\frac{4}{3}\right)^n \tau_0 + k\gamma_w^n = \left(\frac{4}{3}\right)^{0.665} \times 6.394 + 0.971 \times 322.11^{0.665} = 52.935 \text{ lbf/100 ft}^2$$

$$N_{Re} = \frac{\rho v_p^2}{19.36\tau_w} = \frac{11.55 \times 804.568^2}{19.36 \times 52.935} = 7295.601$$

c. Friction factor determination for any flow regime:

$$f_{laminar} = 16 / N_{Re} = 16 / 7295.601 = 0.00219$$

$$f_{transient} = \frac{16N_{Re}}{(3470 - 1370n)^2} = \frac{16 \times 7295.601}{(3470 - 1370 \times 0.665)^2} = 0.01783$$

$$a = \frac{\log(0.665) + 3.93}{50} = 0.076$$

$$b = \frac{1.75 - \log(0.665)}{7} = 0.275$$

$$f_{turbulent} = \frac{a}{N_{Re}^b} = \frac{0.076}{7295.601^{0.275}} = 0.006584$$

$$f_{partial} = (f_{transient}^{-8} + f_{turbulent}^{-8})^{-1/8} = (0.01783^{-8} + 0.006584^{-8})^{-1/8} = 0.006584$$

$$f = (f_{partial}^{12} + f_{laminar}^{12})^{1/12} = (0.006584^{12} + 0.00219^{12})^{1/12} = 0.00658$$

d. Frictional pressure loss calculation inside drillstring:

$$\left(\frac{dp}{dL}\right) = \frac{1.076 f v_p^2 \rho}{10^5 D_p} = \frac{1.076 \times 0.00658 \times 804.568^2 \times 11.55}{10^5 \times 4.5} = 0.1176 \text{ psi/ft}$$

$$\Delta p = \left(\frac{dp}{dL} \right) \Delta L = 0.1176 \times 12440 = 1463.368 \text{ psi}$$

- Annular Flow

a. Velocity:

$$v_a = \frac{24.5q}{D_2^2 - D_1^2} = \frac{24.5 \times 665}{10.711^2 - 5^2} = 181.582 \text{ ft/min}$$

b. Reynolds number:

$$n_a = 3.32 \log \left(\frac{2\mu_p + \tau_y - \tau_o}{\mu_p + \tau_y - \tau_o} \right) = 3.32 \log \left(\frac{2 \times 34 + 24 - 6.396}{34 + 24 - 6.396} \right) = 0.729$$

$$k_a = 1.066 \left(\frac{\mu_p + \tau_y - \tau_o}{511^{n_a}} \right) = 1.066 \left(\frac{34 + 24 - 6.396}{511^{0.729}} \right) = 0.577 \text{ lbf} \cdot \text{sec}^n / 100 \text{ ft}^2$$

$$G = \left(\frac{2n+1}{3n} \right) \times 1.5 = \left(\frac{2 \times 0.729 + 1}{3 \times 0.729} \right) \times 1.5 = 1.68$$

$$\gamma_w = \frac{1.6 \times G \times v}{D_2 - D_1} = \frac{1.6 \times 1.68 \times 181.582}{10.711 - 5} = 85.76 \text{ 1/sec}$$

$$\tau_w = \left(\frac{3}{2} \right)^n \tau_o + k \gamma_w^n = \left(\frac{3}{2} \right)^{0.729} \times 6.396 + 0.577 \times 85.76^{0.729} = 23.47 \text{ Lbf/100 ft}^2$$

$$N_{Re} = \frac{\rho \times v^2}{19.36 \times \tau_w} = \frac{11.55 \times 181.582^2}{19.36 \times 23.47} = 838.69$$

c. Friction factor determination for any flow regime:

$$f_{laminar} = 24 / N_{Re} = 24 / 838.69 = 0.02861$$

$$f_{transient} = \frac{16 \times N_{Re}}{(3470 - 1370n)^2} = \frac{16 \times 838.69}{(3470 - 1370 \times 0.729)^2} = 0.00219$$

$$a = \frac{\log(0.729) + 3.93}{50} = 0.076$$

$$b = \frac{1.75 - \log(0.729)}{7} = 0.269$$

$$f_{\text{turbulent}} = \frac{a}{N_{\text{Re}}^b} = \frac{0.076}{838.69^{0.269}} = 0.01223$$

$$f_{\text{partial}} = \left(f_{\text{transient}}^{-8} + f_{\text{turbulent}}^{-8} \right)^{-1/8} = \left(0.00219^{-8} + 0.01223^{-8} \right)^{-1/8} = 0.00219$$

$$f_a = \left(f_{\text{partial}}^{12} + f_{\text{laminar}}^{12} \right)^{1/12} = \left(0.00219^{12} + 0.02861^{12} \right)^{1/12} = 0.02861$$

d. Frictional pressure loss calculation inside annulus:

$$\left(\frac{dP}{dL} \right) = \frac{1.076 \times f_a \times v^2 \times \rho}{10^5 (D_2 - D_1)} = \frac{1.076 \times 0.02861 \times 181.58^2 \times 11.55}{10^5 (10.711 - 5)} = 0.02053 \text{ psi/ft}$$

$$\Delta p = \left(\frac{dp}{dL} \right) \Delta L = 0.02053 \times 12440 = 255.42 \text{ psi}$$

Finally:

$$\Delta p_p = \Delta p_s + \Delta p_{ds} + \Delta p_b + \Delta p_a = 0 + 1463.368 + 144.04 + 255.42 = 1862.82 \text{ psi}$$

B-7 ROBERTSON AND STIFF FLOW

$q_1 = 100$ gallon/min

- Pipe Flow

a. Velocity:

$$v_p = \frac{0.408q}{D_p^2} = \frac{0.408 \times 100}{(4.5)^2} = 2.015 \text{ ft/sec}$$

b. Reynolds number:

$$\begin{aligned}
 N_{Re} &= \frac{89100 v_p^{2-B} \rho}{A} \left(\frac{0.0416 D_p}{3 + \frac{1}{B}} \right)^B \\
 &= \frac{89100 \times 2.015^{2-0.6186} \times 11.55}{628.65} \left(\frac{0.0416 \times 4.5}{3 + \frac{1}{0.6186}} \right)^{0.6186} \\
 &= 593.305
 \end{aligned}$$

Where:

$A=628.65$ cp, from Robertson and Stiff, Chapter IV

$B= 0.6186$, from Robertson and Stiff, Chapter IV

c. For laminar flow, critical value

$$N_{Rec} = 3470 - 1370B = 3470 - 1370 \times 0.6186 = 2622.55$$

For turbulent flow, critical value

$$N_{Rec} = 4270 - 1370B = 4270 - 1370 \times 0.6186 = 3422.55$$

d. Regime flow determination:

Comparison between N_{Re} and N_{Rec}

If $N_{Re} < N_{Rec} \rightarrow$ flow is laminar.

Friction factor is included in Eq. 5.62

e. Frictional pressure loss calculation inside drillstring:

Laminar:

$$\left(\frac{dp}{dL}\right) = 8.33E - 4 \times 2^{2+B} \times A \left\{ \left(\frac{1+3B}{B} \right) \left[\frac{0.2v_p + \frac{C}{6} D_p}{D_p^{\left(\frac{1+B}{B}\right)}} \right] \right\}^B$$

$$\left(\frac{dp}{dL}\right) = 8.33E - 4 \times 2^{2+0.6186} \times 1.313 \left\{ \left(\frac{1+3 \times 0.6186}{0.6186} \right) \left[\frac{0.2 \times 120.88 + \frac{17.121}{6} 4.5}{4.5^{\left(\frac{1+0.6186}{0.6186}\right)}} \right] \right\}^{0.6186}$$

$$= 0.01416 \text{ psi/ft}$$

Where:

$A = 1.313 \text{ lbf} \cdot \text{sec}^B / 100 \text{ ft}^2$, from Robertson and Stiff, Chapter IV

$C = 17.121 \text{ 1/sec}^B$, from Robertson and Stiff, Chapter IV

$v_p = 2.015 \times 60 = 120.88 \text{ ft/min}$

$$\Delta p = \left(\frac{dp}{dL}\right) \Delta L = 0.01416 \times 12440 = 176.1504 \text{ psi}$$

- Annular Flow

a. Velocity:

$$v_a = \frac{0.408q}{(D_2^2 - D_1^2)} = \frac{0.408 \times 100}{(10.711^2 - 5^2)} = 0.4547 \text{ ft/sec}$$

b. - Reynolds number:

$$N_{Re} = \frac{109000 v_a^{2-B} \rho}{A} \left(\frac{0.0208(D_2 - D_1)}{2 + \frac{1}{B}} \right)^B$$

$$N_{Re} = \frac{109000 \times 0.4547^{2-0.6186} \times 11.55}{628.65} \left[\frac{0.0208 \times (10.711 - 5)}{2 + \frac{1}{0.6186}} \right]^{0.6186} = 81.49$$

c. For laminar flow, critical value $N_{Rec} = 2622.55$

For turbulent flow, critical value $N_{Rec} = 3422.55$

d. Regime flow determination:

Comparison between N_{Re} and N_{Rec}

If $N_{Re} < N_{Rec} \rightarrow$ flow is laminar.

Friction factor is included in Eq. 5.64.

e. Frictional pressure loss calculation inside annulus:

Laminar:

$$\left(\frac{dp}{dL}\right) = 8.33E - 4 \times 4^{1+B} \times A \left\{ \left(\frac{1+2B}{B} \right) \left[\frac{0.2v_a + \frac{C}{8}(D_2 - D_1)}{(D_2 - D_1)^{\left(\frac{1+B}{B}\right)}} \right]^B \right\}$$

$$\left(\frac{dp}{dL}\right) = 8.33E - 4 \times 4^{1+0.6186} \times 1.313 \times \left\{ \left(\frac{1+2 \times 0.6186}{0.6186} \right) \left[\frac{0.2 \times 27.28 + \frac{17.121}{8}(10.711 - 5)}{(10.711 - 5)^{\left(\frac{1+0.6186}{0.6186}\right)}} \right]^{0.6186} \right\}$$

$$= 0.00805 \text{ psi/ft}$$

Where

$$V_a = 0.4547 \times 60 = 27.28 \text{ ft/min}$$

$$\Delta p = \left(\frac{dp}{dL}\right) \Delta L = 0.00805 \times 12440 = 100.142 \text{ psi}$$

Finally:

$$\Delta p_p = \Delta p_s + \Delta p_{ds} + \Delta p_b + \Delta p_a = 0 + 176.1504 + 3.257 + 100.142 = 279.549 \text{ psi}$$

Note: To consider yield stress with this model, use the following equations and estimate the frictional pressure loss for laminar flow by iteration:

- Pipe flow

$$\lambda = \frac{2(AC)^B}{\left(\frac{dp}{dL}\right)} = \frac{2(0.0131 \times 17.12)^{0.6186}}{\left(\frac{dp}{dL}\right)} = \frac{0.7933}{\left(\frac{dp}{dL}\right)}$$

- Annular Flow

$$\lambda = \frac{(AC)^B}{\left(\frac{dp}{dL}\right)} = \frac{0.3966}{\left(\frac{dp}{dL}\right)}$$

Where:

$$A = 0.0131 \text{ Lbf} \cdot \text{sec}^B / \text{ft}^2$$

$$C = 17.12 \text{ 1/sec}^B$$

$$dp/dL = \text{lbf/ft}^2/\text{ft}$$

General equation to estimate friction pressure loss:

- Pipe flow

$$q = \pi \left\{ \left[\frac{1}{2A} \left(\frac{dp}{dL} \right) \right]^{1/B} \left(\frac{B}{3B+1} \right) \left[\left(\frac{D}{2} \right)^{\frac{3B+1}{B}} - \lambda^{\frac{3B+1}{B}} \right] - \frac{C}{3} \left[\left(\frac{D}{2} \right)^3 - \lambda^3 \right] \right\}$$

$$0.2228 = \pi \left\{ \left[\frac{1}{2 \times 0.0131} \left(\frac{dp}{dL} \right) \right]^{1/0.6186} \left(\frac{0.6186}{3 \times 0.6186 + 1} \right) \left[\left(\frac{4.5}{2} \right)^{\frac{3 \times 0.6186 + 1}{0.6186}} - \lambda^{\frac{3 \times 0.6186 + 1}{0.6186}} \right] - \frac{17.12}{3} \left[\left(\frac{4.5}{2} \right)^3 - \lambda^3 \right] \right\}$$

Applying Solve from Excel, we have $dp/dL = 0.0304 \text{ psi/ft}$. Note that λ is also function of dp/dL .

- Annular Flow

$$q = 2(D_2 - D_1) \left\{ \left[\frac{1}{2A} \left(\frac{dp}{dL} \right) \right]^{1/B} \left(\frac{B}{2B+1} \right) \left[\left(\frac{D}{2} \right)^{\frac{3B+1}{B}} - \lambda^{\frac{2B+1}{B}} \right] - \frac{C}{2} \left[\left(\frac{D}{2} \right)^3 - \lambda^3 \right] \right\}$$

$$q = 2(10.711 - 5) \left\{ \left[\frac{1}{2 \times 0.0131} \left(\frac{dp}{dL} \right) \right]^{1/0.6186} \left(\frac{0.6186}{2 \times 0.6186 + 1} \right) \left[\left(\frac{10.711 - 5}{2} \right)^{\frac{3 \times 0.6186 + 1}{0.6186}} - \lambda^{\frac{2 \times 0.6186 + 1}{0.6186}} \right] - \frac{17.12}{2} \left[\left(\frac{10.711 - 5}{2} \right)^3 - \lambda^3 \right] \right\}$$

Applying Solve from Excel, we have $dp/dL = 0.00806$ psi/ft. Note that λ is also function of dp/dL .

Finally:

$$\Delta p_p = \Delta p_s + \Delta p_{ds} + \Delta p_b + \Delta p_a = 0 + 0.0304 \times 12440 + 3.257 + 0.00806 \times 12440$$

$$= 481.277 \text{ psi}$$

$q_2 = 665$ gallon/min

- Pipe Flow

a. Velocity:

$$v_p = \frac{0.408q}{D_p^2} = \frac{0.408 \times 665}{(4.5)^2} = 13.399 \text{ ft/sec or } 803.94 \text{ ft/min}$$

b. Reynolds number:

$$N_{Re} = \frac{89100 v_p^{2-B} \rho}{A} \left(\frac{0.0416 D_p}{3 + \frac{1}{B}} \right)^B = \frac{89100 \times 13.399^{2-0.6186} \times 11.55}{628.65} \left(\frac{0.0416 \times 4.5}{3 + \frac{1}{0.6186}} \right)^{0.6186}$$

$$= 8126.25$$

Where:

$A = 628.65$ cp, from Robertson and Stiff, Chapter IV

$B = 0.6186$, from Robertson and Stiff, Chapter IV

c. For laminar flow, critical value

$$N_{\text{Rec}} = 3470 - 1370B = 3470 - 1370 \times 0.6186 = 2622.55$$

For turbulent flow, critical value

$$N_{\text{Rec}} = 4270 - 1370B = 4270 - 1370 \times 0.6186 = 3422.55$$

d. Regime flow determination:

Comparison between N_{Re} and N_{Rec}

If $N_{\text{Re}} > N_{\text{Rec}} \rightarrow$ flow is Turbulent.

$$a = \frac{\log B + 3.93}{50} = \frac{\log 0.6186 + 3.93}{50} = 0.0744$$

$$b = \frac{1.75 - \log B}{7} = \frac{1.75 - \log 0.6186}{7} = 0.2798$$

$$f = \frac{a}{N_{\text{Re}}^b} = \frac{0.0744}{8126.25^{0.2798}} = 0.00599$$

e. Frictional pressure loss calculation inside drillstring:

$$\left(\frac{dp}{dL} \right) = \frac{f v_p^2 \rho}{25.81 D_p} = \frac{0.00599 \times 13.399^2 \times 11.55}{25.81 \times 4.5} = 0.10698$$

$$\Delta p = \left(\frac{dp}{dL} \right) \Delta L = 0.10698 \times 12440 = 1330.86 \text{ psi}$$

- Annular Flow

a. Velocity:

$$v_a = \frac{0.408q}{(D_2^2 - D_1^2)} = \frac{0.408 \times 665}{(10.711^2 - 5^2)} = 3.024 \text{ ft/sec or } 181.44 \text{ ft/min}$$

b. - Reynolds number:

$$N_{Re} = \frac{109000 v_a^{2-B} \rho}{A} \left(\frac{0.0208(D_2 - D_1)}{2 + \frac{1}{B}} \right)^B$$

$$N_{Re} = \frac{109000 \times 3.024^{2-0.6186} \times 11.55}{628.65} \left[\frac{0.0208 \times (10.711 - 5)}{2 + \frac{1}{0.6186}} \right]^{0.6186} = 1116.31$$

c. For laminar flow, critical value $N_{Rec} = 2622.55$

For turbulent flow, critical value $N_{Rec} = 3422.55$

d. Regime flow determination:

Comparison between N_{Re} and N_{Rec}

If $N_{Re} < N_{Rec} \rightarrow$ flow is laminar.

Friction factor is included in Eq. 5.64.

e. Frictional pressure loss calculation inside annulus:

Laminar:

$$\left(\frac{dp}{dL} \right) = 8.33E - 4 \times 4^{1+B} \times A \left\{ \left(\frac{1+2B}{B} \right) \left[\frac{0.2v_a + \frac{C}{8}(D_2 - D_1)}{(D_2 - D_1)^{\left(\frac{1+B}{B}\right)}} \right] \right\}^B$$

$$\left(\frac{dp}{dL} \right) = 8.33E - 4 \times 4^{1+0.6186} \times 1.313 \times \left\{ \left(\frac{1+2 \times 0.6186}{0.6186} \right) \left[\frac{0.2 \times 181.44 + \frac{17.121}{8}(10.711 - 5)}{(10.711 - 5)^{\left(\frac{1+0.6186}{0.6186}\right)}} \right] \right\}^{0.6186}$$

$$= 0.015023 \text{ psi/ft}$$

$$\Delta p = \left(\frac{dp}{dL} \right) \Delta L = 0.00805 \times 12440 = 186.886 \text{ psi}$$

Finally:

$$\Delta p_p = \Delta p_s + \Delta p_{ds} + \Delta p_b + \Delta p_a = 0 + 1330.86 + 144.04 + 186.886 = 1661.78 \text{ psi}$$

B-8 CASSON FLOW

$q_1 = 100$ gallon/min

- Pipe Flow

a. Velocity:

$$v_p = \frac{0.408q}{D_p^2} = \frac{0.408 \times 100}{(4.5)^2} = 2.015 \text{ ft/sec}$$

b. - Reynolds number:

$$N_{Re} = \frac{928 v_p \rho D_p}{\mu_c} = \frac{928 \times 2.015 \times 11.55 \times 4.5}{26.39} = 3682.8$$

Where:

$\mu_c = 26.39$ cp, from Casson model, Chapter IV

c. Critical value N_{Rec} from Fig.B1.

$$C_a = \frac{D_p^2 \tau_c \rho}{32.174 \mu_c^2} = \frac{(4.5/12)^2 \times 0.06524 \times 86.394}{32.174 \times 0.000551^2} = 81143$$

Where:

$\tau_c = 0.06524$ lbf/ft² from Casson model, Chapter IV

$\rho = 86.394$ lbf/ft³

$\mu_c = 0.0005510$ lbf.sec/ft²

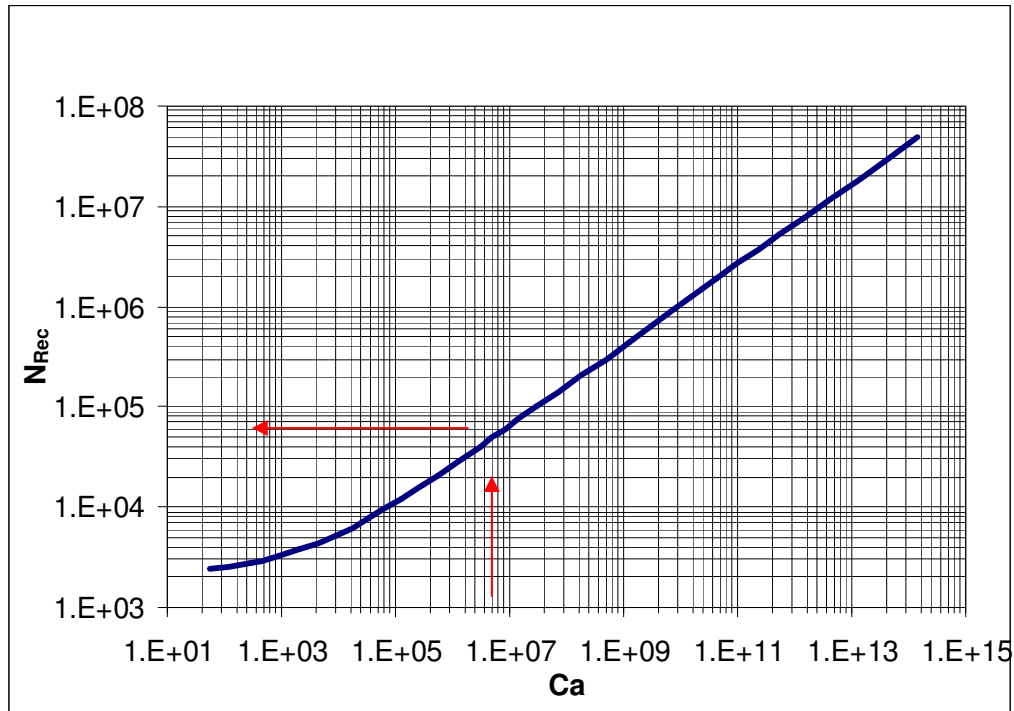


Fig. B1— Critical Reynolds numbers for Casson fluids-example followed.

d. Regime flow determination:

Comparison between N_{Re} and N_{Rec}

$N_{Rec}=14580$ from Fig.B1.

If $N_{Re} < N_{Rec} \rightarrow$ flow is laminar.

Friction factor is included in Eq. 5.70.

e. Frictional pressure loss calculation inside drillstring:

Laminar:

$$q = \frac{\pi D_p^3}{8\mu_c} \left[\frac{D_p \left(\frac{dp}{dL} \right)}{16} - \frac{4}{7} \sqrt{\tau_c} \sqrt{\left(\frac{dp}{dL} \right) D_p} - \frac{64\tau_c^4}{84D_p^3 \left(\frac{dp}{dL} \right)^3} + \frac{\tau_c}{3} \right]$$

Where:

$$q=0.2228 \text{ ft}^3/\text{sec}$$

$$D_p=0.375 \text{ ft}$$

$$\mu_c=0.0005510 \text{ lbf}\cdot\text{sec}/\text{ft}^2$$

$$\tau_c=0.065 \text{ lbf}/\text{ft}^2$$

$$dp/dL= \text{lb}/\text{ft}^2/\text{ft}$$

$$0.2228 = \frac{\pi \times 0.375^3}{8 \times 0.000551} \left[\frac{0.375 \left(\frac{dp}{dL} \right)}{16} - \frac{4}{7} \sqrt{0.065} \sqrt{\frac{\left(\frac{dp}{dL} \right)^{0.375}}{4}} - \frac{64 \times 0.065^4}{84 \times 0.375^3 \left(\frac{dp}{dL} \right)^3} + \frac{0.065}{3} \right]$$

Applying Solve from Excel, we have $dp/dL=0.01436 \text{ psi}/\text{ft}$.

$$\Delta p = \left(\frac{dp}{dL} \right) \Delta L = 0.01436 \times 12440 = 178.6384 \text{ psi}$$

- Annular Flow

a. Velocity:

$$v_a = \frac{0.408q}{(D_2^2 - D_1^2)} = \frac{0.408 \times 100}{(10.711^2 - 5^2)} = 0.4547 \text{ ft}/\text{sec}$$

b. Reynolds number:

$$N_{Re} = \frac{757(D_2 - D_1)v_a\rho}{\mu_c} = \frac{757(10.711 - 5) \times 0.4547 \times 11.55}{26.39} = 860.35$$

c. Critical value N_{Rec} from Fig. A1.

$$C_a = \frac{(D_2 - D_1)^2 \tau_c \rho}{32.174 \mu_c^2} = \frac{\left(\frac{10.711}{12} - \frac{5}{12} \right)^2 \times 0.065 \times 86.394}{32.174 \times 0.00055^2} = 130685.779$$

d. Regime flow determination:

Comparison between N_{Re} and N_{Rec}

$$N_{Rec}=17338 \text{ from Fig.B1.}$$

If $N_{Re} < N_{Rec} \rightarrow$ flow is laminar.

Friction factor is included in Eq. 5.72

e. Frictional pressure loss calculation inside annulus:

Laminar:

$$q = \frac{\pi(D_2 - D_1)^3}{8\mu_c} \times \left[\frac{(D_2 - D_1)\left(\frac{dp}{dL}\right)}{16} - \frac{4}{7}\sqrt{\tau_c} \sqrt{\frac{\left(\frac{dp}{dL}\right)(D_2 - D_1)}{4}} - \frac{64\tau_c^4}{84(D_2 - D_1)^3\left(\frac{dp}{dL}\right)^3} + \frac{\tau_c}{3} \right]$$

Where

$dp/dL = \text{lb/ft}^2/\text{ft}$

$$0.2228 = \frac{\pi\left(\frac{10.711}{12} - \frac{5}{12}\right)^3}{8 \times 0.00055} \times$$

$$\left[\frac{\left(\frac{10.711}{12} - \frac{5}{12}\right)\left(\frac{dp}{dL}\right)}{16} - \frac{4}{7}\sqrt{0.065} \sqrt{\frac{\left(\frac{dp}{dL}\right)\left(\frac{10.711}{12} - \frac{5}{12}\right)}{4}} - \frac{64 \times 0.065^4}{84\left(\frac{10.711}{12} - \frac{5}{12}\right)^3\left(\frac{dp}{dL}\right)^3} + \frac{0.065}{3} \right]$$

Applying Solve from Excel, we have $dp/dL = 0.0090 \text{ psi/ft}$.

$$\Delta p = \left(\frac{dp}{dL}\right)\Delta L = 0.00898 \times 12440 = 111.69 \text{ psi}$$

Finally:

$$\Delta p_p = \Delta p_s + \Delta p_{ds} + \Delta p_b + \Delta p_a = 0 + 178.63 + 3.257 + 111.69 = 293.847 \text{ psi}$$

$q_2 = 665 \text{ gallon/min}$

- Pipe Flow

a. Velocity:

$$v_p = \frac{0.408q}{D_p^2} = \frac{0.408 \times 665}{(4.5)^2} = 13.399 \text{ ft/sec}$$

b. - Reynolds number:

$$N_{Re} = \frac{928 v_p \rho D_p}{\mu_c} = \frac{928 \times 13.399 \times 11.55 \times 4.5}{26.39} = 24489.25$$

Where:

$\mu_c = 26.39$ cp, from Casson model, Chapter IV

c. Critical value N_{Rec} from Fig.B1.

$$C_a = \frac{D_p^2 \tau_c \rho}{32.174 \mu_c^2} = \frac{(4.5/12)^2 \times 0.06524 \times 86.394}{32.174 \times 0.000551^2} = 81143.14$$

Where:

$\tau_c = 0.06524$ lbf/ft² from Casson model, Chapter IV

$\rho = 86.394$ lbm/ft³

$\mu_c = 0.0005510$ lbf.sec/ft²

d. Regime flow determination:

Comparison between N_{Re} and N_{Rec}

$N_{Rec} = 14577$ from Fig.B1.

If $N_{Re} < N_{Rec} \rightarrow$ flow is turbulent.

$$f = \frac{0.0791}{N_{Re}^{0.25}} = \frac{0.0791}{24489.25^{0.25}} = 0.00632$$

e. Frictional pressure loss calculation inside drillstring:

$$\left(\frac{dp}{dL} \right) = \frac{f v_p^2 \rho}{25.81 D_p} = \frac{0.00632 \times 13.399^2 \times 11.55}{25.81 \times 4.5} = 0.11289$$

$$\Delta p = \left(\frac{dp}{dL} \right) \Delta L = 0.11289 \times 12440 = 1404.36 \text{ psi}$$

- Annular Flow

a. Velocity:

$$v_a = \frac{0.408q}{(D_2^2 - D_1^2)} = \frac{0.408 \times 665}{(10.711^2 - 5^2)} = 3.024 \text{ ft/sec}$$

b. Reynolds number:

$$N_{Re} = \frac{757(D_2 - D_1)v_a\rho}{\mu_c} = \frac{757(10.711 - 5) \times 3.024 \times 11.55}{26.39} = 5721.797$$

c. Critical value N_{Rec} from Fig. A1.

$$C_a = \frac{(D_2 - D_1)^2 \tau_c \rho}{32.174 \mu_c^2} = \frac{\left(\frac{10.711}{12} - \frac{5}{12}\right)^2 \times 0.065 \times 86.394}{32.174 \times 0.00055^2} = 130685.779$$

d. Regime flow determination:

Comparison between N_{Re} and N_{Rec}

$N_{Rec} = 17338$ from Fig.B1.

If $N_{Re} < N_{Rec} \rightarrow$ flow is laminar.

Friction factor is included in Eq. 5.72

e. Frictional pressure loss calculation inside annulus:

Laminar:

$$q = \frac{\pi(D_2 - D_1)^3}{8\mu_c} \times \left[\frac{(D_2 - D_1)\left(\frac{dp}{dL}\right)}{16} - \frac{4}{7}\sqrt{\tau_c} \sqrt{\frac{\left(\frac{dp}{dL}\right)(D_2 - D_1)}{4}} - \frac{64\tau_c^4}{84(D_2 - D_1)^3\left(\frac{dp}{dL}\right)^3} + \frac{\tau_c}{3} \right]$$

Where:

$$q = 1.48162 \text{ ft}^3/\text{sec}$$

$$\mu_c = 0.0005510 \text{ lbf}\cdot\text{sec}/\text{ft}^2$$

$$\tau_c = 0.065 \text{ lbf}/\text{ft}^2$$

$$dp/dL = \text{lb/ft}^2/\text{ft}$$

$$1.48162 = \frac{\pi \left(\frac{10.711}{12} - \frac{5}{12} \right)^3}{8 \times 0.00055} \times \left[\frac{\left(\frac{10.711}{12} - \frac{5}{12} \right) \left(\frac{dp}{dL} \right)}{16} - \frac{4}{7} \sqrt{0.065} \sqrt{\frac{\left(\frac{dp}{dL} \right) \left(\frac{10.711}{12} - \frac{5}{12} \right)}{4}} - \frac{64 \times 0.065^4}{84 \left(\frac{10.711}{12} - \frac{5}{12} \right)^3 \left(\frac{dp}{dL} \right)^3} + \frac{0.065}{3} \right]$$

Applying Solve from Excel, we have $dp/dL = 0.01873 \text{ psi/ft}$.

$$\Delta p = \left(\frac{dp}{dL} \right) \Delta L = 0.01873 \times 12440 = 233.0012 \text{ psi}$$

Finally:

$$\Delta p_p = \Delta p_s + \Delta p_{ds} + \Delta p_b + \Delta p_a = 0 + 1404.36 + 144.04 + 233.012 = 1781.415 \text{ psi}$$

Table B1 and **B2** show a comparison between pressure drop results calculated with the various models at two flow rates.

Table B1— Pressure Drop Results Calculated with the Various Models
($q=100 \text{ gpm}$)

Model	Newt.	B-P	Power Law	API-RP13D	H-B	Unified	R&S "original"	Casson
$\Delta p_{ds}, \text{psi}$	47.846	249.7	118.53	118.66	170.56	190.14	176.15	178.73
$\Delta p_a, \text{psi}$	8.24	218.88	39.73	100.33	94.85	134.27	100.14	111.69
$\Delta p_b, \text{psi}$	3.26	3.26	3.26	3.26	3.26	3.26	3.26	3.26
$\Delta p_p, \text{psi}$	59.346	471.84	161.52	222.25	268.67	327.67	279.55	293.68

Table B2— Pressure Drop Results Calculated with the Various Models
($q=665 \text{ gpm}$)

Model	Newt.	B-P	Power Law	API-RP13D	H-B	Unified	R&S "original"	Casson
$\Delta p_{ds}, \text{psi}$	1709.9	1819.15	1380.49	1380.03	2003.3	1463.4	1330.86	1404.4
$\Delta p_a, \text{psi}$	98.7	246.2	140.2	212.28	181.79	255.42	186.889	233.01
$\Delta p_b, \text{psi}$	144.04	144.04	144.04	144.04	144.04	144.04	144.04	144.04
$\Delta p_p, \text{psi}$	1952.7	2209.39	1664.73	1736.35	2329.13	1862.9	1661.789	1781.4

APPENDIX C

C-1 Enlargement and Contraction

Appendix C proposes a method to calculate hydraulics correcting by tool joints effect, for a flow rate of 100 gallon/min. Newtonian fluid.

- Pipe

Gradual Enlargement

Table C1— Angles for Internal Upset (Drillpipe) for Given Example

Pipe				tool joint			angle calculation	
OD,in	wt(lbf/ft)	Grade	d,in	miu,in	dou,in	d-dou	$\theta/2$	θ
4.5	20	D,E	3.6400	2	3.0000	0.6400	17.7500	35.5000
5	19.5	D,E	4.2760	2	3.6875	0.5885	16.4000	32.8000
5	25.6	D,E	4.0000	2	3.3750	0.6250	17.3500	34.7000
5.5	21.9	D,E	4.7780	2	4.0000	0.7780	21.2500	42.5000
5.5	24.7	D,E	4.6700	2	4.0000	0.6700	18.5200	37.0400
3.5	15.5	X,G,S	2.6020	2	1.9375	0.6645	18.3800	36.7600
4.5	20	X,G,S	3.6400	2	2.8125	0.8275	22.4800	44.9600
5	19.5	X,G,S	4.2760	2	3.5625	0.7135	19.6300	39.2600
5	25.6	X,G,S	4.0000	2	3.3125	0.6875	18.9600	37.9200
5.5	21.9	X,G,S	4.7780	2	3.8125	0.9655	25.7700	51.5400
5.5	24.7	X,G,S	4.6700	2	3.8125	0.8575	23.2100	46.4200

$$\theta \leq 45^\circ$$

$$K_e = 2.6 \sin\left(\frac{\theta}{2}\right) (1 - \beta^2)^2 = 2.6 \sin\left(\frac{39.26}{2}\right) \left[1 - \left(\frac{3}{4.276}\right)^2\right]^2 = 0.2276.$$

Where β is the ratio of diameters of small to large pipes, dimensionless

$$\beta = d_{TJ}/D_p$$

Note: internal diameter of pipe for this example is 4.276 because is the data that we have been cover in table C1.

The mechanical energy loss, Fe , between two different successive diameters can be expressed by comparing the Bernoulli equation at two points. See Eq.7.2.

$$v = \frac{0.408q}{d_{TJ}^2} = \frac{0.408 \times 100}{(3)^2} = 4.533 \text{ ft/sec}$$

$$F_e = K_e \left(\frac{v^2}{2gc} \right) = 0.2276 \left(\frac{4.533^2}{2 \times 32.2} \right) = 0.07263 \text{ lbf ft/lbm.}$$

The pressure loss then is calculated by multiplying the fluid density with mechanical energy loss for gradual enlargements.

$$\Delta p_e = 0.052 F_e \rho = 0.052 \times 0.07263 \times 11.55 = 0.0436 \text{ psi.}$$

Gradual Contraction

$$\theta \leq 45^\circ$$

$$K_c = 0.8 \sin\left(\frac{\theta}{2}\right)(1 - \beta^2) = 0.8 \sin\left(\frac{39.26}{2}\right) \left(1 - \left(\frac{3}{4.276}\right)^2\right) = 0.1365$$

Where β is the ratio of diameters of small to large pipes, dimensionless

$$\beta = d_{TJ}/D_p$$

Then;

$$F_c = K_c \left(\frac{v^2}{2gc} \right) = 0.1365 \left(\frac{4.533^2}{2 \times 32.2} \right) = 0.04355 \text{ lbf ft/lbm}$$

$$\Delta p_c = 0.052 F_c \rho = 0.052 \times 0.04355 \times 11.55 = 0.02616 \text{ psi}$$

Note the convergence or divergence angle can be estimated using tables and figures in Chapter VI. Also, see Fig. 7.3 and Tables 7.1, 7.2.

- Annulus

Gradual Enlargement and Contraction

The procedure is the same followed in Sections 7.1.1 and 7.1.2. However, notice that the velocity used to estimate the pressure loss by enlargement and contraction corresponds to the narrow annulus. See Fig. 7.4.

Table C2— Angles for External Upset (Annulus) for Given Example

Pipe				tool joint			angle calculation	
D,in	wt(lbf/ft)	Grade	d,in	meu,in	Dou,in	Dou-D	$\theta/2$	θ
4.5	20	D,E	3.6400	1.5	4.7810	0.2810	10.6100	21.2200
5	19.5	D,E	4.2760	1.5	5.1880	0.1880	7.1400	14.2800
5	25.6	D,E	4.0000	1.5	5.1880	0.1880	7.1400	14.2800
5.5	21.9	D,E	4.7780	1.5	5.5630	0.0630	2.4000	4.8000
5.5	24.7	D,E	4.6700	1.5	5.5630	0.0630	2.4000	4.8000
3.5	15.5	X,G,S	2.6020	2.5	3.7810	0.2810	6.4100	12.8200
4.5	20	X,G,S	3.6400	2.5	4.7810	0.2810	6.4100	12.8200
5	19.5	X,G,S	4.2760	2.5	5.1880	0.1880	4.3000	8.6000
5	25.6	X,G,S	4.0000	2.5	5.1880	0.1880	4.3000	8.6000
5.5	21.9	X,G,S	4.7780	2.5	5.5630	0.0630	1.4400	2.8800
5.5	24.7	X,G,S	4.6700	2.5	5.5630	0.0630	1.4400	2.8800

$$\theta \leq 45^\circ$$

$$K_e = 2.6 \sin\left(\frac{\theta}{2}\right) (1 - \beta^2)^2 = 2.6 \sin\left(\frac{8.6}{2}\right) \left[1 - \left(\frac{6.75}{10.711}\right)^2\right]^2 = 0.07086$$

Where β is the ratio of diameters of small to large pipes, dimensionless

$$\beta = D_{TJ}/D_2$$

The mechanical energy loss, Fe , between two different successive diameters can be expressed by comparing the Bernoulli equation at two points. See Eq.7.2

$$v_a = \frac{0.408q}{(D_2^2 - D_{TJ}^2)} = \frac{0.408 \times 100}{(10.711^2 - 6.75^2)} = 0.5899 \text{ ft/sec}$$

$$F_e = K_e \left(\frac{v^2}{2gc} \right) = 0.07086 \left(\frac{0.5899^2}{2 \times 32.2} \right) = 0.00038 \text{ lbf ft/lbm.}$$

The pressure loss is then calculated by multiplying the fluid density with mechanical energy loss for gradual enlargements.

$$\Delta p_e = 0.052 F_e \rho = 0.052 \times 0.00038 \times 11.55 = 0.00023 \text{ psi.}$$

Gradual Contraction

$$\theta \leq 45^\circ$$

$$K_c = 0.8 \sin \left(\frac{\theta}{2} \right) (1 - \beta^2) = 0.8 \sin \left(\frac{8.6}{2} \right) (1 - 0.63^2) = 0.036$$

Where β is the ratio of diameters of small to large pipes, dimensionless

$$\beta = D_{TJ} / D_2$$

Then;

$$F_c = K_c \left(\frac{v^2}{2gc} \right) = 0.036 \left(\frac{0.5899^2}{2 \times 32.2} \right) = 0.0002 \text{ lbf ft/lbm}$$

$$\Delta p_c = 0.052 F_c \rho = 0.052 \times 0.0002 \times 11.55 = 0.00012 \text{ psi}$$

C-1.1 Estimation of Pump Pressure Considering Enlargement and Contraction correction

Add to drillstring friction pressure losses calculated (with any correction) the pressure losses caused by enlargement and contraction of each tool joint. Do the same for the annulus friction pressure losses. See Eq. 7.9. Table B1 shows the values for pressure drop in the annulus and in the drillstring for Newtonian fluid.

$$\Delta p_p = \Delta p_s + [\Delta p_{ds} + (\Delta p_e + \Delta p_c) N_{TJ}] + [\Delta p_a + (\Delta p_e + \Delta p_c) N_{TJ}] + \Delta p_b.$$

Where $N_{TJ} = 12440\text{ft}/30\text{ft} = 415$

$$\Delta p_p = 0 + [47.84 + (0.0436 + 0.02616) \times 415] + [8.24 + (0.00023 + 0.00012) \times 415] + 3.257 = 88.6 \text{ psi}$$

C-2 Equivalent Diameter

Use the following equation to estimate equivalent diameter, D_e , in drillstring (between inside pipe and tool joint diameters).³¹

- Pipe

$$De_p = \left[\frac{L_2 d_{TJ}^4 D_P^4}{L_1 D_P^4 + (L_1 - L_2) d_{TJ}^4} \right]^{1/4} = \left[\frac{21 \times 3^4 \times 4.276^4}{21 \times 4.276^4 + (21 - 336) \times 3^4} \right]^{1/4} = 4.089 \text{ in}$$

Where:

$$d_{TJ} = 3 \text{ in.}$$

$$D_P = 4.276 \text{ in.}$$

$$L_1 = 21 \text{ in, from drilling manual (i.e. pin + box tong length).}$$

$$L_2 = 28 \text{ ft} \times 12 = 336 \text{ in. (length of one pipe without tool joint)}$$

- Annulus

$$De_a = \left[\frac{L_2 D_{TJ}^4 D_1^4}{L_1 D_1^4 + (L_1 - L_2) D_{TJ}^4} \right]^{1/4} = \left[\frac{21 \times 6.75^4 \times 5^4}{21 \times 5^4 + (21 - 336) \times 6.75^4} \right]^{1/4} = 5.06 \text{ in}$$

Where:

$$D_{TJ} = 6.75 \text{ in.}$$

$$D_1 = 5 \text{ in.}$$

Finally, calculate friction pressure losses in the drillstring and annulus as showed in appendix B, but use equivalent diameter in the calculation of frictional pressure drop.

Note: use $D_p = De_p$ for the estimation of pressure drop in the drillstring and $D_2 = De_a$ to estimate pressure drop in the annulus.

$q_1 = 100$ gallon/min

- Pipe Flow

$$v_p = \frac{0.408q}{D_p^2} = \frac{0.408 \times 100}{(4.089)^2} = 2.4402 \text{ ft/sec}$$

$$\mu_a = R_{300} = 58 \text{ cp}$$

$$N_{Re} = \frac{928 De_p v_p \rho}{\mu_a} = \frac{928 \times 4.089 \times 2.4402 \times 11.55}{58} = 1843.93$$

If $N_{Re} < N_{Rec} \rightarrow$ flow is laminar.

$$f = 16 / N_{Re} = 16 / 1843.93 = 0.008677$$

$$\left(\frac{dp}{dL} \right) = \frac{f v_p^2 \rho}{25.81 De_p} = \frac{0.008677 \times (2.4402)^2 \times 11.55}{25.81 \times 4.089} = 0.0057 \text{ psi/ft}$$

$$\Delta p_{ds} = \left(\frac{dp}{dL} \right) \Delta L = 0.0057 \times 12440 = 70.343 \text{ psi}$$

- Annular Flow

$$v_a = \frac{0.408q}{(D_2^2 - De_a^2)} = \frac{0.408 \times 100}{(10.711^2 - 5.06^2)} = 0.4578 \text{ ft/sec}$$

$$N_{Re} = \frac{757(D_2 - De_a)v_a \rho}{\mu_a} = \frac{757 \times (10.711 - 5.06) \times 0.4578 \times 11.55}{58} = 389.988$$

If $N_{Re} < N_{Rec} \rightarrow$ flow is laminar.

$$f = 16 / N_{Re} = 16 / 389.988 = 0.04103$$

$$\left(\frac{dp}{dL} \right) = \frac{f v_a^2 \rho}{25.81(D_2 - D_{e_a})} = \frac{0.04103 \times (0.4578)^2 \times 11.55}{25.81 \times (10.711 - 5.06)} = 0.00068 \text{ psi/ft}$$

$$\Delta p_a = \left(\frac{dp}{dL} \right) \Delta L = 0.00068 \times 12440 = 8.471 \text{ psi}$$

- Frictional pressure losses across the bit, Δp_b :

$$\Delta p_b = \frac{156 \rho q^2}{(D_{N1}^2 + D_{N2}^2 + D_{N3}^2)^2} = \frac{156 \times 11.5 \times 100^2}{(28^2 + 28^2 + 28^2)^2} = 3.257 \text{ psi}$$

$$\Delta p_p = 0 + 70.343 + 3.257 + 8.471 = 82.07 \text{ psi}$$

C-3 Two Different IDs

This proposed approach estimate the frictional pressure drop in the annulus and in the drillstring considering the actual pipe/tool joint length and diameter in the calculation. Follow the example in appendix B.

- Pipe:

- Estimation of total drillstring length, $L_{\text{total } dp}$:

$$L_{\text{total } dp} = (L_2 N_{DP} - L_1 N_{TJ}) = (12440 - 21 \times 415 / 12) = 11713.75 \text{ ft}$$

- Use the inner diameter of the drillstring to estimate the frictional pressure drop, Δp_{ds} :

$$\Delta p_{ds} = \left(\frac{dp}{dL} \right) \Delta L = 0.0038 \times 11713.75 = 44.51 \text{ psi}$$

Where:

$L_{\text{total } dp}$ = total drill pipe length, ft

N_{DP} = numbers of drillpipe

Δp_{ds} = frictional pressure drop in the drillstring, psi.

$(dp/dL)_{ds}$ = pressure gradient, psi/ft. See Chapter V.

c. Estimation of total tool joint length, $L_{\text{total } TJ}$:

$$L_{\text{total } TJ} = 21 \times 415 / 12 = 726.25 \text{ ft}$$

d. Use ID of tool joint and respective length to calculate its contribution in the pressure loss to the drillstring, Δp_{TJ} .

$$v_p = \frac{0.408q}{D_p^2} = \frac{0.408 \times 100}{(3)^2} = 4.533 \text{ ft/sec}$$

$$\mu_a = R_{300} = 58 \text{ cp}$$

$$N_{Re} = \frac{928 d_{TJ} v_{TJ} \rho}{\mu_a} = \frac{928 \times 3 \times 4.533 \times 11.55}{58} = 2513.09$$

If $N_{Re} < N_{Rec} \rightarrow$ flow is turbulent.

$$f = 0.0791 / N_{Re}^{0.25} = 0.0791 / (2513.09)^{0.25} = 0.01117$$

$$\left(\frac{dp}{dL} \right) = \frac{f v_p^2 \rho}{25.81 D_p} = \frac{0.01117 \times (4.533)^2 \times 11.55}{25.81 \times 3} = 0.00343 \text{ psi/ft}$$

$$\Delta p_{TJ} = \left(\frac{dp}{dL} \right) \Delta L = 0.00343 \times 726.25 = 2.49 \text{ psi}$$

e. Add drillstring and tool joint frictional pressure drop to estimate the total drillstring friction pressure losses.

$$(\Delta p_{\text{Total 2IDs}})_{ds} = 44.51 + 2.49 = 47.00 \text{ psi}$$

- Annulus:

Use the same procedure to estimate the total frictional pressure drop in the annulus, $(\Delta p_{\text{Total 2IDs}})_a$, followed in the pipe section but use the annulus data.

Finally,

$$\Delta p_p = 0 + 47.00 + 10.25 + 3.257 = 60.51 \text{ psi}$$

C-4 Enlargement and Contraction Plus Equivalent Diameter

$$\Delta p_p = 0 + [70.25 + (0.044 + 0.02624) \times 415] + [10.27 + (0.00023 + 0.00012) \times 415] + 3.257 = 113.072 \text{ psi}$$

C-5 Enlargement and Contraction plus Two Different IDs

$$\Delta p_p = 0 + [69.42 + (0.044 + 0.02624) \times 415] + [10.25 + (0.00023 + 0.00012) \times 415] + 3.257 = 113.072 \text{ psi}$$

$$\Delta p_p = 0 + 69.42 + 10.25 + 3.257 = 112.22 \text{ psi}$$

APPENDIX D

Table D1— Rheological Properties for Eight Rheological Models

Mud density, ppg=		11.55		P,psi=		14.7			
Mud type:		SBM-oil		T, F=		150			
γ_N (sec ⁻¹)	τ_{fann}	τ_{new}	τ_{B-M} (API13RP)	τ_{P-L}	τ_{API}	τ_{H-B} (full range)	τ_{Casson}	τ_{R-S}	$\tau_{Unified}$
1021.80	98.16	108.92	98.16	85.46	98.17	100.09	101.16	96.44	97.48
510.90	61.89	54.46	61.89	62.65	61.89	63.66	61.78	63.45	61.47
340.60	49.08	36.31	49.79	52.25	47.25	49.35	47.42	49.87	46.94
170.30	34.14	18.15	37.70	38.30	34.17	32.70	31.56	33.43	30.93
10.22	10.67	1.09	26.33	10.86	11.23	10.16	10.92	10.16	9.55
5.11	8.54	0.54	25.97	7.97	8.54	8.80	9.52	8.94	8.30
AAPE		46.538	60.48599	6.8871	1.512089	2.8978288	4.66646946	2.91378324	4.73638305
		Newton.	B-M _(API13RP)	P-L _(full range)	API _(P-L)	H-B _(full range)	Casson	R-S	Unified
μa 6 points=		51.04	μp_{API} = 0.0710	n = 0.45	np = 0.67	n = 0.7129	μpc = 0.0551	B = 0.6186	np = 0.67
μa 1 point=		58.00	τy_{API} = 25.61	k = 3.84	na = 0.40	k = 0.6686	τOC = 6.5238	A = 1.3130	na = 0.73
					kp = 0.97	τo = 6.66		C = 17.12	kp = 0.97
					ka = 4.45				ka = 0.58
									LSYP = 6.40
									R = 0.27

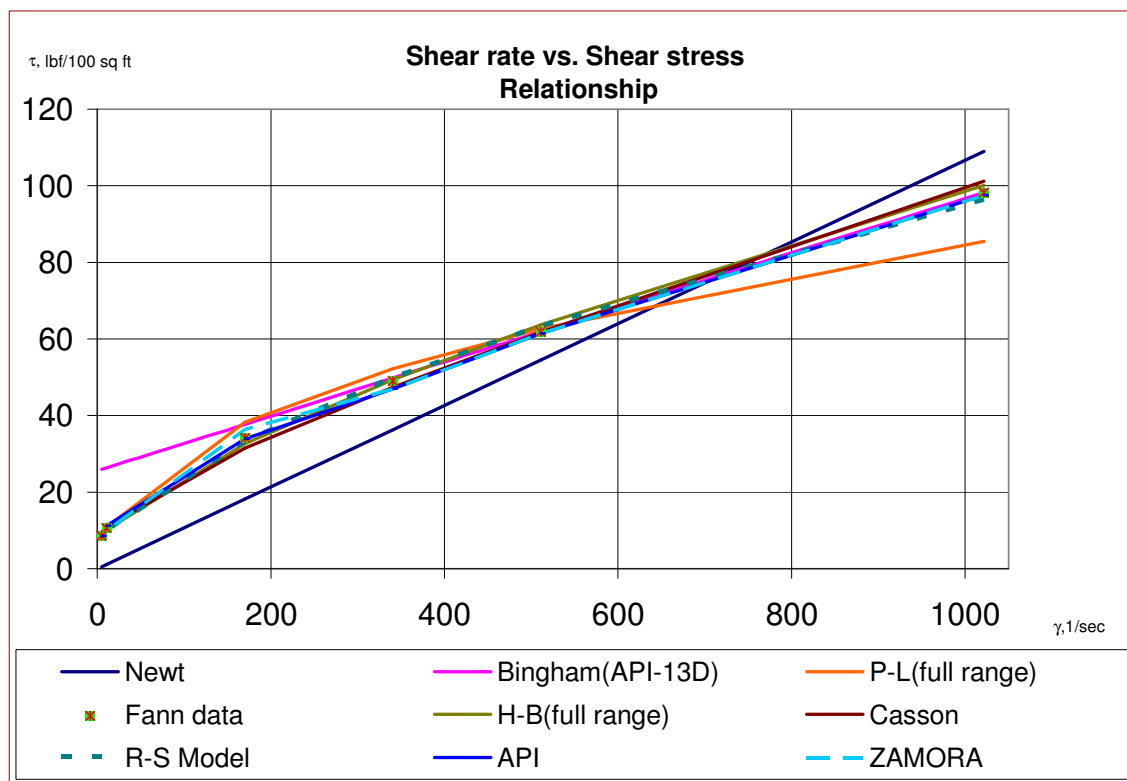


Fig. D1— Rheograms for eight rheological models at 150°F.

APPENDIX E

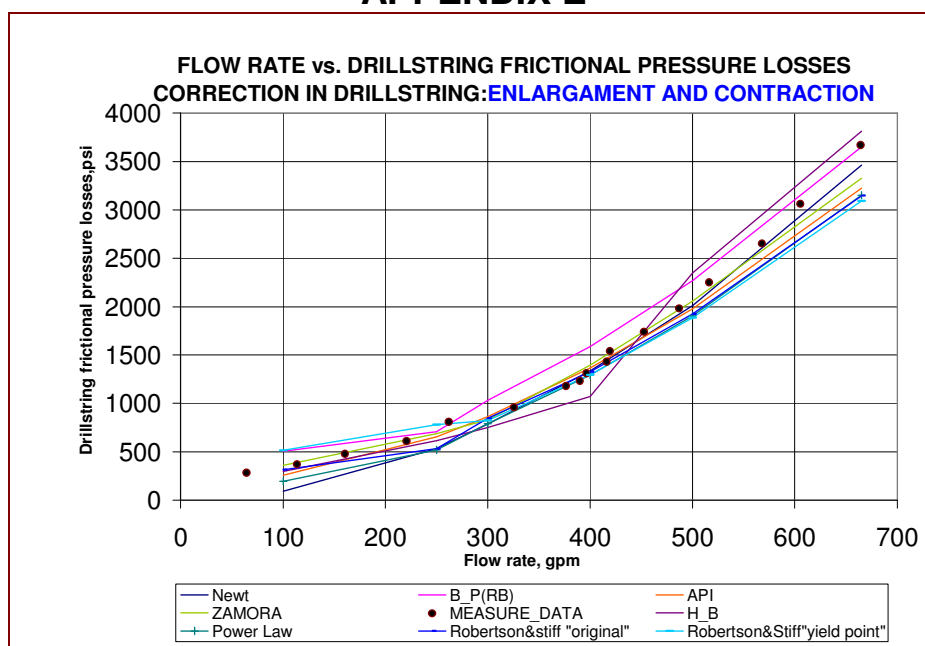


Fig. E1— Flow rate vs. drillstring pressure loss with E&C correction.

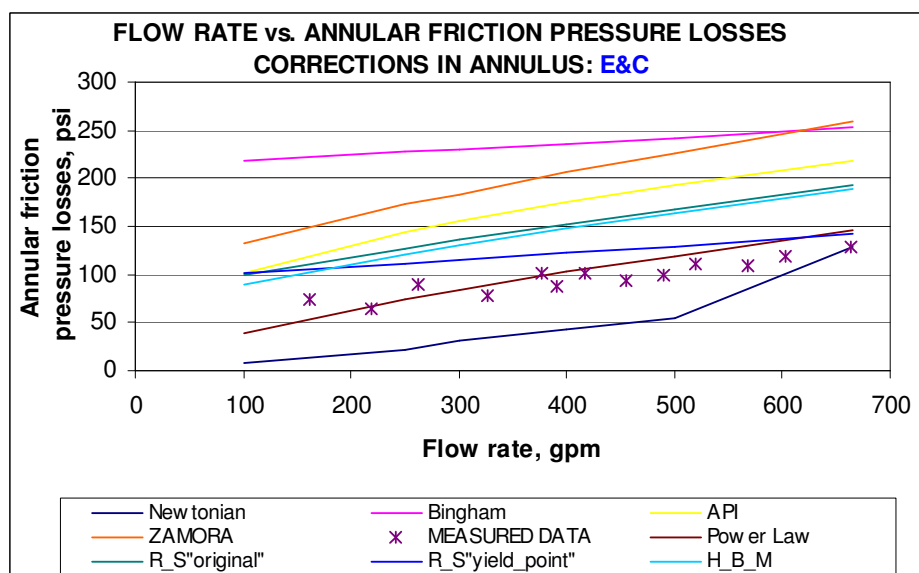


Fig. E2— Flow rate vs. annular pressure loss with E&C correction.

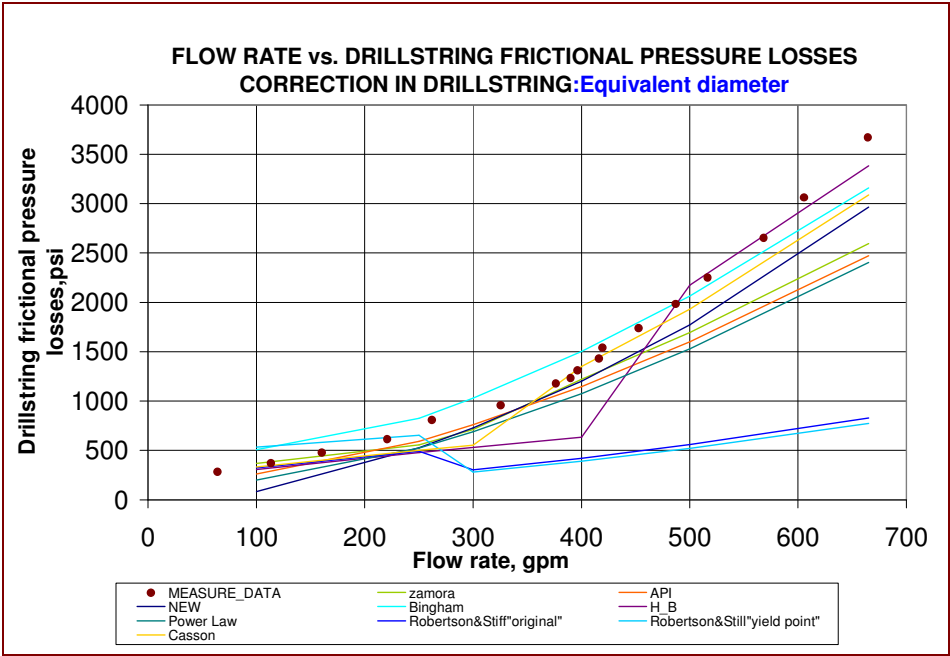


Fig. E3— Flow rate vs. drillstring pressure loss with ED correction.

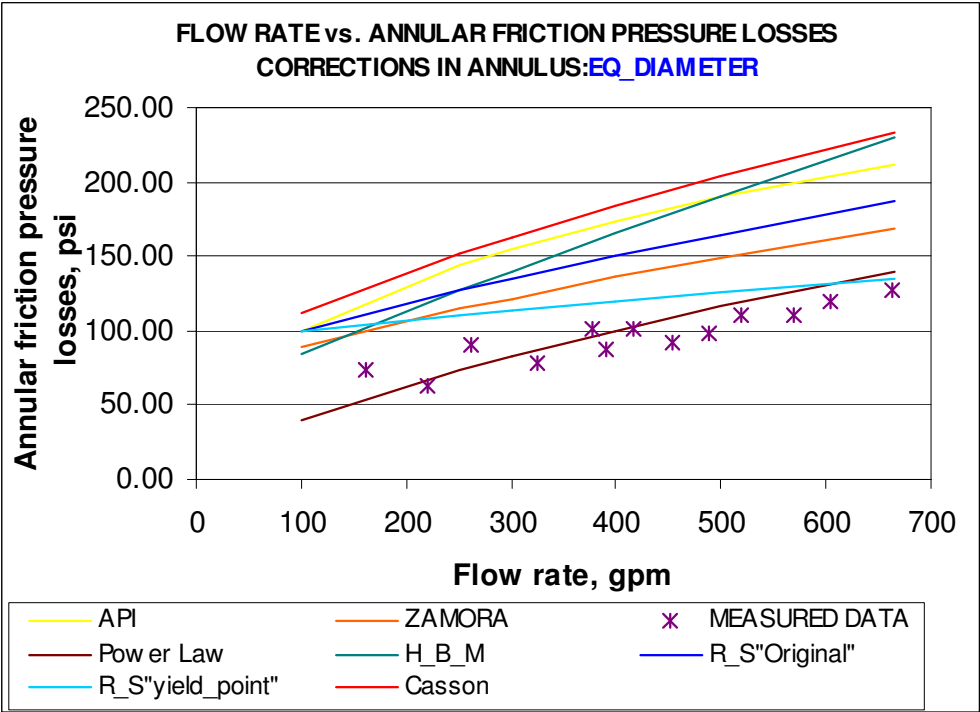


Fig. E4— Flow rate vs. annulus pressure loss with ED correction.

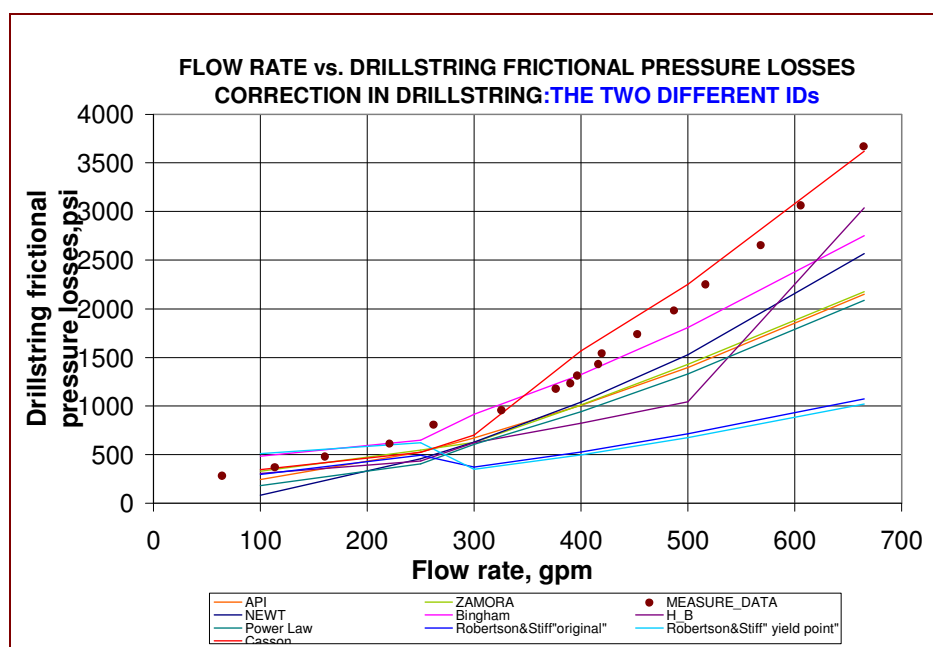


Fig. E5— Flow rate vs. drillstring pressure loss with 2IDs correction.

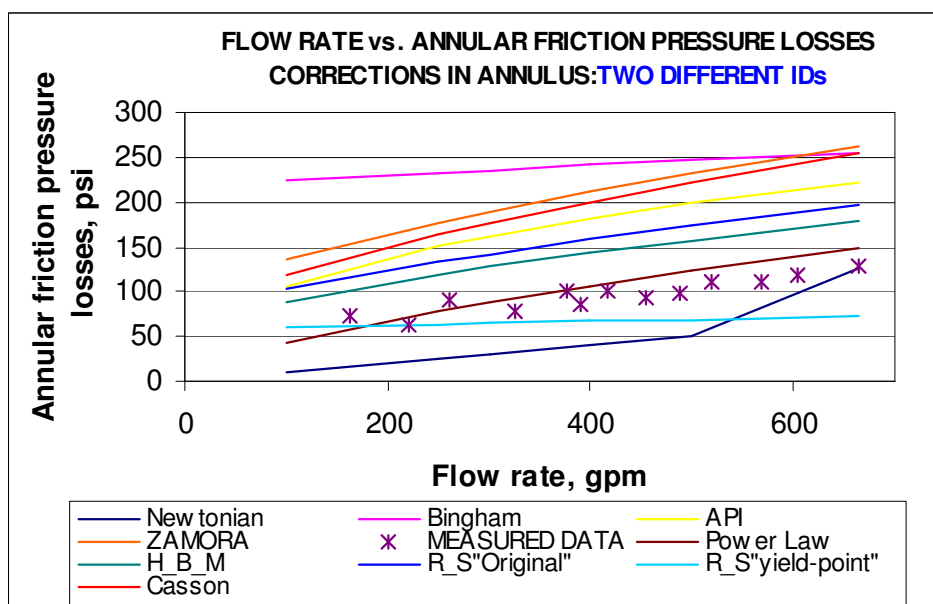


Fig. E6— Flow rate vs. annular pressure loss with correction for 2IDs.

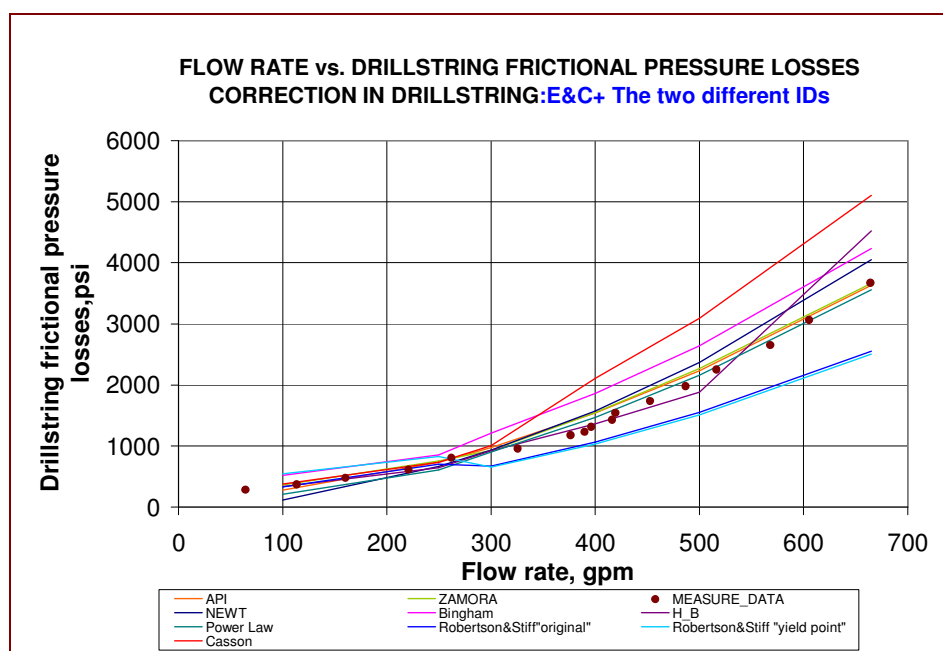


Fig. E7— Flow rate vs. drillstring pressure loss with correction for E&C+2IDs.

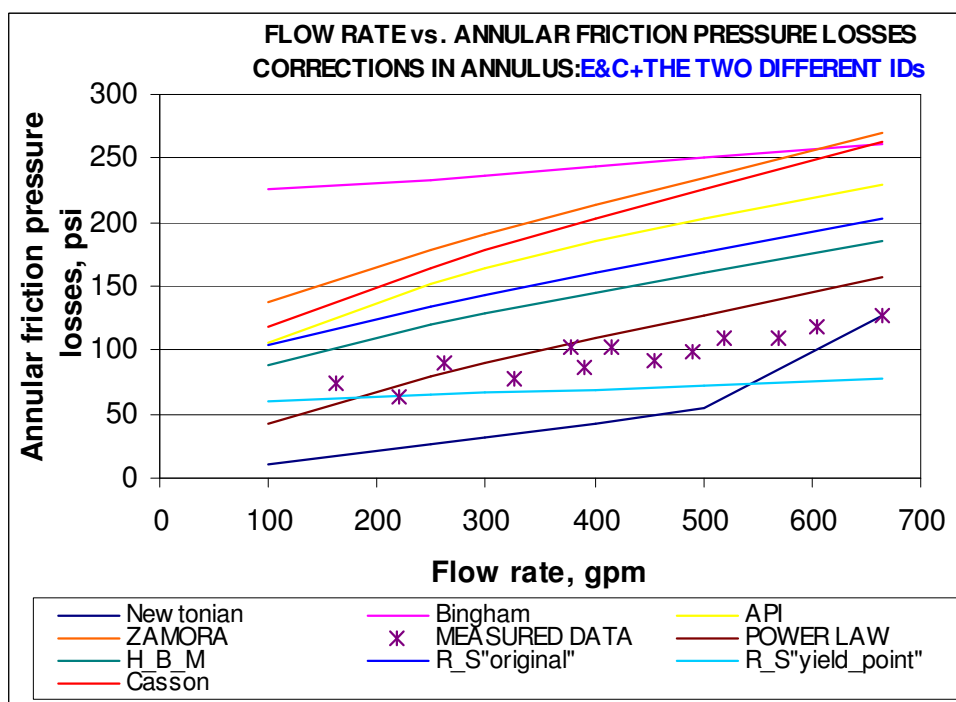


Fig. E8— Flow rate vs. annular pressure loss with correction for E&C+2IDs.

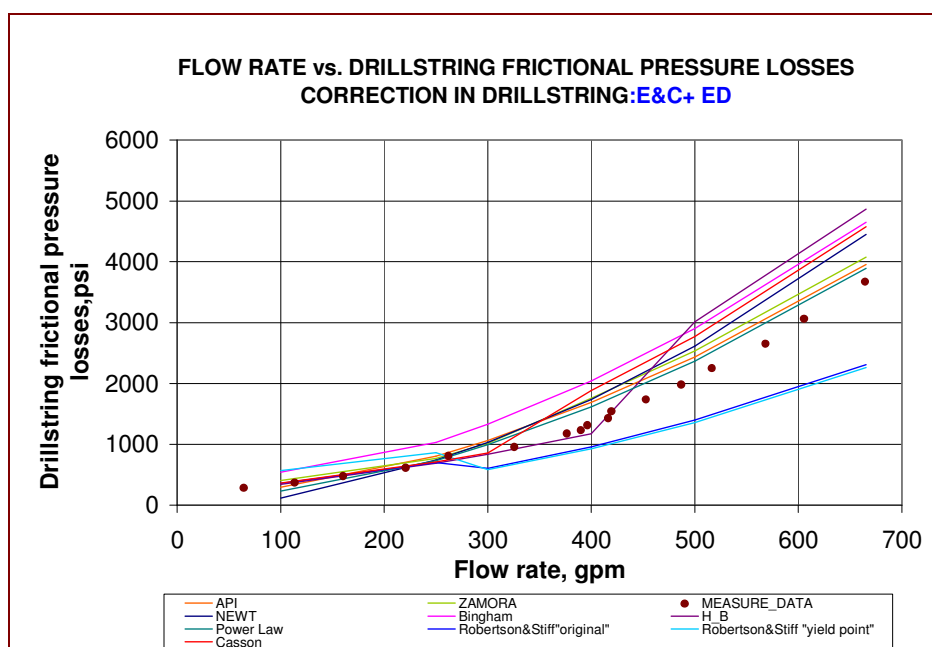


Fig. E9—Flow rate vs. drillstring pressure loss with correction for E&C+ ED.

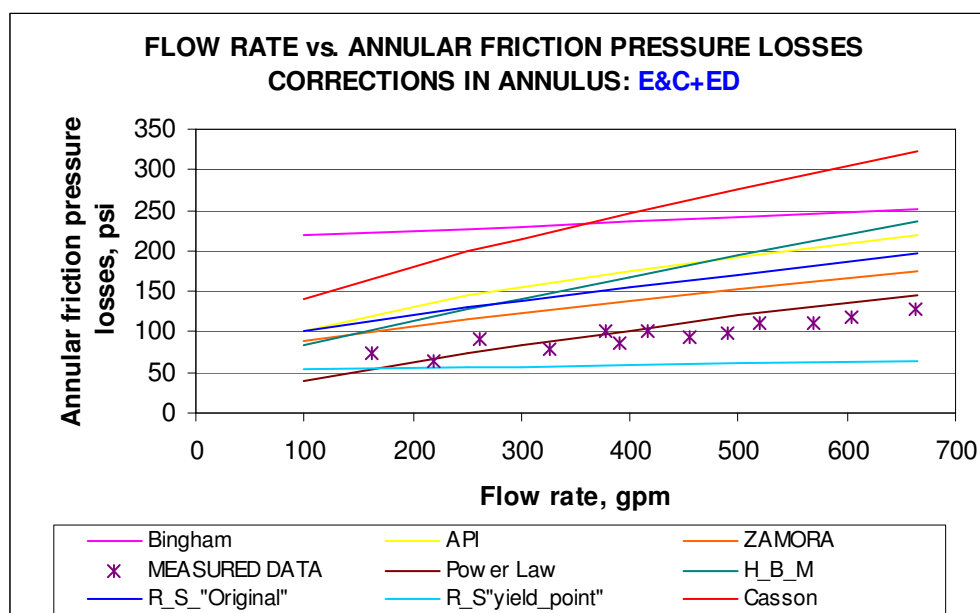


Fig. E10—Flow rate vs. annular pressure loss with correction for E&C+ ED.

VITA

Name: Marilyn Viloria Ochoa

Address: Urb,La Paz,calle 96E#53A-66, Maracaibo/Zulia-Venezuela

Born: Maracaibo-EDO-Zulia (Venezuela)

Education: Zulia University
Venezuela, B.S.—Petroleum Engineering, 1994

Zulia University-CIED_PDVSA
Venezuela, M.A. — Drilling Engineering, 1997

Zulia University
Venezuela, M.A. — Petroleum Engineering, 1998

Texas A&M University
USA, Ph.D.— Petroleum Engineering, 2006